Investigation into the relationship between aluminium treatment and the superoxide dismutase (SOD) enzyme system in *Lolium perenne* (*L. perenne* cv. Nui)

A thesis presented in partial fulfilment of the requirements for the degree of Master of Science (with Honours) in Plant Biology
at Massey University

Samuel James Gregory
2009

ABSTRACT

Lolium perenne cv. Nui is a cultivar of ryegrass grown throughout New Zealand in pastures due to favourable traits such as high palatability for livestock and its ability to withstand intensive grazing. However, the productivity of pastures is reduced when levels of aluminium and other metals accumulate in soils to toxic levels, a phenomenon referred to as the 'acid soil syndrome'. In response to this toxicity, plants activate a series of antioxidant reactions, with one catalysed by the superoxide dismutase (SOD) enzymatic system. The enzyme system comprises three isoenzymes, a Cu/ZnSOD, FeSOD and a MnSOD which catalyse the same reaction but differ in amino acid sequence, molecular mass and the metal ion co-factor (hence Cu/ZnSOD, FeSOD and MnSOD). Together these isoenzymes combat the damaging effect of superoxide radicals which accumulate due to metal toxicity. In this thesis, the isolation of genes encoding isoenzymes of the SOD enzyme from *L. perenne* cv. Nui is described. As well, the growth of *L. perenne* cv. Nui and changes in expression of the SOD genes encoding each isoenzyme in response to aluminium treatment (0.2mM $AlCl_3$) is investigated.

A 1072 bp FeSOD gene sequence and a 705 bp MnSOD gene sequence were isolated from shoot tissue of *L. perenne* cv. Nui using a combination of RT-PCR with degenerate primers and 3'-RACE. The FeSOD gene comprised 572 bp of the coding sequence and 500 bp of 3'-UTR while the MnSOD gene comprised 508 bp of coding sequence and a 197 bp 3'-UTR. By alignment of each sequence with the gene from the database with highest identity it was predicted that the translation start codon (ATG) is located a further 196 bp upstream for the FeSOD gene (aligned with an *Oryza sativa* FeSOD sequence as a reference) and a further 152 bp upstream for the MnSOD sequence (aligned with a *Triticum aestivum* MnSOD sequence as a reference). Using RT-PCR with degenerate primers, a 313 bp CuSOD sequence was predominantly cloned from shoot tissue of *L. perenne* cv. Nui, but it was not possible to generate the 3'-UTR using 3'-RACE.

For growth analysis, seedlings of *L. perenne* cv. Nui were germinated and acclimatised in Hoagland's solution, and then subjected to either aluminium treatment (0.2mM

$AlCl_3$) or no treatment to act as a control over a designated time course of 0, 4, 8, or 24 hours. Two growth trials were conducted that differed in the age of seedlings used and plant tissues were separated into root and shoot tissues. Similar growth trends were observed in both trials, but the sampling regime in the second growth trial meant that statistical analysis could be carried out. In this trial, analysis revealed that over a time course of 24 hours exposure to 0.2mM aluminium, both root and shoot tissue fresh weight did not significantly differ when compared to the control (no aluminium). A general trend of an increase in root and shoot fresh weight was observed in plants treated with aluminium, but this trend was not significant at P=0.05. No significant change in fresh weight partitioning from shoot to root, or root to shoot in response to aluminium was also observed.

Using semi-quantitative Reverse Transcriptase-Polymerase Chain Reaction (sqRT-PCR) and primers based around the 3'-UTR with RNA isolated from plants grown in the second hydroponic trial, it was determined that under the conditions used, expression of the FeSOD and MnSOD genes isolated in this study were neither up-regulated or down-regulated in response to aluminium treatment in both shoot and root tissue. Further, using degenerate primers to detect expression of one or more genes encoding the Cu/ZnSOD isoenzyme, total expression of the Cu/ZnSOD isoenzyme was also unresponsive to aluminium treatment.

ACKNOWLEDGEMENTS

My expression of gratitude, firstly, must go to my supervisor Professor Michael McManus for his excellent guidance in helping me through to completion of my Masters degree. Michael, you have given me space in achieving what I have completed at Massey to date, and also given me a push in the right direction when it has been needed so I thank you for that.

To Susanna, your help with all aspects of lab work has been greatly appreciated especially in relation to primer design and sequence analysis work. Special thanks must also be given to the other MTM lab workers that I have had the privilege of working with, namely, Sarah, Nick, Jibran, Phoung, Aluh, Caleb, Matt, Afsana, Alvina and Diantha for providing a relaxed lab environment to work in.

Special thanks must be given to Massey University in relation to offering me a Massey University Maori Masterate Scholarship which has allowed me to pursue my academic path. Also, to IMBS for the successful application of travel grants to attend Plant Biology conferences in New Zealand.

Finally, I'd like to acknowledge my friends and family. Mum and Dad, you have always helped me push for success both academically and on the sporting field which I will always be grateful for. I can only look forward in both disciplines now with your ongoing help. To Gabrielle for your ongoing persistence and ability in allowing me to carry out my life ambitions. You have always been there for me which I appreciate. To Corkill and Dazza, you make me laugh.

TABLE OF CONTENTS

LIST OF FIGURES

LIST OF TABLES

LIST OF ABBREVIATIONS

A_{260}	Absorbance at 260 nm
Al	Aluminium
$AlCl_3$	Aluminium chloride
Amp	Ampicillin
bp	Base pair
°C	Degrees celcius
$CaCl_2$	Calcium chloride
cDNA	Complementary deoxyribonucleic acid
cm	Centrimetre
cv.	Cultivar
d	Day
DEPC	Diethylpyrocarbonate
DF	Dilution factor
DNA	Deoxyribonucleic acid
dNTP	Deoxynucleotide triphosphate
DTT	Dithiothreitol
E. coli	*Echerichia coli*
EDTA	Ethylenediaminetetraacetic acid
EtBr	Ethidium bromide
FW	Fresh weight
g	g force
g	Grams
h	Hour
HCl	Hydrochloric acid
IPTG	Isopropyl-β-$_D$-thiogalactopyranoside
Kb	Kilo basepair
KCl	Potassium chloride
L	Litre
LB	Luria-Bertani (media or broth)
L. perenne	*Lolium perenne*

LiCl	Lithium chloride
M	Molar, moles per litre
mM	Millimolar
mg	Milligram
MQ Water	Water purified by a Milli-purification system
min	Minute
mL	Millilitre
NaOAc	Sodium acetate
NCBI	National Centre for Biotechnology Information
ng	Nanogram
nm	Nanometre
n	Night
NaCl	Sodium chloride
NaOH	Sodium hydroxide
NZ	New Zealand
OD	Optical density
PCR	Polymerase chain reaction
PCR Water	Filtered, sterile MQ water
PEG	Polyethylenglycol
pH	-Log $[H^+]$
RACE	3´-rapid amplification of cDNA ends
RNA	Ribonucleic acid
RNase	Ribonuclease
rpm	Revolutions per minute
RT-PCR	Reverse transcriptase-polymerase chain reaction
s	Second
SDS	Sodium dodecyl sulphate
sqRT-PCR	Semi-quantitative RT-PCR
TAE	Tris-Acetate-EDTA
Tris	Tris (hydroxymethyl) aminomethane
µg	Microgram
µl	Microlitre
µM	Micromolar
U	Units

UTR	Untranslated region
UV	Ultraviolet light
V	Volts
v/v	Volume per volume
w/v	Weight per volume
w/w	Weight per weight
X-Gal	5-Bromo-4-chloro-3-indolyl-β-$_D$-galactopyranoside

1. Introduction

1.1 Overview

All plants, like other aerobic organisms evolved in the presence of oxygen have developed processes that harness the energetic potential of this molecule (Navrot et al., 2007). But as an important molecule it must also be reduced during respiration and different pathways are involved in the reduction. This reduction of oxygen can occur in a number of ways with one being a stepwise system where oxygen accepts electrons one by one and leads to the formation of a reactive oxygen species (ROS) known as the superoxide anion (Basu et al., 2001) .

ROS are generated by aerobic metabolism and include active molecules derived from oxygen including singlet oxygen, peroxides, hydroxyl radicals, superoxide anions and hydrogen peroxide. In most living cells, ROS play a key role as signaling molecules especially in response to a number of various stresses or threats to plant integrity. They may act as messengers to induce gene transcription or trigger protein activation but the levels of these oxidants must be tightly controlled as increased levels may lead to cell damage (Bowler et al., 1992; Navrot et al., 2007).

Under stress conditions such as heavy metal contamination, ROS have been observed to increase to levels which cause damage to plant integrity in a process known as oxidative stress. The accumulation of ROS can include superoxide radicals which are relatively unreactive but can form species damaging to cellular components, such as hydroxyl radicals in the presence of metals (Huang et al., 2009; Rangel et al., 2009). Hydroxyl radicals are able to react indiscriminately, causing lipid peroxidation, protein oxidation and DNA damage. Under aluminium stress, for instance, an initial accumulation of ROS is observed which impairs mitochondrial metabolism but also generates an intracellular signal for the control of such species (Navrot et al., 2007) This signal allows for the induction of antioxidant genes and/or activation of detoxifying genes that prevent oxidation.

In general the activation of the antioxidant pathway follows transduction events as a consequence of ROS signaling. This pathway consists of a number of enzymic and non-

enzymic components which work in concert to detoxify ROS. One of these components is the superoxide dismutase (SOD) enzyme system which is responsible for the catalysation on the superoxide anion to hydrogen peroxide. This enzyme has been identified as a major step in the reduction of ROS and its induction under a number of stresses has been observed.

Two components that form the basis of this study are the metal aluminium and the SOD system which is the first line of defence against the formation of high levels of ROS. Aluminium toxicity is reported to cause an increase in ROS production, which triggers the antioxidant pathway, of which the superoxide dismutase enzyme system is an integral component. This thesis therefore examines the response of perennial ryegrass (Lolium perenne) to aluminium treatment in terms of the induction of a spectrum of SOD genes.

1.2 Aluminium Toxicity and the Acid Soil Syndrome

1.2.1 Formation of Acidic Soils

Acidic soils are those with a pH of <5.5 and represent up to 30-40% of arable soils globally (Pan et al., 2001; Tamas et al., 2001; Simonovicova et al., 2004; Poozesh et al., 2007). These soils represent a major limitation to world-wide agriculture as a number of elite pasture species cannot tolerate growing in low pH soil (Basu et al., 2001).

Each year the area of acidic soils gradually increases due to industrial and agricultural practices which affect soil pH. Examples of industrial practices include the phenomenon of acid rain and the environmental pollution caused by aluminium smelters which elevate the possibility of acid rain (Zhang et al., 2007). The increased use of nitrogen-based fertilizers is also seriously affecting soil pH as part of poor agricultural management practices. Such fertilizers are applied to meet the needs of the plant for certain elements, but if applied routinely, they cause a build-up of nitric acid in soils leading to a drop in soil pH (Whitehead, 2000; Cruz et al., 2006). Nitrification caused by such fertilizer applications causes displacement of cations and a build up of nitric acid which leads to further acidification of soils (Whitehead, 2000; Fukuda et al., 2007).

Although liming causes the soil pH to be elevated to alleviate acidic conditions, it is an expensive option for small farmers (Rangel et al., 2007; Scott et al., 2008).

In New Zealand, areas surrounding the central North Island which were active forestry regions (*Pinus radiata*) and sheep/beef agricultural systems have now reverted to dairying and this has resulted in intensive inputs of N-based fertilizers into the soil. At present, the dairying boom currently seen in New Zealand could be accompanied by a potential increase in acidic soils around the country (Siegel, 2002; Dominguez-Valdivia et al., 2008; Whitcombe et al., 2008).

1.2.2 Aluminium and Acidic Soils

Aluminium is an essential micronutrient for plants and is the most abundant metal in the earth's crust, comprising up to 7% of its mass (Pan et al., 2001; Matsumoto, 2002; Epstein & Bloom, 2005). Normally, aluminium exists as insoluble aluminosilicates or oxides under neutral or alkaline pH conditions but its speciation changes in response to acidity (Tamas et al., 2005; Zheng & Yang, 2005). At pH 5.0 or lower, aluminium is solubilised into its phytotoxic form Al^{3+} (known as the octahedral hexahydrate, $Al(H_2O)_6^{3+}$) (Kochian, 1995; Matsumoto, 2002; Zheng & Yang, 2005). The adverse effects of acidic soils on plant health have been shown to be directly correlated with concentrations of Al ions in the soil substrate (Jones et al., 2006; Fukada et al., 2007).

Some soils are naturally acidic due to parental rock makeup and weathering processes which release previously bound metal ions such as aluminium (Siegel, 2002) and increase the concentration of toxic Al^{3+} ions in the soil solution (Ryan et al., 2009). Aluminium ions (Al^{3+}) accumulate in the soil substrate to phytotoxic concentrations in a process known as the 'Acid Soil Syndrome'. This syndrome results in aluminium and other metals such as iron and manganese accumulating under acidic conditions from previously bound forms (Kochian et al., 2004). Plants that grow in such regions have evolved tolerance strategies to alleviate the toxicity of heavy metals.

In contrast, poor agricultural processes that can lead to a reduction in soil pH could have dire consequences for agriculture in New Zealand as a number of elite pasture species are thought to be sensitive to Al-toxicity (Whitcombe et al., 2008). Acid soils of tropical

and sub-tropical countries that produce a number of staple food products (i.e. rice) have found Al-toxicity to be a major constraint (Meriga et al., 2003; Scott et al., 2008; Sharma et al., 2007; Liu et al., 2009). Such toxicity in relation to aluminium cations causes differential responses in a number of plant species with certain genotypes also varying widely in their ability to grow and yield on acid soils (Ryan et al., 2009).

1.2.3 Aluminium Toxicity

Aluminium toxicity has been implicated in crop yield reduction from as early as 1918 when barley (*Hordeum vulgare*) and rye (*Secale cereale*) crops exhibited decreased productivity on acid soils (Zheng & Yang, 2005). Since that time, aluminium has been viewed as a very important growth limiting factor at even micromolar concentrations (Tamas et al., 2005; Zheng & Yang, 2005; Poozesh et al., 2007).

Toxicity results in a rapid inhibition of root growth, beginning in a matter of a few minutes under lab conditions (Jones et al., 2006; Sun et al., 2007; Mimmo et al., 2009; Zhou et al., 2009). This inhibition causes the root system to become damaged, limiting both nutrient and water uptake to the plant (Jones et al., 2006; Poozesh et al., 2007; Zhang et al., 2007). The signs of root systems suffering from aluminium toxicity include stunted root growth, reduction in root hair development and swollen root apices (Matsumoto, 2002). Following these root symptoms, signaling occurs from the roots to the shoots, and the vegetative tissues eventually also show toxicity symptoms as observed in rice seedlings cultivated in a full nutrient solution treated with 80 and 160 µM of $Al_2(SO)_4$ (Sharma & Dubey, 2007).

At the tissue level, the root apex is observed to be the most affected by aluminium toxicity (Zheng & Yang, 2005). Regions of the root apex, including the distal transition, apical elongation and meristematic zones, have been observed to show detrimental effects when the roots are exposed to high aluminium concentrations experiments, including, but not limited to, reduced cell division and elongation as well as abnormal cellular division. (Rangel et al., 2007; Achary et al., 2008; Giannakoula et al., 2008; Mimmo et al., 2009). Rangel et al., (2007) identified the elongation zone and also the transition zone as major sites of Al damage by applying agarose blocks loaded with 200 µM Al in the form of $AlCl_3$ to these zones in *Phaseolus vulgaris.*

During early research into the symptoms of aluminium toxicity, it was believed that cell division was the primary cause of injury (Taylor & Foy, 1985; Richards et al., 1998; Pintro et al., 1998). Taylor & Foy (1985) identified a decrease in cell division in root tissue while working on mechanisms of aluminium tolerance in wheat cultivars (*Triticum aestivum*) treated with 74 µM Al supplied as $AlK(SO_4)_2$, while Pintro et al. (1998) observed a decrease in cell division in root tissue of Al-sensitive varieties of *Zea mays* that were treated with 10.3 µM of $AlCl_3$. This theory has been strongly refuted recently and now there is strong evidence that inhibition of cell elongation is the main cause of aluminium injury (Zheng & Yang, 2005). This is because cell division is a relatively slow process while cell elongation has been observed to decrease in as little as 30 min after treatment in some species (Furukawa et al., 2007; Rangel et al., 2007; Zhang et al., 2007; Zhen et al., 2007).

Further research at the cellular level has pinpointed a number of sub-cellular structures that are affected by aluminium toxicity including the plasma membrane, cell walls, cytoskeleton and nucleus (Achary et al., 2008). At a molecular level, evidence points to aluminium (Al^{3+}) showing strong binding affinities to a number of oxygen donor ligands including nucleic acids and phospholipids, eventually resulting in a reduction of cell extension and elongation (Kochian et al., 2004; Zheng & Yang, 2005; Achary et al., 2008; Yang et al., 2008). In one such study by Achary et al. (2008), comet assays (an assay for DNA damage) were carried out on root cells of *Allium cepa* (onion) after treatment with 50 µM aluminium added as $AlCl_3$.

Pan et al (2001) studied the effect of a range of aluminium concentrations (0.1-50mM) on the inhibition of root growth in barley and found that a number of root tip cells had lost viability due to cell death at concentrations as low of 0.1 µM. This result was subsequently studied by Achary et al (2008) who observed that even under micromolar concentrations (10-200 µM) of $AlCl_3$, DNA damage occurred that finally resulted in root cell death. Cell death in relation to increased oxidative stress induced by aluminium toxicity has also been shown to be correlated with, but is only one factor underlying cell death by Meriga et al. (2004), Simonovicova et al. (2004) and Tamas et al. (2005).

Signal transduction pathways are also negatively affected by aluminium toxicity, as the plasma membrane can be affected by the metal binding with the lipid components (causing rigidification), and so ion fluxes can be altered (Jones et al., 2006; Ali et al., 2008; Giannakoula et al., 2008; Zhou et al., 2009).

As aluminium toxicity results in substantial stress to plants, a number of defensive mechanisms are induced to control these negative effects. A major effect is that the toxicity results in a high number of reactive oxygen species accumulating (which is common to any plant stress) resulting in the process termed oxidative stress (Morgan et al., 2008). Consequently, a series of cellular changes are induced to alleviate the affects of oxidative stress (collectively termed the antioxidant pathway). An overview of the accumulation of ROS and the detoxification of these compounds is shown in Figure 1.1.

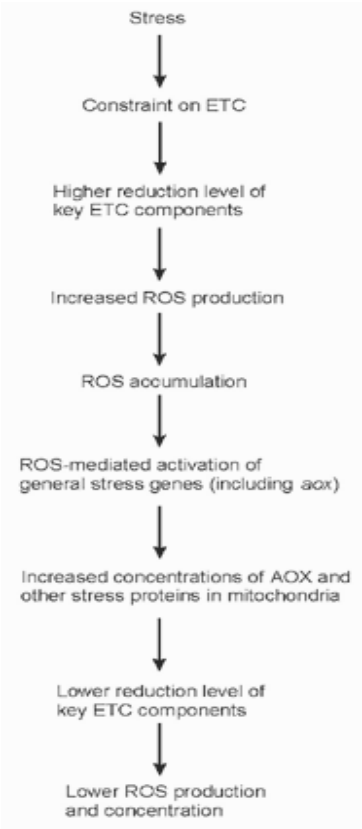

Figure 1.1. Flow diagram of how Al-toxicity can result in oxidative stress. This model represents plant mitochondria (ETC – Electron Transport Chain, AOX – Antioxidant Genes)

1.3 Formation of ROS and Oxidative Stress

Like all aerobic organisms, plants have evolved in the presence of oxygen and have developed metabolic pathways to utilize its energetic potential (Navrot et al., 2007). One potentially damaging effect of this facet is the deleterious production of reactive oxygen species (ROS) that are produced during normal respiration, photosynthesis and nitrogen fixation (Bowler et al., 1992; Dalton, 1995).

Oxidative stress develops when a shift in balance between ROS (oxidants) and the antioxidant pathway occurs. Inhibition of the antioxidant pathway or an accumulation of ROS overcomes the antioxidant pathway leading to oxidative stress and cellular injury (Mates, 2000; Prasad, 2004).

Due to ROS having a highly transient nature and high chemical reactivity, a number of degradative changes occur quickly. Proteins undergo oxidation and degradation while lipids may undergo peroxidation (Mates, 2000; Navrot et al., 2007). Peroxidation of essential membrane lipids is a result of ROS reacting with unsaturated fatty acids in the plasma membrane (Basu et al., 2001).

ROS are generated under any plant stress, whether it is pathogen attack, salinity or drought (Simonovicova et al., 2004). In common with this, aluminium toxicity is also known to trigger the production of ROS through the activation of various enzymatic and non-enzymatic reactions (Wang et al., 2009; Zhou et al., 2009). Common ROS include hydroxyl radicals, hydrogen peroxide, nitric oxide and the superoxide anion. Most of these superoxide radicals are formed during normal cellular reactions and occur due to misdirection of electrons which are then donated to oxygen (Mates, 2000; Bowler et al., 1992; Navrot et al., 2007). For instance, Dalton (1995) and Bowler et al. (1992) outline the formation of superoxide anions in plant mitochondria as shown in Equation 1.1.

$$\mathbf{O_2 + 4e + 4H^+ \rightarrow 2H_2O}$$

Equation 1.1 : Reduction of O_2 catalysed by cytochrome oxidase. NADH dehydrogenase may produce O_2^- from this reaction by misdirecting electrons

Usually this reaction is catalysed by cytochrome oxidase which is efficient at the reduction without producing intermediates such as superoxide anions or hydrogen peroxide. However, other components of the electron transport chain are not so efficient such as NADH dehydrogenases which directly reduce oxygen to superoxide anions (Dalton, 1995; Bowler et al., 1992).

Electron leakages, like those set out above, are believed to be enhanced by the presence of heavy metals resulting in an accumulation of ROS such as the superoxide anion (Prasad, 2004). In animal systems, studies have shown that rat kidney mitochondria incubated in mercuric ions form four times as much hydrogen peroxide (when compared to the control), which suggests some impairment of the respiratory chain electron transport (Mates, 2000; Prasad, 2004).

Meriga et al (2004) were able to show that aluminium increased the production of a number of ROS which resulted in increased amounts of lipid peroxidation and DNA damage in rice seedlings (*Oryza sativa*). Seedlings were grown in plastic containers containing 80 µmol/L of external Al supply in a Yoshida culture solution and harvested at different time points (maximum lipid peroxidation was seen after 56 hrs). Simonovicova et al (2004) also concluded that aluminium treatment induced ROS production by analyzing enhanced hydrogen peroxide levels in relation to cell death in barley (*Hordeum vulgare*) and observed that H_2O_2 production was highly elevated in as little as 48 hours after treatment with 2mM $AlCl_3$.

Achary et al (2008) also related oxidative stress to aluminium in a dose responsive manner. Onion (*Allium cepa*) bulb roots were subjected to varying concentrations of aluminium (0-200 µM) with results showing an increase in the amount of ROS forming in response to increased aluminium concentration. The increased aluminium caused DNA damage (as determined by the comet assay) and cell death in root cells which conformed to a dose-response manner. Further research on other elements including cadmium, chromium and nitrogen toxicity have also shown that plants react in much the same way by the induction of ROS and subsequent damage (Vitoria et al., 2001; Liu et al., 2007; Dominguez-Valdivia et al., 2008; Rodrıguez-Serrano et al., 2009).

1.3.1 The Antioxidant Pathway

Avoidance of the production of ROS would be considered to be the first line of defence against their harmful effects but this step can only be limited, not avoided. Therefore aerobic organisms such as plants contain systems which can control and detoxify ROS, thus limiting toxic effects (Gratao et al., 2006).

The term antioxidant describes any compound that is able to detoxify ROS without itself undergoing conversion to a harmful radical. Antioxidant enzymes are involved in either processing ROS or catalyzing the reactions that take place in an effort to reduce harmful radicals (Asada, 1994; Gratao et al., 2006). Although the antioxidant pathway has the same end goal, it consists of both enzymic and non-enzymic components.

1.3.1.1 Antioxidant Pathway – The non-enzymic system

The plant non-enzymic antioxidant system consists of relatively high levels of ascorbate, glutathione (GSH), α-tocopherol and a number of other smaller non-enzymic antioxidants. Both are relatively important in the antioxidant pathway but the levels of these compounds must be tightly controlled, as cells with enhanced GSH levels have been shown to experience oxidative stress due to changes in the overall redox state in chloroplasts (O'Brien et al., 2004; Ruley et al., 2004; Gratao et al., 2006). All three named non-enzymic components (above) are responsible for detoxification of $^1O_2$ and OH ROS (Sharma & Dubey, 2007).

1.3.1.2 Antioxidant Pathway – The enzymic system

The major ROS scavenging enzymes involved in the antioxidant pathway in plants include superoxide dismutase (SOD), catalase (CAT), guaiacol peroxidase (GOPX), ascorbate peroxidase (APX), dehydroascorbate reductase (GR), monodehydrateascorbate reductase (MDHAR), glutathione reductase (GR) and glutathione peroxidase (GPX) (Boscolo et al., 2003; Kuo & Kao, 2003; Polesskaya et al., 2004; Ruley et al., 2004; Simonovicova et al., 2004). These enzymes combine with the non-enzymic components to detoxify ROS to oxygen and water using ascorbate, reduced glutathione and NADPH as electron donors (Gupta et al., 1993; Ezaki et al.,

2004). ROS undergo a series of oxidation/reduction reactions in what as known as the Halliwell-Asada pathway (Fig 1.2) (Gratao et al., 2006).

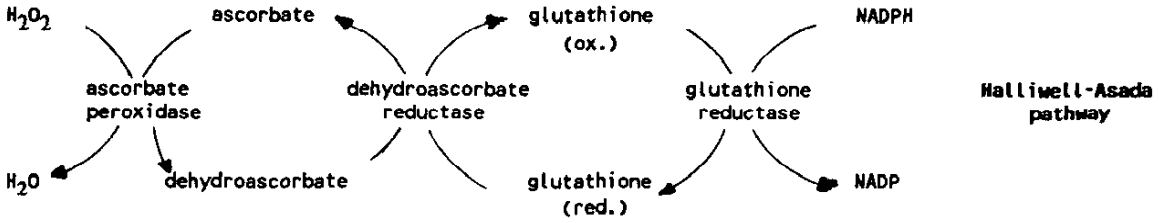

Figure 1 The Halliwell-Asada pathway.

Figure 1.2 – The Halliwell-Asada pathway describes components of the antioxidant pathway that are catalysed in concert

The first antioxidant enzyme to be covered is of great importance. SOD is primarily the first line of defence in detoxifying the superoxide anion (O_2^-), as it is removed by converting it to hydrogen peroxide (H_2O_2) and oxygen in the reaction:

$$\mathbf{2O_2^- + 2H^+ \rightarrow H_2O_2 + O_2}$$

Equation 1.2 : SOD catalysed reaction showing formation of hydrogen peroxide (H_2O_2) and oxygen (O_2) from superoxide anions (O_2^-)

This enzyme is unique as its activity determines the concentrations of O_2^- and H_2O_2 and is therefore central to the antioxidant pathway defence response (Bowler et al., 1992; Guo et al., 2006). SOD will be discussed in detail later in this introduction (refer to section 1.4).

Hydrogen peroxide, or the product of the SOD reaction, then undergoes a series of successive reactions to produce water and oxygen as end-products. This is mainly achieved by the activity of catalase (CAT) and guaiacol peroxidase (GOPX). Hydrogen peroxide is directly eliminated by CAT in peroxisomes and by GOPX in the cytosol, vacuole and other extracellular spaces (Boscolo et al., 2003; Sharma & Dubey, 2007; Dominguez-Valdivia et al., 2008).

CAT has an extremely high catalytic rate, but low substrate affinity and is abundant in peroxisomes. It is also thought to have another important role in protecting SOD against inactivation by high levels of H_2O_2 (Gratao et al., 2006). Depending on the plant species, isoenzymes (as distinct genes) of CAT can differ in number, from two in barley to as many as twelve in mustard (Gratao et al., 2006). Variability in CAT activity has been observed since the antioxidant pathway has been studied in relation to environmental stresses. Achary et al (2008) found that aluminium stress caused an inhibition of CAT activity in *Allium cepa*, while Kuo & Kao (2003) observed an increase in CAT activity in relation to aluminium stress in *Oryza sativa* where detached rice leaves treated with 5mM $AlCl_3$ induced a higher activity of CAT when compared with the control.

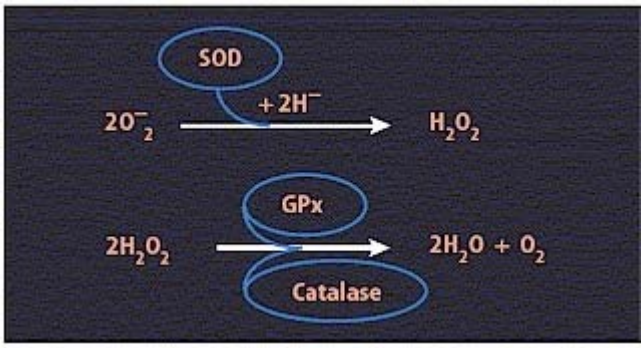

Figure 1.3. Inactivation of the superoxide anion by antioxidant components. SOD firstly converts it to H_2O_2, which is then converted to H_2O and O_2 by the other antioxidant pathway components

Ascorbate peroxidase (APX) uses ascorbate as a substrate for the removal of H_2O_2 from plant cells. The APX protein family consists of at least five different isoforms which include apoplastic and thylakoid forms (Gratao et al., 2006; Morgan et al., 2008). Sharma & Dubey (2007) found significant increases in APX enzyme activity in rice seedlings when exposed to toxic levels (100mM) of aluminium. Conclusive evidence for the induction of this enzyme in relation to aluminium is also well documented by other workers (Kuo & Kao, 2003; Meriga et al., 2004; Simonovicova et al., 2004; Achary et al., 2008).

Guaiacol Peroxidase (GOPX) can be distinguished from APX when isolated from plant systems. Differences exist in the amino acid sequence and also physiological function. A number of elements at toxic levels are able to induce the activity of GOPX significantly such as cadmium, nitrogen and lead (Polesskaya et al., 2004; Ruley et al., 2004; Guo et al., 2006). Enhancement of the enzyme activity also increases significantly under aluminium stress (Boscolo et al., 2003; Simonovicova et al., 2004).

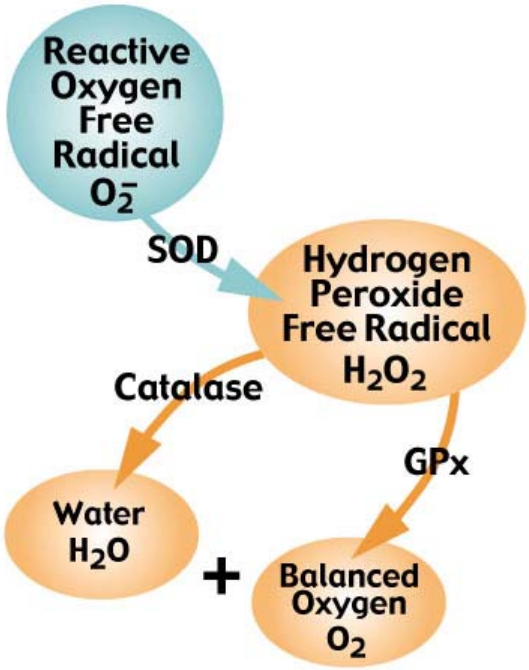

Figure 1.4. Diagrammatic representation of how the antioxidant system in plants detoxify ROS

1.4 Superoxide Dismutase (SOD)

SOD was first isolated in 1938 from bovine blood and was originally thought to be involved in copper storage. It was originally referred to as indophenol oxidase, tetrazolium oxidase and erythrocuprein until its catalytic function was discovered by McCord and Fridovich in 1969 (cited in Bowler et al., 1992; Gratao et al., 2006).

The importance of SOD is in the activity of the enzyme which reacts with superoxide anions (O_2^-) in a disproportionation reaction (one molecule which is oxidized while another identical molecule is reduced) to form hydrogen peroxide and oxygen in the reaction shown as equation 1.3:

$$\mathbf{2O_2^- + 2H^+ \rightarrow H_2O_2 + O_2}$$

Equation 1.3 : SOD catalysed reaction showing formation of hydrogen peroxide (H_2O_2) and oxygen (O_2) from superoxide anions (O_2^-)

In plants this reaction is constitutive, albeit occurring at a very slow rate, but can be catalysed at accelerated levels and is thus an important line of defence during times of stress when ROS levels substantially increase (Dalton, 1995; Prasad, 2004; Corpas et al., 2006; Gratao et al., 2006).

As a family of metalloenzymes, SOD exists in three forms (designated as isoenzymes) that is dependent on the metal co-factor; Cu/Zn SOD, MnSOD, and FeSOD. All three function with high similarity (which is to detoxify superoxide anions) but are found in different cellular compartments inside plants (Van Camp et al., 1994; Morgan et al., 2008). All SOD's are nuclear encoded with N-terminal sequences directing transport to various organelles but only the FeSOD and MnSOD enzymes are structurally similar, with the Cu/ZnSOD structurally unrelated (Bowler et al., 1992). Cu/Zn SOD is commonly found in the cytosol, MnSOD in the mitochondria and FeSOD in chloroplasts, although differences have been observed for example MnSOD has been associated with chloroplasts (Gratao et al., 2006).

Due to the importance of SOD in aerobic organisms, a number of aspects have been analysed which include biochemical and molecular properties, structure, expression and phylogenetic distribution (Corpas et al., 2006). Dalton (1995) and Gratao et al (2006) have documented the structure and mass of each isoform. Cu/Zn SODs isolated from *Pisum*, *Phaseolus* and *Zea* exist as a dimer with a molecular mass of 31-33 kD, and MnSOD as a tetramer with a molecular mass of 90kD (Dalton, 1995; Gratao et al., 2006).

The use of electrophoresis allows each SOD isoform to be isolated and detected due to their metal co-factor and relative molecular masses (Dalton, 1995; Prasad, 2004). Further, the use of specific inhibitors allows for easy detection as specific isoenzymeactivity as cyanide (KCN) and H_2O_2 react differently to each form. Cu/Zn SOD is sensitive to both treatments, MnSOD is resistant to both, and FeSOD is sensitive to H_2O_2 only (Del Rio et al., 1985; Bowler et al., 1992; Murao et al., 2004).

Both FeSOD and MnSOD in plants are structurally similar and have other chemically similar characteristics while sequence data suggests that the three types of SOD fall into distinct phylogenetic families. It is believed that FeSOD and MnSOD may have evolved from a common ancestor while Cu/Zn SOD evolved recently and independently (Bowler et al., 1994; Prasad, 2004; Murao et al., 2004; Corpas et al., 2006; Gratao et al., 2006).

Further analysis into the proportion of each SOD in plant tissue has been carried out in olive (*Olea europaea*) (Corpas et al., 2006). All three isozymes were characterized by expression analysis showing Cu/Zn SOD, FeSOD and MnSOD resulting in 82, 17 and 0.8% of SOD expression respectively in whole leaves analysed but it was unclear whether one gene per isoform was responsible for this expressed ratio. This result is commonly observed in other plants, where Cu/Zn SOD contributes greatly to total SOD expression in a number of tissues but expression of the three isoenzymes differs in relation to species and also age. (Corpas et al., 2006). Further analysis has shown that isozyme proportions differed in cell tissues i.e. FeSOD was most abundant in palisade mesophyll cells (Corpas et al., 2006).

Research such as Corpas et al (2006) has provided insights into the complexity of the SOD gene family and its evolutionary nature. Depending on the plant species, environmental conditions and plant age, the spectrum of isoenzyme present and the number of genes coding each isoenzyme can differ. For example, sunflower has only one isoform, a Cu/Zn SOD while eight SOD genes comprising all three forms of SOD have been identified in *Arabidopsis thaliana.* This shows the variety that can be produced (some plants may contain one isoenzyme with one gene encoding that form while others such as *Arabidopsis* have eight genes encoding the SOD isoenzymes) (Corpas et al., 2006; Morgan et al., 2008).

1.4.1 Aluminium Toxicity and SOD Expression

Research into the induction of SOD gene expression in relation to each of the isoforms has yet to be carried out to the best of my knowledge in *Lolium perenne* in respect to aluminium toxicity. To date, research on total SOD expression has been carried out on a number of staple food varieties such as onion and rice.

For example, Sharma & Dubey (2007) raised rice seedlings in sand cultures containing a medium of 160µM of the Al^{3+} ion ($AlCl_3$) which resulted in increased levels of H_2O_2 and O_2^-. To combat oxidative stress, increases in levels of antioxidative components followed, with significant increases in SOD expression activity (total expression is that which includes all three isoenzymes). Interestingly, Kuo & Kao (2003) who used detached rice leaves treated with 5mM $AlCl_3$, found total SOD expression activity was reduced.

Simonovicova et al (2004) studied the effect of aluminium stress in barley roots and observed a high correlation in induced total SOD expression activity and root length inhibition. Their work appeared to show that SOD is involved intimately with detoxification of aluminium at toxic levels by reducing the impact of ROS by its conversion to hydrogen peroxide (Simonovicova et al., 2004).

Research into aluminium stress and SOD enzyme activity in other plant species (rice, maize, onion) further provides evidence that SOD enzyme activity is induced and

involved in detoxifying ROS that are generated by aluminium toxicity (Boscolo et al., 2003; Meriga et al., 2004; Achary et al. 2008; Zhou et al., 2009).

1.5 Genetic Engineering of plants with SOD genes

The over expression of SOD genes in transgenic plants to ameliorate aluminium toxicity has resulted in a number of contrasting results over the last two decades (O'Brien et al., 2004). Basu et al (2001) isolated a wheat cDNA coding for a MnSOD isoenzyme, and under the control of the CaMV35S promoter this was expressed in *Brassica napus* and the transformants exhibited enhanced total SOD enzyme activity. When stressed with aluminium, leaf disks exhibited reduced electrolyte leakage and reduced inhibition of root growth (Basu et al., 2001). Gupta et al (1993) also over expressed a chloroplast localized Cu/Zn SOD gene which resulted in increased resistance to chilling and high light intensity when compared to controls.

Bowler et al (1992) and Van Camp et al (1994) provide contrasting views when over-expression of a Cu/Zn SOD gene in wheat and barley did not significantly alter resistance to cadmium stress. Both authors suggest a possible increase in H_2O_2 could cause further oxidative stress and suggested over-expression of further antioxidant components to increase resistance. Thus the future of breeding programmes designed to ameliorate the effect of aluminium toxicity on pasture species revolves around the discovery of key genes in the antioxidant pathway and genes involved in detoxification (Bowler et al., 1992; Van Camp et al., 1994; Sawaki et al., 2009).

1.6 *Lolium perenne* c.v Nui

Cultivar Nui is a New Zealand variety that was released in 1962 by DSIR Grasslands and showed favourable traits for the agricultural market (Seawright, 2005). Of importance to this study is the ability of the cultivar to thrive best on soils with a pH between 5.5 and 7.5 (Sartie, 2006). Al-toxicity in *Lolium perenne* and its response has not been well documented.

Perennial ryegrass (*Lolium perenne*) cultivar Grasslands Nui, accession number A11106 (AgResearch Grasslands, Palmerston North, New Zealand) was used for this study. It is a member of the family Gramineae, sub-family Poeideae within the tribe Poeae. Perennial ryegrass is favoured as a forage crop due to its pasture persistence, palatability and ability to withstand high grazing intensity.

1.7 Aim (s) and Hypothesis of Current Research

High use of N-based fertilizers in New Zealand is affecting soil acidity. In turn, this acidity gives rise to the 'acid soil syndrome' where phytotoxic levels of aluminium accumulate in pasture. This results in oxidative stress to species such as *Lolium perenne* and (as postulated) induction of the antioxidant system including the SOD system in response to Al-toxicity.

Hypothesis

That there are associated SOD isoenzymes that have a high correlation with aluminium stress in *Lolium perenne*. Although constitutively present, the expression of one or more of the genes encoding these isoenzymes will be further enhanced in response to aluminium treatment.

Aims

- Using degenerate primers and RT-PCR to clone at least one gene for each of the three SOD isoenzymes (if all three exist) in *L.perenne* c.v Nui.

- Analyse the expression of all genes isolated that code for each isoenzyme in terms of up- or down-regulation in response to Al-treatment

1.8 Note on nomenclature

For the purposes of this thesis, the SOD enzyme system is divided into three isoenzymes (isoforms and isoenzymes are terms used synonymously) designated Cu/ZnSOD, FeSOD and MnSOD. Each isoenzyme may further be coded by a single gene product, or comprise a multi-gene family (so increasing the number of isoenzymes that can be designated as either a Cu/ZnSOD, FeSOD or MnSOD isoenzyme).

It is accepted that post-translational modifications can introduce a tier of heterogeneity to a single isoenzyme, but this level of processing was not examined in this thesis.

2. Methods and Materials

2.1 Propagation

2.1.0 Germination and Establishment of Ryegrass Seedlings

Seeds of *Lolium perenne* c.v Nui were pre-sterilised by washing in 1 % bleach solution (sodium hypochlorite 4% (v/v)) for 5 min in 50 mL falcon tubes, then transferred to sterile MQ water. This was repeated three times in succession. To ensure sterile conditions were met for germination, autoclaved Whatman paper (No. 42) was used to line the bottom of sterile petri plates. Twenty-five seeds were placed on the Whatman paper which was kept moist by the addition of sterile MQ water during seed germination. To promote germination, the sterile Petri dishes were incubated in a growth hood under continuous lighting (85 µmol photons m^{-2} s^{-1}) at 21ºC. Germinated ten-day old seedlings were then transferred to pottles (250 mL capacity) at a rate of ten seedlings per pottle. Seedlings were kept under continuous light (85 µmol photons m^{-2} s^{-1}) at 21ºC until a sufficient root system had developed (> 2cm). These seedlings remained at 21°C throughout germination which ranged from 13 days to 15 days (first hydroponic trial seedlings remained under lighting for 13 days while in the second trial, seedlings remained under lighting for 15 days) before being transferred to the hydroponic system.

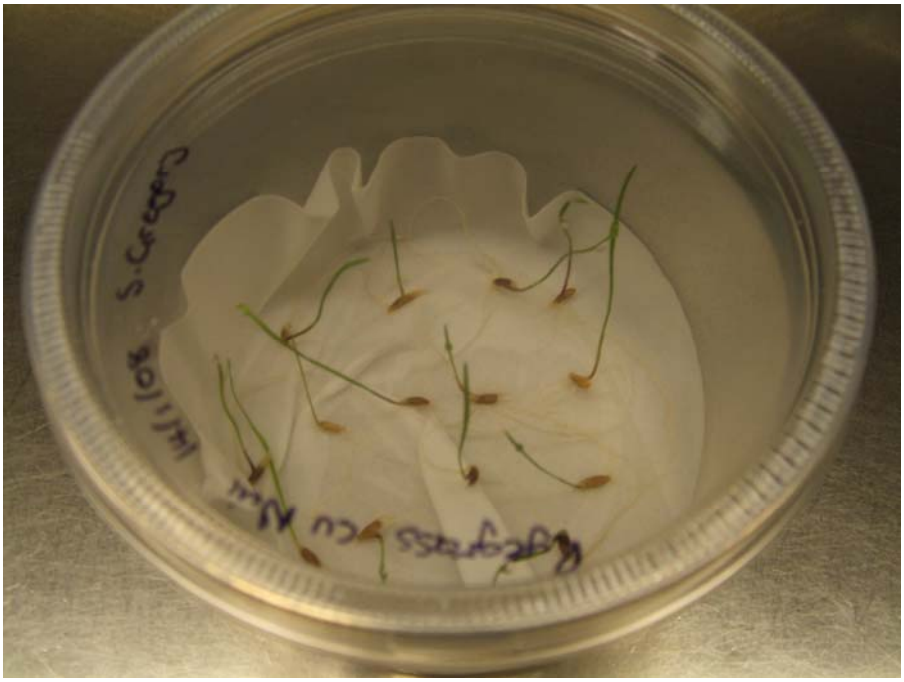

Figure 2.1. *L. perenne* germinated seedlings under sterile conditions. Seedlings are maintained on moist sterile Whatman paper, with 10 seedlings per pottle, and incubated at 21ºC.

2.2 Hydroponics and Aluminium Treatment

2.2.1 Establishment of the hydroponic growth system

Seedlings of sufficient age (section 2.10) were inserted into pre-formed holes in a polystyrene tray, and held in place using foam inserts. The tray was placed over Hoagland's media in a 20-L capacity container with the media covering the protruding roots below the polystyrene tray (Figure 2.2). The Hoagland's solution (Table 2.1) consisted of one-third strength macronutrients and full strength micronutrients to maintain a low osmotic pressure as well as to avoid possible ion toxicity and adverse interactions of certain nutrients (Gibeaut et al., 1997). An air pump was placed into the plastic container to facilitate continuous element availability and for aeration of Hoagland's solution. Natural light conditions for the summer period (13 hr daylight / 11 hr night) were observed (artificial lighting conditions were not used) and the room kept at a constant temperature of 24 °C.

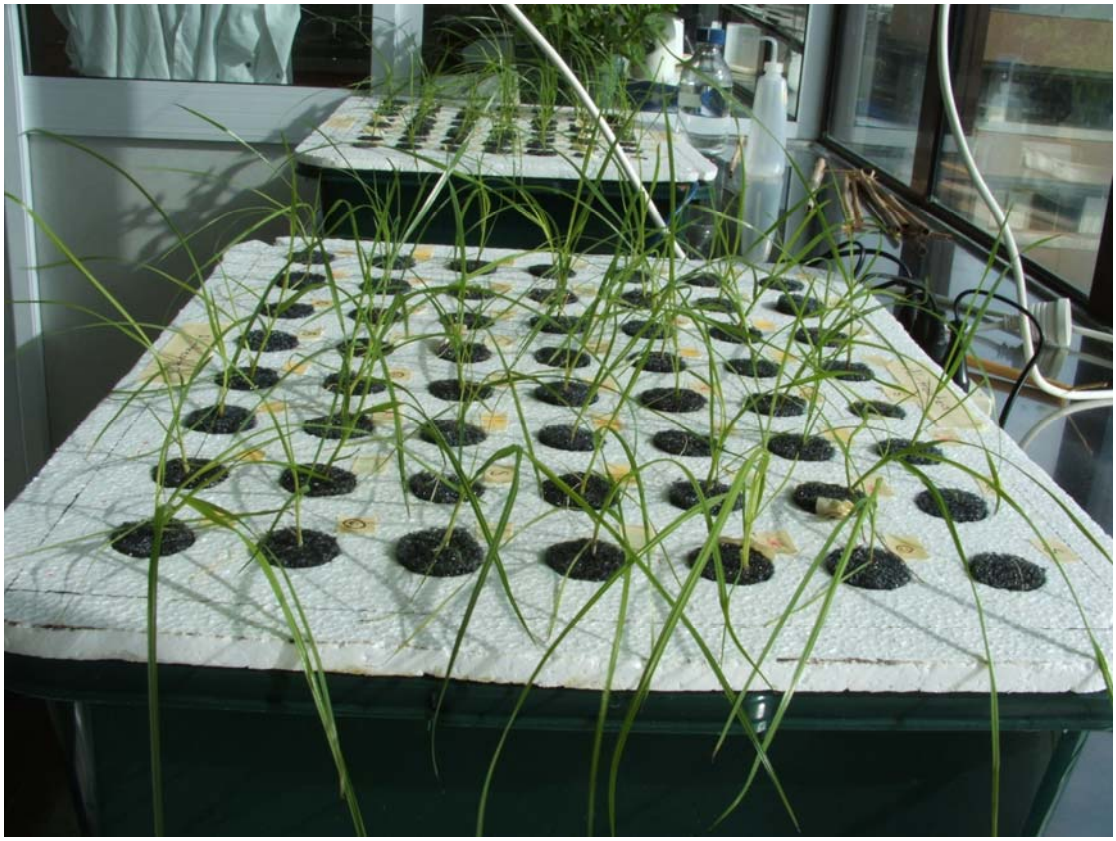

Figure 2.2. Control and Al-treated containers. *L.perenne* seedlings are held in place with foam inserts over a 20 L capacity container holding a modified Hoagland's solution, Table 2.1.

Table 2.1. Composition of the Hoagland solution with one-third strength macro and full strength micronutrients (Gibeaut et al., 1997)

A. Macronutrients	Working concentration (mM)	Weight (g) per litre of 10x stock solution
KNO_3	1.25	1.264
$Ca(NO_3)_2$	1.50	3.543
$MgSO_4$	0.75	1.849
KH_2PO_4	1.00	1.360

B. Micronutrients	Working concentration (µM)	Weight (mg) per litre of 100x stock solution
KCl	50.0	372.8
H_3BO_3	50.0	309.2
$MnSO_4$	10.0	151.0
$ZnSO_4$	2.0	57.5
$CuSO_4$	1.5	37.5
$(NH_4)_6Mo_7O_{24}$	0.075	9.30
Na_2O_3Si	0.1	2.10
Fe Na EDTA	72.0	2642.8

Experimental Design

For each experiment, a total of one hundred and twelve seedlings were used in the hydroponic setup with the number divided to obtain fifty-six seedlings per tray (Figure 2.2). These were left until sufficient tissue growth had occurred (18-21 days) for use in RNA extraction. Twelve seedlings were designated for each timepoint (0,4,8,24 h) used for expression analysis. Eight seedlings per tray were set aside as spares in case of poor plant health. All seedlings were placed randomly around the tray using a random number sequence generator (**www.random.org**) to prevent bias in sampling data.

2.2.2 Aluminium Treatment

To ensure that any changes in gene expression observed were due to Al-treatment alone, the pH of the solution was slowly reduced by 0.1 units per day from an original pH of 5.5 with the addition of 2 M HCl and kept constant at pH 4.8. This was carried out before the addition of $AlCl_3$, so as to acclimatise the seedlings to a pH of 4.8 prior to Al-treatment.

Once sufficient tissue growth had occurred (determined by removing a spare seedling, dissecting it into root and shoot tissue followed by weighing then multiplying by the number of remaining seedlings in solution for each time point) one of the containers was treated with a 0.2 M $AlCl_3$ solution to give a final concentration in solution of 0.2 mM $AlCl_3$. The 0hr control time was taken before the addition of the Al solution. After the addition of $AlCl_3$, a stop watch was used to determine the next harvesting point.

2.2.3 Harvesting of Plant Material

Seedlings were removed from the Hoagland's solution and immediately placed on ice-cold paper towels on an ice bucket. All twelve seedlings per time point were sectioned at the root/shoot junction using a razor blade and pooled and weighed (trial I) or individually weighed (trial II). All root and shoot tissues (per time point) were then pooled together and snap frozen in liquid nitrogen in 50 mL falcon tubes and stored at -80°C for RNA extraction.

2.3 Molecular Methods

2.3.0 RNA Extraction

The modified Hot Borate Method as described by Hunter and Reid (2001) was used for the isolation of total RNA, with a few minor changes.

Reagents

- Extraction buffer (Buffer XT) : 0.2 M sodium borate decahydrate containing 0.03 M EGTA, 1.0% (w/v) SDS, 1.0% (w/v) sodium deoxycholate salt, 10 mM DTT, 1.0% (v/v) nonidet P-40 (IGEPAL), and 2% (w/v) polyvinylpyrrolidone-40 (PVP-40)
- Proteinase K : (20mg/mL in DEPC-treated water)
- 2 M KCl
- 0.4 M LiCl

Plant tissue was powdered in liquid nitrogen and added to the warmed extraction buffer (80°C) at a ratio of 5 mL buffer to 1 g tissue powder and the mixture vortexed for 30 s. An aliquot (37.5 µL) of Proteinase K was added per gram fresh weight of tissue and the suspension was incubated, with shaking, at 42°C for 1.5 h. After this period, a 0.08 volume of 2 M KCl was added and the mixture swirled gently on ice for 30 min, centrifuged at 14,000 rpm for 20 min at 4°C and the supernatant transferred to a fresh tube. After carefully determining the volume of the supernatant, one volume of 4 M LiCl was added, the contents mixed gently and the RNA precipitated overnight at 4°C. The following day, the precipitate was collected by centrifugation at 14,000 rpm for 30 min at 4°C. After discarding the supernatant, the remaining LiCl was carefully drained on absorbent paper and the pellet was resuspended in 200 µL of sterile DEPC-treated water and 20 µL of 3 M sodium acetate, pH 5.2 added. The suspension was then pipetted to microfuge tubes, followed by the addition of 200 µL of chloroform/isoamyl alcohol (24:1). After vortexing for 30 s, centrifugation was conducted at 14,000 rpm for 5 min at 4°C, and the upper (aqueous) layer transferred to a fresh microfuge tube. This step was repeated again with the addition of chloroform/isoamyl (24:1) and the use of a fresh microfuge tube. One volume of isopropanol was then added to the upper (aqueous) layer, the solution mixed gently, and then placed on ice for 1 h. The precipitate was then

collected by centrifugation at 14,000 rpm for 30 min at 4°C, the pellet washed with 80% (v/v) ethanol and centrifuged at 14,000 rpm for 10 min to attain a clean pellet. The supernatant was then removed by pipetting and the pellet air dried for 10 min before the addition of 20 µL of DEPC-treated water to suspend the pellet and the samples placed in -80°C for eventual RNA quantification and for use in experiments.

2.3.1 RNA Quantification

RNA was diluted 100-fold (typically) in RNAse-free water, and the absorbance of the dilution measured at 260 nm and 280 nm on an SP8-400 UV/visible spectrophotometer (Pye Unicam) or on an Ultrospec 3000 UV/visible spectrophotometer (Pharmacia Biotech). The quality of the RNA sample was determined by calculating the OD260/D280 ratio, which is equal to 2.0 if the RNA preparation is pure. The concentration of RNA in the undiluted sample was determined as follows:

[RNA] µg μL^{-1} = Abs260nm x 40 µg mL^{-1} / 1000 x DF
The yield of RNA per g of fresh weight tissue was calculated as follows:

RNA yield µg g^{-1} FW = [RNA] µg μL^{-1} x 20 µL / FW g

2.3.2 Reverse transcriptase – Polymerase chain reaction

RT-PCR was conducted using the two-step ThermoScript™ RT-PCR System (Invitrogen) following the manufacturer's instructions. The first step comprised cDNA synthesis from total RNA and the second step constitutes amplification by PCR using the appropriate primers (Table 2.2). For cDNA synthesis, 1 µg of total RNA was routinely used which was combined with 1 µL of 50 µM Oligo $(dT)_{20}$ primer , 2 µL of 10 mM dNTP mix and the volume adjusted to 12 µL with RNase-free water. This combined RNA and primer mix was denatured by incubating at 65°C for 5 min and then placing the solution on ice.

For each reverse transcription reaction, the following components of the reaction mix were added to another tube: 4 µL of the 5x cDNA synthesis buffer, 1 µL of 0.1 M DTT, 1 µL of RNaseOUT™ (40 U/µL), 1 µL of RNase-free water (provided with the kit), and

1 µL of ThermoScript RT (15 U/µL). The mixture was vortexed gently, added into the reaction tube containing the RNA and primer, and incubated at 55°C for 60 min. At the conclusion of this step, the mixture was incubated at 85°C for 5 min to terminate the reaction. To prevent RNA-DNA complex formation, 1 µL of RNase H (provided in the kit) was added and the mixture was incubated at 37°C for 20 min.

For the amplication of the synthesised cDNA, the following components were mixed: 10 µL of PCR Master Mix, 2 µL each of the appropriate forward and reverse primers, 1 µL of the cDNA synthesis reaction and 5 µL of PCR water. The PCR programme setting varied depending on the primers used and the expected PCR product size.

2.3.3 3' RACE (Rapid Amplification of cDNA ends)

3' RACE was carried out as per the manufacturers instructions (Invitrogen). Firstly, RT-PCR was conducted using the two-step ThermoScript™ RT-PCR System (Invitrogen) following the manufacturer's instructions. The first step comprised cDNA synthesis from total RNA and the second step constitutes the amplification by PCR using gene-specific primers (Table 2.2).

For cDNA synthesis, 1 µg of total RNA was routinely used which was combined with 1 µL of 50 µM 3 Race Oligo $(dT)_{20}$ primer (Figure 2.3) , 2 µL of 10 mM dNTP mix and the volume adjusted to 12 µL with RNase-free water. The combined RNA and primer was denatured by incubating at 65°C for 5 min and then placing the solution on ice. cDNA synthesis is then completed as seen in section 2.32.

For the amplication of the synthesised cDNA, the following components were mixed: 10 µL of PCR Master Mix, 2 µL each of the gene-specific forward and universal amplification (UAP) primer as seen in Figure 2.3. One µL of the cDNA synthesis reaction and 5 µL of PCR water were also added. The PCR programme setting varied depending on the primers used and the expected PCR product size. Fig 2.4 details the capture of an unknown 3' untranslated region which is specific to a given gene.

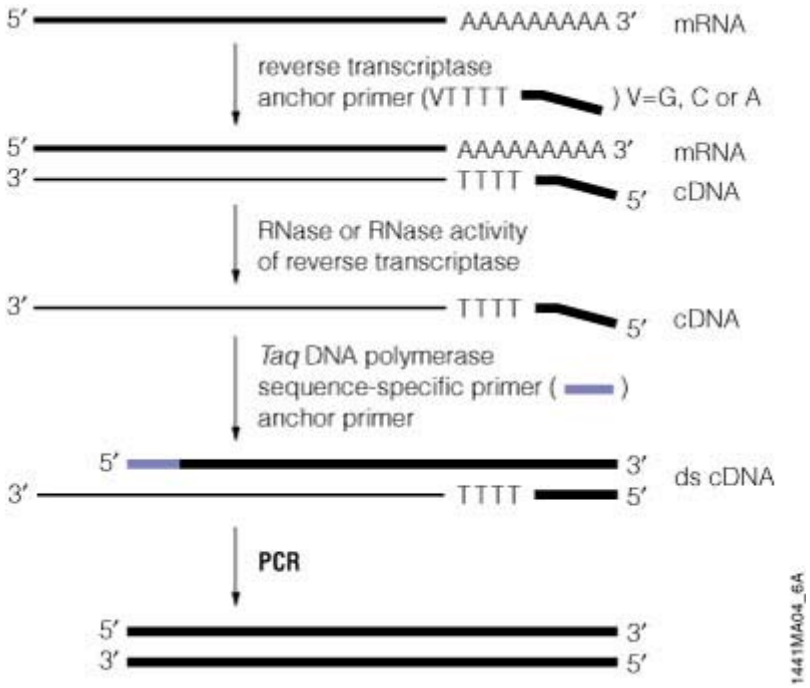

Figure 2.3. Diagrammatic approach to the capture of 3' UTR sequences using the 3' RACE protocol. The 3′-RACE procedure uses an oligo(dT) primer/adaptor as a primer for the reverse transcription reaction. The oligo(dT) primer anneals to the poly(A)+ tail of the mRNA. This oligo(dT) primer/adaptor is also used as the anchor primer in the subsequent amplifications along with a primer complementary to known sequences within the gene (the gene-specific primer)

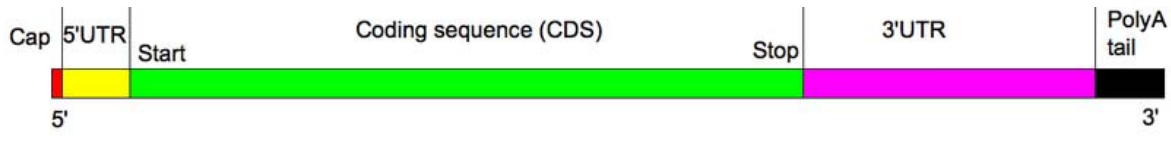

Figure 2.4. Structure of a typical plant protein coding mRNA including the untranslated regions (UTRs). The 3' UTR is a particular domain of messenger RNA (mRNA).

2.3.4 Semi-quantitative RT-PCR expression analysis

Linearity studies were first conducted on each primer set to determine the optimum number of cycles in the PCR reaction. Linearity studies were also conducted on the control primer set (Actin) in both root and shoot tissue. The PCR programme was similar to the RT-PCR reaction (section 2.32) but had slight changes in the amount of cDNA added to each reaction. Preliminary reactions to achieve the same expression intensity per reaction were carried out using Actin which in turn provided the amount of cDNA to be used per time point in both shoot and root samples when examining the expression of specific SOD genes.

2.3.5 Purification of PCR Products

Purification was achieved using the High Purification Kit (Roche Applied Science). After PCR amplification, 40 µL of the product mix was added to 500 µL of Binding Buffer and mixed well in a sterile microfuge tube. This mix was then transferred into the supplied High Pure filter tube and connected to a collection tube. The assembly was then centrifuged at 13,000 rpm for 1 min at 15-25°C and the flowthrough solution discarded. The filter tube was then reconnected with the same collection tube and 500 µL of Wash Buffer then added to the upper reservoir and the assembly centrifuged at 13,000 rpm for 1 min. Again, the flowthrough solution was discarded and the collection tube reconnected to the filter tube. Another 200 µL of Wash Buffer was then added to the upper reservoir and the assembly centrifuged again at 13,000 rpm for 1 min. The filter tube was then connected to a clean 1.5 mL microcentrifuge tube and 100 µL of Elution Buffer added to the upper reservoir. After 1 min (to allow the buffer to absorb into the reservoir) the assembly was then centrifuged for 1 min at 13,000 rpm. The microcentrifuge tube, containing the purified DNA, was then stored at 4°C for later use.

2.3.6 DNA Ligation

DNA ligation was carried out using a 1:3 molar ratio of vector:insert. The molar ratio was calculated using the equation below:

$$\frac{\text{Amount of vector(ng)} \times \text{size of insert (kb)}}{\text{Size of vector (kb)}} \times \text{molar ratio of } \frac{\text{insert}}{\text{vector}} = \text{amount of insert}$$

The ligation reaction was carried out using 1 unit of T4 DNA ligase (Promega, Madison, USA) per 50 ng of vector and the calculated amount of DNA insert, with the appropriate volume of 2x T4 DNA ligation buffer (supplied by the manufacturer). The ligation reaction was made up to a final volume of 10 µL with sterile distilled water and incubated at 25°C overnight.

2.3.7 Preparation of E.coli (strain DH5α) Competent Cells

Cells of the *E.coli* strain, DH5α, (GIBCO BRL) were inoculated from glycerol stocks into 10 mL of LB (Luria-Bertani) broth (1 % (w/v) tryptone, 0.5 % (w/v) yeast extract, 1 % (w/v) NaCl, pH 7.5) and incubated overnight at 37°C, with shaking at 180 rpm. From this overnight culture, 400 µL of broth was transferred to a fresh 40 mL of LB broth and the culture grown for 2-2.5 h at 37°C until the OD_{600} reached approximately 0.40. The cell culture was then poured into a sterile, pre-chilled centrifuge tube and centrifuged at 3000 x g for 5 min at 4°C. The supernatant was then discarded and the pellet gently re-suspended in 10 mL of ice-cold 60mM $CaCl_2$ before an additional 10mL of 60mM $CaCl_2$ was poured into the tube and the mixture incubated on ice for 30 min. After centrifugation for 5 min at 3000 x g at 4°C, the supernatant was poured off and the pellet gently re-suspended in 4 mL of 60mM $CaCl_2$ containing 15 % (v/v) glycerol. Aliquots (300 µL) of the competent cells were then snap frozen in liquid nitrogen and stored at -80°C until required.

2.3.8 Plasmid DNA Transformation Into E.coli (DH5α)

Transformation was achieved using the heat shock method. To do this, competent cells were thawed on ice for 5 min, then 50 µL aliquots were added to 5 µL of ligation reaction (section 2.36), the suspension gently mixed and incubated on ice for 10 min. The suspension was heat shocked at 42°C for 30 s, followed immediately by the addition of 500 µL LB (without antibiotic). The mixture was then incubated at 37°C for 1 h with shaking at 180 rpm. The putative transformed cells (250 µL) were then spread onto LB plates with the appropriate antibiotic (typically 100µg/mL Ampicillin). Prior to this addition of cells (ca. 30min), an aliquot (100 µL) of 100mM IPTG and 20 µL of 50 mg/mL X-gal was applied to the surface of the LB^{Amp100} plates and allowed to absorb at 37°C. The LB^{Amp100} plates with the plated cell suspension were then left for 5 min for the cells to absorb into the agar, the plates then sealed with parafilm and placed in an inverted position and incubated at 37°C overnight.

2.3.9 Selection of Transformants

Successful transformation of an insert into the pGEM-T and pGEM-T Easy Vectors interrupts the coding sequence of β-galactosidase. Therefore colonies produced after incubation on IPTG/X-Gal plates are white or blue, with colonies containing an insert appearing as white. These colonies, along with a few blue colonies, were selected for plasmid isolation sequencing. A fresh LB^{Amp100} plate was then sectioned by drawing grids onto its base to form a grid of 50 squares. Screened colonies were then introduced to each square to allow for growth and incubated overnight at 37°C for eventual sequencing.

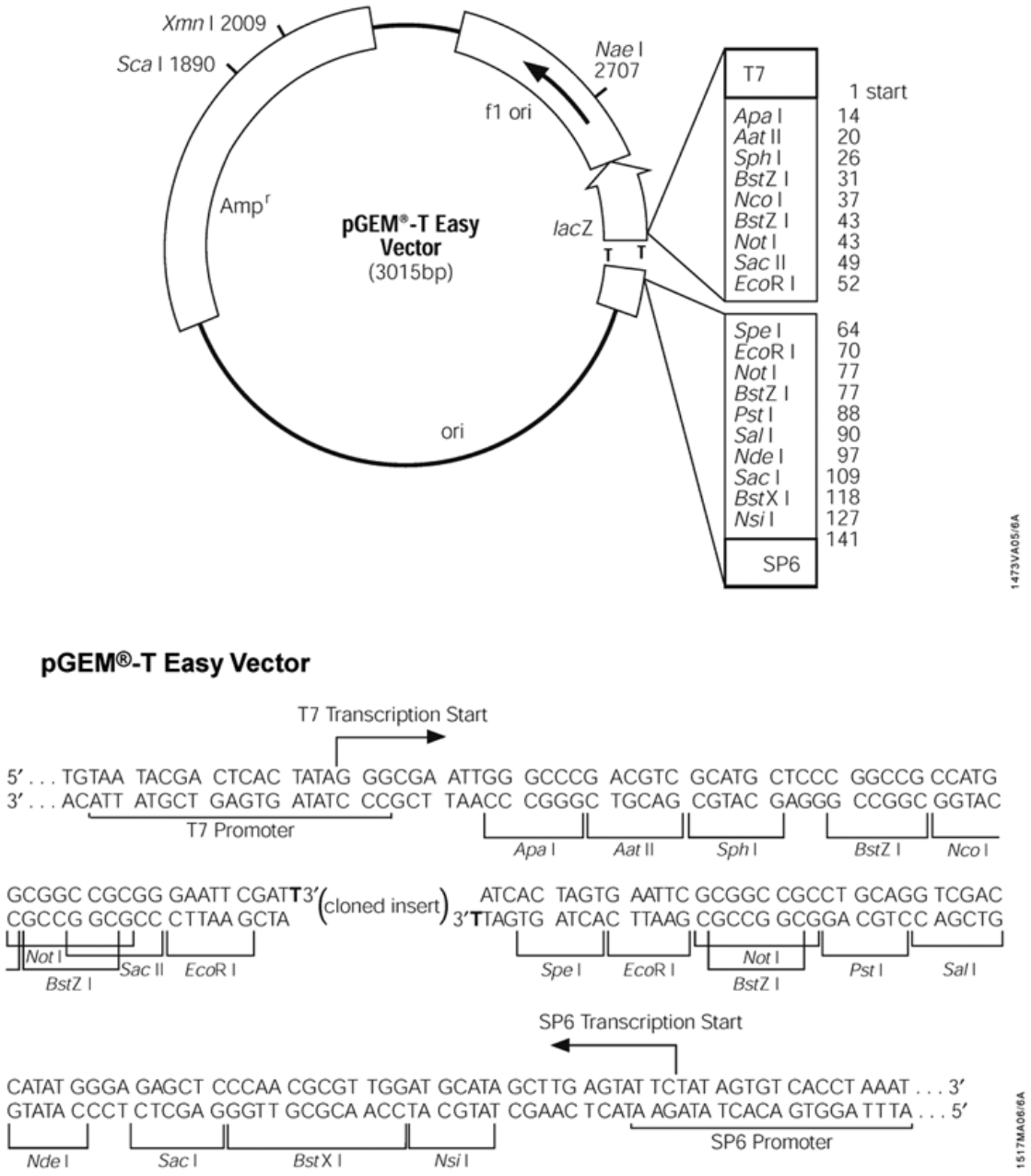

Figure 2.5. pGEM-T Easy vector map with sequence reference points. Also the sequence of the promoter and multiple cloning site of pGEM is shown.

2.4 Preparation of Plasmid DNA

One method of plasmid DNA extraction, relying on the alkaline lysis of bacterial cells, was used for this study.

2.4.1.0 Alkaline lysis/PEG precipitation mini prep method

Reagents and culture medium:

- Lauria Bertani (LB) broth: [1% (w/v) tryptone, 0.5% (w/v) yeast extract, and 1% (w/v) NaCl, pH 7.5]
- Solution A: (25 mM Tris-HCl, pH 8.0, containing 50 mM glucose, and 10mM EDTA)
- Solution B: (0.2 M NaOH, 1% (w/v) SDS)
- Solution C (3 M potassium acetate, 2 M acetic acid)

Cells of *E.coli* (section 2.39) were grown for approximately 16 h at 37°C in 10 mL of LB broth with the appropriate antibiotic for selection. The cells were then pelleted at 10,000 x g for 10 min, the supernatant discarded and the pellet resuspended in 200 µL of cold Solution A, mixed by vortexing, and transferred to an 1.5-mL Eppendorf. An aliquot (300 µL) of Solution B was then added, the solution mixed by slow inversion, then incubated at room temperature for 5 min, before 300 µL of cold Solution C was added and the mixture incubated on ice for 5 min followed by centrifugation at 20,000 x g for 10 min. The resulting supernatant was then transferred to a clean 1.5-mL Eppendorf, 2.5 µL of 10mg/mL RNase A added, the mixture vortexed for 30 sec and then incubated at 37°C for 20 min. Chloroform:iso-amyl alcohol (24:1) (400 µL) was then added, the mixture vortexed for 30 s and centrifuged at 20,000 x g for 1 min. The upper (aqueous) layer was then transferred to a fresh Eppendorf and the chloroform:iso-amyl alcohol step repeated again. Isopropanol (400 µL) was then added to the pooled aqueous fractions, and after mixing the precipitated DNA was collected, the supernatant removed, and the pellet washed with 500 µL of 70 % (v/v) ethanol, followed by centrifugation at 20,000 x g for 2 min. The resulting DNA pellet was then dried under vacuum for 5 min and resuspended with 32 µL of sterile MQ water. Eight micro-litres

of sterile 4 M NaCl and 40 µL of sterile 13 % (v/v) PEG_{8000} was then added, the mixture placed on ice for 20 min, then centrifuged at 20,000 x g for 20 min at 4°C. The DNA pellet was then washed with 500 µL of 70 % (v/v) ethanol, centrifuged at 20,000 x g for 2 min, the pellet then air-dried for 10 min and then resuspended in 25 µL of 10 mM Tris-HCl (pH 8.0).

Autosequencing and Online Services

2.4.1.1 Autosequencing Reaction – BigDye Terminator v3.1

The flowing reactants were added together in a 0.2-mL PCR tube:

Template (Plasmid DNA ~ 100ng/µL)	3 µL
10 µM primer (M13F)	2 µL
Sequence Buffer	3 µL
BigDye Terminator v3.1	2 µL (add last)
PCR Water	10 µL
	20 µL

Template DNA is outlined in section 2.4

Each reaction was subjected to an autosequence programme as set out below:

27 cycles of:

1) 96°C ----- 30 sec
2) 50°C ----- 15 sec
3) 60°C ----- 4 min

Each reaction was then kept at 4°C before precipitation (section 2.41) and then sequenced

2.4.1 Precipitation of terminator DNA and automated DNA sequencing

The prepared DNA after the terminator reaction (section 2.412) required precipitation and purification before automated sequencing could be performed. The product of terminator dye reaction was precipitated with the addition of 2 µL of EDTA (125 mM), 2 µL of Sodium acetate (3 M), and 50 µL of 100 % (v/v) ethanol. The mixture was inverted 5 times, incubated at room temperature for 15 min, and then centrifuged (20,000 x g) at 4°C for 30 min. The pellet was washed twice with 70 µL of 70 % (v/v) ethanol, then collected by centrifugation at 4°C at 20,000 x g for 5 min, air dried and the samples submitted to the Allan Wilson Centre, Institute of Molecular BioSciences, Massey University, Palmerston North, NZ for automated sequencing.

2.4.2 Agarose gel electrophoresis

Reagents:

- 25 x TAE buffer : 1 M Tris (pH 8.0) containing 0.5 M acetic acid, 25 mM EDTA
- 10 x SUDS : 100 mM EDTA (pH 8.0) containing 50 % (v/v) glycerol, 1 % (w/v) SDS, 0.025 % (w/v) bromophenol blue
- 1 kB Plus DNA ladder (Life Technologies)
- Ethidium Bromide (EtBr, 10 µg/mL)

Agarose gel electrophoresis was used to analyse PCR products. Agarose was dissolved in 1 x TAE buffer, with heating, to give a 1 % (w/v) solution. After cooling, this was then poured into an assembled horizontal gel apparatus containing a well-forming comb and the molten agarose allowed to set for 20 min before being immersed in 1 x TAE buffer. The well-forming comb was then removed prior to loading DNA samples. DNA samples were prepared by the addition of 2 µL of 10 x SUDS. Unless mentioned, all gels were loaded with 5 µL of HyperLadder loaded separately. Electrophoresis was carried out at 100 V for 40 min, after which the gels were stained in an EtBr bath for 10 min, then destained in sterile MQ water for 10 min and visualised on a short wavelength (340 nm) UV Transilluminator (Gel Doc 2000, Bio-Rad) and photographed.

2.5 Sequence Analysis and Primer Design

Sequence Analysis

Sequences were analysed using the Chromas Lite V.2.01 programme (Technelysium Ptd Ltd, 2005) to identify nucleotide base matches in the chromatogram. The NCBI (National Centre for Biotechnological Information) database was used to search for matches of a given inputted sequence against the database. By using BLAST (Basic Local Alignment Search Tool) (http://www.ncbi.nlm.nih.gov/), sequences can be matched with database sequences for similarity by comparing nucleotide or protein sequences. The programme performs a statistical calculation to determine the significance of each match.

Sequence data obtained were then analysed using Clustal W (European Molecular Biology Laboratory, 2009) (http://www.ebi.ac.uk/Tools/clustalw2/index.html) which is an online sequence alignment programme which allows for unknown sequences to be matched/aligned and the programme given a similiarity index (%) of matched nucleotide bases.

Primer Design

Primers were designed and based around the probable formation of dimer formation (no formation) and secondary structure (weak/N/A). These were calculated using the online oligo calculator (Sigma-Aldrich, 2009) (http://row.sigma-genosys.eu.com/) by inputting a sequence of nucleotide bases to be used for a primer. Similar melting temperatures (°C) between forward and reverse primers were also taken into account.

Table 2.2. Primer sequences used in this study

Primer name	Sequence
CuSOD –F degenerate	5' CCTGGACTTCATGGCTTCCAT 3'
CuSOD-R degenerate	5' TCTTCCGCCAGCGTTTCCAGTG 3'
MnSOD-F degenerate	5' ACMMGAARCACCAYCARACTTA 3'
MnSOD-R degenerate	5' TGMARGTAGTAGGCATGYTCCCA 3'
FeSOD-F degenerate	5' TYCACTGGGGKAAGCAYCA 3'
FeSOD-R degenerate	5' TCMARRTAGTAAGCATGCTCCCA 3'
3' RACEoligoT Adapter	5' GACTCGAGTCGACATCGATTTTTTTTTTTTTTTTV 3'
3'RACE Adapter	5' GACTCGAGTCGACATCG 3'
MnSOD 3'RACE-F	5' CTAATCAGGACCCTCTGGT 3'
FeSOD 3'RACE-F	5' AACCCACTTGCTTTTGGA 3'
CuSOD- gene specific-F	5' CTCTTGCTAAGCTCATGTCC 3'
CuSOD-gene specific-R	5' TCCTGGACTTCATGGCTTC 3'
MnSOD-UTR-F	5' GCAAACCTGATTCCTTTGTT 3'
MnSOD-UTR-R	5' AACCAATGATTTTGCAGAGAG 3'
FeSOD-UTR-F	5' TTGTGAACCTTGGTGAACC 3'
FeSOD-UTR-R	5' ACAGAATGAATGAAACTACGGC 3'

3. Results

3.1 RT-PCR Amplification of SOD Isoforms in *L. perenne*

In order to determine whether genes coding for all three known isoenzymes of the SOD enzyme system (Cu/ZnSOD, FeSOD, MnSOD) exist in *L. perenne,* degenerate primers were used in a RT-PCR protocol. This was carried out due to the fact that a number of higher plant species, such as sunflower, contain a gene (or genes) coding for only one isoform, e.g. a Cu/ZnSOD. Also, the number of genes expressed that code for one or more isoforms can change depending on plant species and age (Corpas et al., 2006). To clone SOD genes from *L. perenne*, plant material was separated into root and shoot tissue and separated tissue from all 9 seedlings pooled together in their respective tissue type and total RNA extracted from this. Following RNA extraction, RT-PCR was carried out on each RNA sample which had been treated with 0.2 mM $AlCl_3$ for a given time, or had remained as untreated (control plants).

Initially, SOD cDNAs were obtained with the use of degenerate primers (Corpas et al., 2006) to amplify the conserved region that was anticipated to occur in Cu/ZnSOD, FeSOD or MnSOD genes in *L. perenne* (Table 2.2). From the study of Corpas et al., 2006, product sizes of 435 bp (MnSOD), 312 bp (CuSOD) and 435 bp (FeSOD) were expected.

The PCR products amplified with the use of degenerate primers were purified (section 2.35), ligated into the pGEM vector (section 2.36) and transformed into the *E.coli* strain DH5α. The white colonies from the transformation, which used LB Amp^{100} plates with IPTG and X-Gal for selection, were picked and cultured in LB Amp^{100} broths. Plasmids were isolated (section 2.4) and purified (section 2.4) and sent for DNA autosequencing. To maximise the chances of obtaining SOD genes, 100 colonies (50 from 4 hr Al-treated roots, 50 from 24 hr Al-treated roots) were sequenced for each putative isoenzyme from the Al-treated root tissue at the time points indicated.

3.1.1 Sequence analysis of clones generated using degenerate Cu/ZnSOD primers

PCR products obtained using the Cu/ZnSOD degenerate primers were ~300 bp in size (Fig 3.1.0) and were consequently used for sequencing. The size of each insert correlated well with the expected size found by Corpas et al., 2006. To identify a gene sequence that would show a high correlation with aluminium treatment, 100 colonies were sequenced (in total) for 4 hr and 24 hr Al-treated root samples. This also provided information on the degeneracy of the CuSOD primers and how close the sequence is to the Cu/ZnSOD sequence (or sequences) expressed in *L. perenne*.

All sequences obtained contained the same sequence (313 bp) apart from one sequence which was named CuSOD9 (colony 9 of 100) which was 318 bp in length. This sequence was identical to the other CuSOD genes but also contained a five bp insertion (Fig 3.1.1A) and was consequently used initially for alignment and identity studies for the CuSOD isoform. Translation of the CuSOD9 sequence around the five bp insertion resulted in an inserted valine amino acid and the conversion of an isoleucins to an arginine residue. All other 99 sequences contained an isoleucine amino acid rather than the arginine residue (Fig 3.1.1B). An alignment of the amino acid sequences between CuSOD1 and CuSOD9 demonstrated a frame shift in the amino acid sequence, such that residues C-terminal to the valine and arginine in CuSOD9 differed from the other 99 CuSOD sequences analysed (Fig 3.1.1C). Thus CuSOD1 was used for further analysis.

In terms of nucleotide comparison, the full length sequence (colony 1) had an identity of 84 % with a *Oryza sativa* Japonica Group cultivar Wuyujing 3 copper/zinc-superoxide dismutase mRNA sequence identified in the NCBI database (Table 3.1.0). An 84 % identity with a *Oryza sativa* Japonica Group mRNA for copper/zinc-superoxide dismutase sequence was also observed. Also, 81 % identity with two sequences: a *Pennisetum glaucum* Cu-Zn superoxide dismutase mRNA and *Oryza sativa* (indica cultivar-group) cytoplasmic copper/zinc-superoxide dismutase mRNA sequence was also observed. Of note is 71% identity with an *Olea europaea* Cu/Zn-superoxide dismutase mRNA sequence. This is interesting due to the fact that *O.europaea* is the plant species from which the sequence of the degenerate primers were constructed by Corpas et al., (2006).

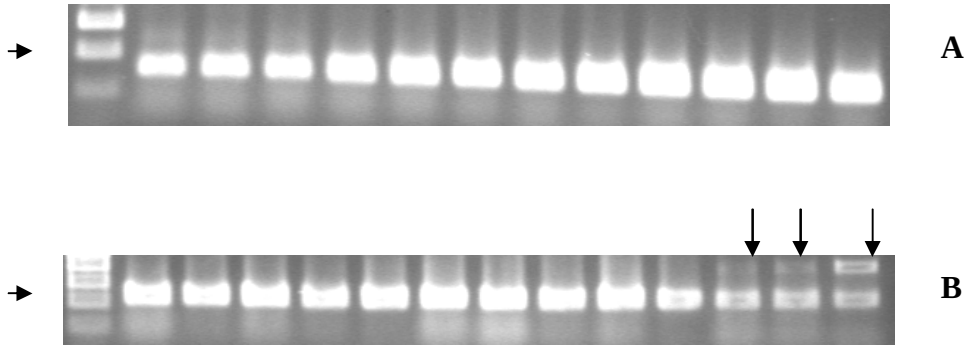

Figure 3.1.0 Examples of PCR generated DNA inserts from the pGEM vector using Cu/ZnSOD degenerate primers (A) and FeSOD degenerate primers (B). Colonies were screened for the correct size insert as detailed by Corpas et al., (2006). The arrow (to the left) marks the 0.4 kb band. This figure illustrates the screening of white and blue colonies for PCR inserts as all colonies in (A) are white and contain the ~300 bp insert while in (B) three blue colonies are selected (far right, marked with arrows) which contain two bands which do not correspond to the FeSOD insert (~435 bp). These colonies are slightly larger in size

A

```
CuSOD1          CATGCTGGTGATCTTGGAAACGTGACAGCTGGAGAGGATGGTGTTGCTCCCATCAATGTT 180
CuSOD9           CATGCTGGTGATCTTGGAAACGTGACAGCTGGAGAGGATGGTGTTGCTCCCATCAATGTT 180
                 ************************************************************

CuSOD1          GTTGACAAGCAT-----ATCCCCCTTACTGGACCACATTCAATCATTGGCCGTGCTGTTG 235
CuSOD9           GTTGACAAGCATGTGAGATCCCCCTTACTGGACCACATTCAATCATTGGCCGTGCTGTTG 240
                 ************     ****************************************
```

B

```
CuSOD 9 amino acid sequence

CCT GGA CTT CAT GGC TTC CAT GTG CAC GCT CTT GGT GAC ACC ACC AAT GGC TGC ATG TCT ACT GGA
CCA CAC TTC AAC CCC GCT GGT CAT GTG CAT GGG GCA CCA GAG GAT GAA ATC CGC CAT GCT GGT GAT
CTT GGA AAC GTG ACA GCT GGA GAG GAT GGT GTT GCT CCC ATC AAT GTT GTT GAC AAG CAT GTG AGA
TCC CCC TTA CTG GAC CAC ATT CAA TCA TTG GCC GTG CTG TTG TTG TCC ATG GTG ATG CTG ATG ATC
TTG GCA AGG GCG GAC ATG AGC TTA GCA AGA GCA CTG GAA ACG CTG GCG GAA RAA

Corresponding CuSOD 1 amino acid sequence

CCT GGA CTT CAT GGC TTC CAT GTG CAC GCT CTT GGT GAC ACC ACC AAT GGC TGC ATG TCT ACT GGA
CCA CAC TTC AAC CCC GCT GGT CAT GTG CAT GGG GCA CCA GAG GAT GAA ATC CGC CAT GCT GGT GAT
CTT GGA AAC GTG ACA GCT GGA GAG GAT GGT GTT GCT CCC ATC AAT GTT GTT GAC AAG CAT ATC CCC
CTT ACT GGA CCA CAT TCA ATC ATT GGC CGT GCT GTT GTT GTC CAT GGT GAT GCT GAT GAT CTT GGC
AAG GGC GGA CAT GAG CTT AGC AAG AGC ACT GGA AAC GCT GGC GGA AGA A
```

GTG = Valine AGA = Arginine ATC = Isoleucine CCC = Proline

C

```
CuSOD1          PGLHGFHVHALGDTTNGCMSTGPHFNPAGHVHGAPEDEIRHAGDLGNVTAGEDGVAPINV  60
CuSOD9          PGLHGFHVHALGDTTNGCMSTGPHFNPAGHVHGAPEDEIRHAGDLGNVTAGEDGVAPINV  60
                ************************************************************

CuSOD1          VDKHIPLTGPHSIIGRAVVVHGDAD--DLGKGGHELSKSTGNAGGR  104
CuSOD9          VDKHVRSPLLDHIQSLAVLLLSMVMLMILARADMSLARALETLAEE  106
                ****        *   **          *      *
```

H = Histidine V = Valine R = Arginine

Figure 3.1.1 A Clustal W alignment illustrating the 5 bp insertion (A) of the CuSOD9 sequence used for expression analysis with resulting amino acid change (B) and (C). Screening of colonies for gene sequences that may show an association with Al-treatment using CuSOD degenerate primers revealed only one sequence (CuSOD9) that differed from 100 that were sequenced.

Accession	Description	Max score	Total score	Query coverage	E value	Max ident
EU325984.1	*Oryza sativa* Japonica Group cultivar Wuyujing 3 copper/zinc-superoxide dismutase mRNA	336	336	95%	4e-89	84%
D01000.1	*Oryza sativa* Japonica Group mRNA for copper/zinc-superoxide dismutase	336	336	95%	4e-89	84%
EF495351.1	*Pennisetum glaucum* Cu-Zn superoxide dismutase mRNA,	311	311	98%	1e-81	81%
DQ058108.1	*Oryza sativa* (indica cultivar-group) cytoplasmic copper/zinc-superoxide dismutase mRNA	311	311	98%	1e-81	81%
AF426829.1	*Olea europaea* Cu/Zn-superoxide dismutase mRNA, partial cds	289	289	99%	5e-75	79%

Table 3.1.0. NCBI BLAST-n analysis of the putative CuSOD sequence showing the highest identity sequences from the database. All sequences apart from *O.europaea* obtained from the analysis of the CuSOD sequence revealed high identities with graminaceous species.

3.1.2 Sequence analysis of degenerate FeSOD primer sequences

PCR amplified products obtained using the FeSOD degenerate primers were ~400 bp in size (Fig 3.1.0). As with CuSOD sequencing, 100 colonies (in total) from 4hr (50) and 24 hr (50) Al-treated root DNA were sent for analysis. The alignment results from the NCBI BLAST database indicated that the FeSOD primers were also aligning to a highly conserved region, in the sense that many of the colonies sequenced contained the same sequence. Interestingly the BLAST results also showed high identity matches with MnSOD gene sequences. Two sequences from the original cloning were analysed that differed from one another. One had high identity to FeSOD genes and the other high identity to MnSOD genes. The other 98 colonies had identity to FeSOD genes but were smaller or incomplete sequences when compared with the 438 bp FeSOD sequence used for further analysis.

Alignment results of the 439 bp primary FeSOD sequence indicated that it was most closely related to a *Zea mays sodB* gene sequence corresponding to a chloroplastic iron-superoxide dismutase (Table 3.1.1). The aligned FeSOD sequence had an identity of 82% with this *Zea mays* sequence and also had an identity of 80% with a *Zea mays* partial mRNA corresponding to the iron superoxide dismutase *fsd1* gene. A 79% and 80% max identity was observed to an *Oryza sativa* Japonica Group mRNA for an iron-superoxide dismutase sequence and *Oryza sativa* (indica cultivar-group) iron-superoxide dismutase (Fe-SODb) gene sequence respectively. An *Arabidopsis thaliana* putative iron superoxide dismutase 3 gene sequence followed as the main hits for this sequence with 69% max identity.

The second isolated sequence that was generated using the degenerate FeSOD primers showed identity to MnSOD sequences in the database and is thus designated as an MnSOD gene sequence. This consisted of a 444 bp sequence which showed high identity with three *Triticum aestivum* sequences in the NCBI BLAST-n database. A sequence described as a *Triticum aestivum* manganese superoxide dismutase (SOD3.2) mRNA - nuclear gene encoding mitochondrial protein returned the highest identity of 86%, while two other *T.aestivum* sequences, referred to as a *Triticum aestivum* manganese superoxide dismutase (SOD) gene sequence and *Triticum aestivum* manganese superoxide dismutase (SOD3.1) mRNA - nuclear gene encoding

mitochondrial protein sequences gave 85% max identity with the inputted MnSOD sequence discovered in this study (Table 3.1.2). Also, 85% max identity to a *Saccharum officinarum* (sugar cane) superoxide dismutase (Mn-SOD) gene sequence was observed along with an identity of 83% to a *Zea mays* Mn-superoxide dismutase (Sod3.4) gene sequence (Table 3.1.2).

Accession	Description	Max score	Total score	Query coverage	E value	Max ident
NM_001111401.1	*Zea mays* chloroplastic iron-superoxide dismutase (sodB), mRNA	443	443	98%	5e-121	82%
AB014056.1	*Oryza sativa* Japonica Group mRNA for iron-superoxide dismutase	399	399	99%	5e-108	79%
AJ854254.1	*Zea mays* partial mRNA for iron superoxide dismutase (fsd1 gene)	356	356	85%	5e-95	80%
AY770495.1	*Oryza sativa* (indica cultivar-group) iron-superoxide dismutase (Fe-SODb) mRNA	304	406	99%	3e-79	80%
AY065458.1	*Arabidopsis thaliana* putative iron superoxide dismutase 3 (At5g23310) mRNA	167	167	84%	5e-38	69%

Table 3.1.1. NCBI BLAST-n analysis of the putative FeSOD sequence showing the highest identity sequences from the database.

Accession	Description	Max score	Total score	Query coverage	E value	Max ident
U73172.1	*Triticum aestivum* manganese superoxide dismutase (SOD3.2) mRNA	540	540	96%	2e-150	86%
GQ246460.1	*Saccharum officinarum* super-oxide dismutase (Mn-SOD) mRNA	536	536	96%	3e-149	85%
EF392662.1	*Triticum aestivum* manganese superoxide dismutase (SOD) mRNA	536	536	96%	3e-149	85%
U72212.1	*Triticum aestivum* manganese superoxide dismutase (SOD3.1) mRNA	522	522	96%	6e-145	85%
L19463.1	*Zea mays* Mn-superoxide dismutase (Sod3.4) mRNA,	491	491	96%	1e-135	83%

Table 3.1.2. NCBI BLAST-n analysis of the putative MnSOD sequence showing the highest identity sequences from the database

3.1.3 Sequence analysis of clones amplified using the degenerate MnSOD primer sequences

The use of the MnSOD degenerate primers was inconclusive when analysing 100 sequences from 4 hr and 24hr Al-treated root using NCBI BLAST as the database search tool. No sequences of higher plant origin in the database showed identity to the inputted sequence but other organisms showed positive identity (data not shown). The amplified MnSOD sequences showed identity to a number of bacterial and human sequences but identity was generally low. Most sequences generated in this study had an identity of 54% to a mitochondrial manganese superoxide dismutase (MnSOD2) gene from *Phytophthora nicotianae* and 64% identity to a manganese-containing superoxide dismutase (SOD2) mRNA from *Homo sapiens* cell-line MCF-1. Generally, these two sequences in the database returned the highest identity hits to inputted sequences (colonies 1-100) using the degenerate MnSOD primers although there were a few sequences (of the 100) that did not show identity to these two sequences. However, for any of the 100 sequences, no identity was observed to higher or lower plant SOD sequences using BLAST as the search tool.

3.1.4 Sequence alignment of the three isoform sequences

To determine how closely related the three SOD gene sequences identified in this study were from one another, Clustal W, an online alignment tool, was used (Fig 3.1.2). All three sequences are quite dissimilar from each other with ranges from 46% to 57% similarity at the nucleotide level (NOTE: one of the sequences obtained using the FeSOD primers is referred to as the MnSOD sequence).

With regard to the CuSOD and FeSOD sequences, only a 48% identity was observed which was the highest identity between the three isoforms. A 57% identity was observed between FeSOD and MnSOD with 46% identity percentage between CuSOD and MnSOD sequences.

Amino acid identity between the three SOD sequences was much lower when compared with the nucleotide identity (Fig 3.1.3). The identity in amino acid sequence between the CuSOD and FeSOD sequence was 19% while the CuSOD and MnSOD sequence

had an identity score of 23%. The FeSOD and MnSOD identity was much higher with a score of 38% (Table 3.1.3).

Figure 3.1.2. Clustal W alignment of the CuSOD, MnSOD and FeSOD genes sequences isolated in this study. The (*) denotes complete conservation.

```
FeSOD           HWGKHQQDYVDGLNKQLDTSPFYGHTLEDMVKEAYNNGNPLPEYNNAAQVWNHHFFWESM 60
MnSOD           HWGKHHATYVANYNKALEQ---LDAAVSKGDASAVVQLQGAIKFNGGGHV-NHSIFWKNL 56
CuSOD           --------------PGLHG--FHVHALGDTTNGCMSTG---PHFNPAGHV--HGAPEDEI 39
                              *                               *    *  *

FeSOD           QPG--GGGSPEAGVL-QQIEKDFGSFANFREEFMLSA-LSLLGSGWVWLVLKRNERKLSV 116
MnSOD           KPTNEGGGEPPHGKLGWAIDEDFGSFDKLVKKMNAEG-AALQGSGWVWLALDKEAKKLSV 115
CuSOD           RHAGDLGNVT-------AGEDGVAPINVVDKHIPLTGPHSIIGR---AVVVHGDADDLGK 89
                      *                                   *             *

FeSOD           VNTRNAINPLAFGD--IPIISLDLWEHAYYL- 145
MnSOD           ETTANQDPLVTKGANLIPLLGIDVWEHAYYLE 147
CuSOD           GGHELSKSTGNAGGR---------------- 104
                           *
```

Figure 3.1.3. Clustal W alignment of CuSOD, MnSOD and FeSOD SOD genes for amino acid identity. Genes are aligned based on sequence number and identity observed from BLAST results by using degenerate primers. (*) stand for conserved amino acid between the three sequences.

	CuSOD	**FeSOD**	**MnSOD**
CuSOD	-	**48%** (19%)	**46%** (23%)
FeSOD	**48%** (19%)	-	**57%** (38%)
MnSOD	**46%** (23%)	**57%** (38%)	-

Table 3.1.3. Alignment scores (%) of SOD gene sequences obtained using degenerate primers in this study. Scores are based on alignment values from Clustal W and are given as percentages. Nucleotide identity is listed first (bold) with consequent amino acid identity in brackets between two listed SOD genes.

3.2 Amplification of the 3'-UTR corresponding to the SOD isoenzymes of *L. perenne*

Species such as *Arabidopsis* have a number of genes that code for each isoform, and so to study the expression of specific genes, RACE may potentially provide a route to design primers specific to only one gene and in doing so allow for the study of expression of this gene in isolation. Thus to obtain gene specificity for each isoform found in *L. perenne*, RACE or Rapid Amplification of cDNA Ends was utilised. This step was initiated due to the possibility of a number of genes coding for each SOD isoform in ryegrass as has been observed in a number of other higher plant species. A number of genes coding for each isoenzyme would not be discriminated using degenerate primers in the expression studies.

RACE is a variation of RT-PCR that amplifies unknown cDNA sequences corresponding to the 3′- or 5′-untranslated region of the mRNA. In this thesis, the amplification of the 3'-UTR (3'RACE) was used (Fig. 2.3 and Fig 2.4). The procedure works by the conversion of mRNA to cDNA using the RT reaction (reverse transcription) with an oligo dT adapter primer. A user designed GSP (gene-specific primer) for each isoform then amplifies specific cDNA by PCR. This GSP anneals to a region of known exon sequences and an adapter primer targets the poly A tail region (Fig 2.3).

3.2.1 Screening of putative inserts using SOD gene-specific primers

Gene-specific primers were designed based on the sequence information that was obtained from sequences previously generated using degenerative MnSOD, FeSOD and CuSOD primers (Section 3.1). SOD gene-specific primers (Table 2.2) were designed based on their low formation of secondary structures, close melting temperatures and the prevention of dimer formation. Amplified products were purified (Section 2.35) and ligated into the pGEM vector and transformed into *E.coli* strain DH5α. After plating onto selection media, 20 colonies were selected for each primer set (corresponding to either the MnSOD, FeSOD and CuSOD genes).

3.2.2 Analysis of 3' UTR sequences corresponding to the FeSOD gene isolated using degenerate primers

Of the 20 colonies submitted for DNA sequencing all returned high identity hits with the same FeSOD sequence in the NCBI database (all the same). For analysis, the largest 3'-UTR sequence was used, as well as forming the basis of the design of FeSOD gene-specific primers used in expression analysis.

To determine the start of the 3'-UTR region in the consensus FeSOD sequence, the STOP codon (TGA), was located using tBLASTx. To do this, an alignment with the STOP codon to an *Oryza sativa* sequence with highest identity was determined and the subsequent 3'-UTR region identified (Fig 3.2.1).

A 500 bp FeSOD 3'-UTR region was observed which corresponded well with the *Oryza sativa* FeSOD sequence in BLASTn used to detect the STOP codon (Fig 3.2.1) while the full 3'-UTR region is shown in Figure 3.2.2. This 500 bp sequence was most closely related to an *Oryza sativa* (indica cultivar-group) iron-superoxide dismutase (Fe-SODb) mRNA sequence with 85 % identity and this was used to identify the STOP codon (Fig 3.2.1). The second most identical sequence is another *Oryza sativa* Japonica Group mRNA for iron-superoxide dismutase sequence from a different accession (same sequence) and then a *Zea mays* clone 222965 superoxide dismutase, chloroplast mRNA sequence with 91 % identity (Table 3.2.1). If the coding region amplified using the degenerate primers is included (439 bp), with the further 133 bp region of the coding sequence generated as part of the 3' RACE procedure and the 500 bp 3' UTR, a total sequence of 1072 bp is obtained (Fig 3.2.3). Using a FeSOD sequence from *O.sativa* (AB014056.1) as a reference sequence, a comparison with the full-length mRNA predicts that a further 196 bp of coding sequence is still required to obtain the full length coding sequence from *L . pere*nne (Fig 3.2.4).

To confirm that the FeSOD 3'-UTR sequence is part of the same gene as that of the partial coding sequence generated using the FeSOD degenerate primers, a 50 bp sequence that overlapped from that generated using the degenerate primers (Fig. 3.1.2) with the same region generated using 3'-RACE (Fig. 3.2.3) was compared and found to be identical (data not shown).

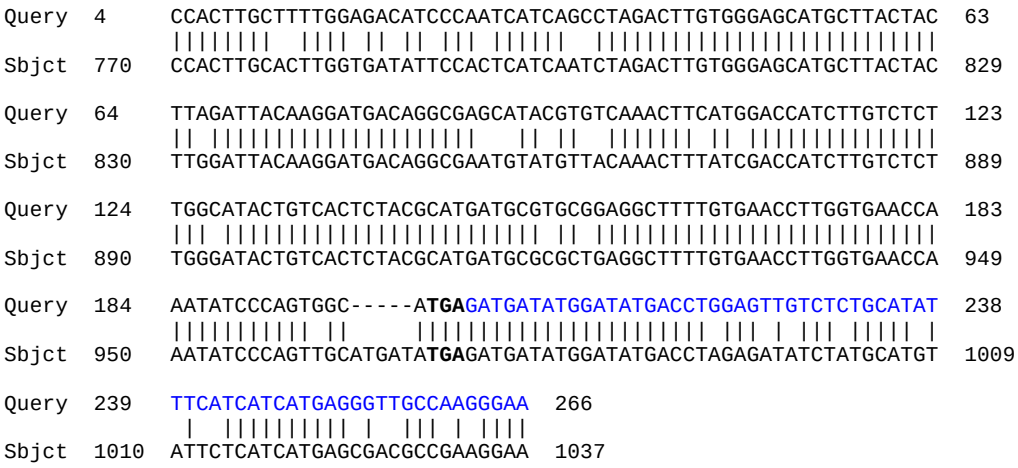

Fig 3.2.1. Results from the NCBI database BLAST-n analysis of the putative FeSOD reading frame and partial 3'-UTR sequence identifying the STOP (TGA) codon. Query = FeSOD sequence generated in this study. Subject (AY770495.1) = *Oryza sativa* sequence in the NCBI database. The blue highlighted query is the start of the 3' UTR

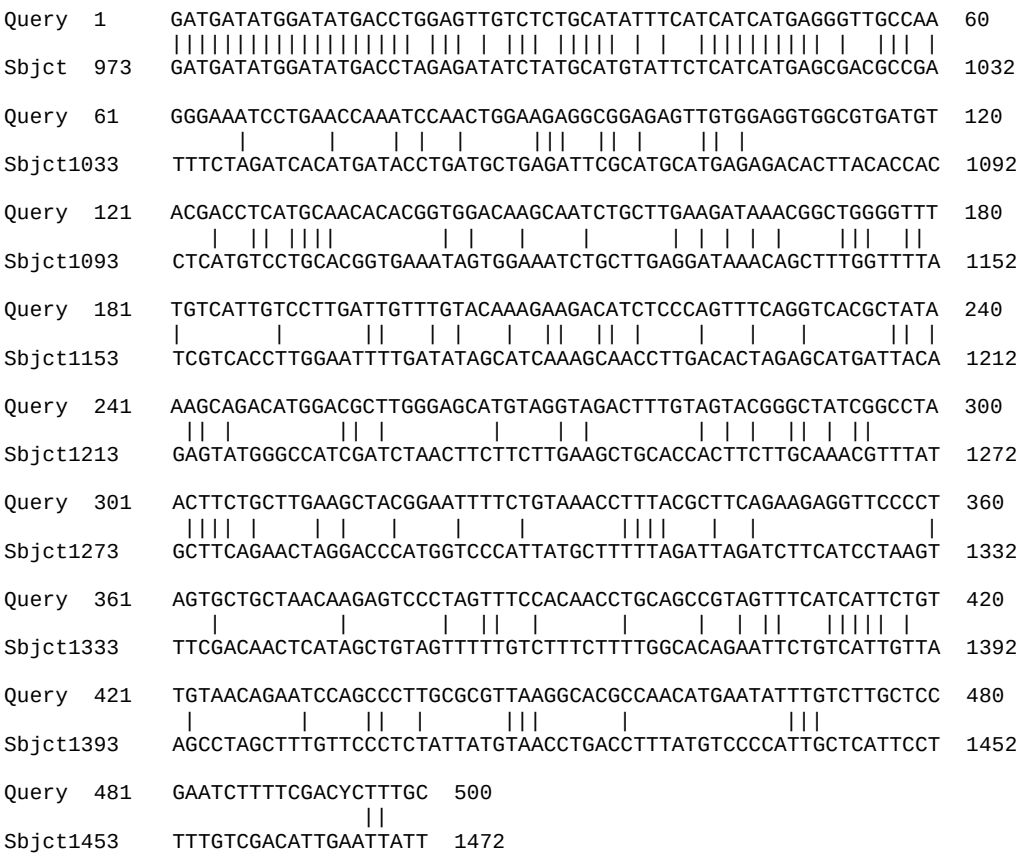

Figure 3.2.2. Results from the NCBI database BLAST-n analysis of the putative FeSOD 3'-UTR sequence. Query = FeSOD 3'-UTR sequence. Subject (AY770495.1) = *Oryza sativa* sequence in the NCBI database (see Table 3.2.1)

Accession	Description	Max score	Total score	Query coverage	E value	Max ident
AY770495.1	*Oryza sativa* (indica cultivar-group) iron-superoxide dismutase (Fe-SODb) mRNA, complete cds, alternatively spliced	307	307	35%	4e-80	85%
AB014056.1	*Oryza sativa* Japonica Group mRNA for iron-superoxide dismutase, complete cds	307	307	35%	4e-80	85%
EU960262.1	*Zea mays* clone 222965 superoxide dismutase, chloroplast mRNA, complete cds; nuclear gene for chloroplast product	284	284	27%	5e-73	91%
NM_001111401.1	*Zea mays* chloroplastic iron-superoxide dismutase (sodB), mRNA >dbj|AB201543.1| Zea mays sodB mRNA for chloroplastic iron-superoxide dismutase, complete cds	284	284	27%	5e-73	91%
DQ517439.1	*Gymnadenia conopsea* Fe-superoxide dismutase (Fe-SOD) mRNA, complete cds	123	123	27%	1e-24	74%

Table 3.2.1 Sequences producing significant alignments to the 500 bp 3'-UTR FeSOD sequence of *L. perenne*

TTCACTGGGGGAAGCACCAGCAGGATTACGTGGACGGCTTGAACAAGCAGCTCGA
CACCAGCCCCTTCTACGGCCACACTCTGGAGGATATGGTCAAGGAGGCCTACAACA
ACGGCAACCCTCTGCCGGAGTACAACAATGCTGCACAGGTCTGGAACCACCACTTT
TTCTGGGAATCAATGCAGCCCGGAGGCGGTGGCTCGCCTGAGGCTGGTGTACTGCA
GCAAATTGAGAAGGATTTCGGCTCGTTTGCTAATTTCAGGGAAGAGTTTATGCTCTC
GGCGTTATCCCTACTGGGGTCTGGATGGGTTTGGCTTGTCTTGAAGAGAAACGAGA
GGAAACTCTCGGTAGTTAACACACGAAATGCCATCAACCCACTTGCTTTTGGAGAC
ATCCCAATCATCAGCCTAGACTTGTGGGAGCATGCTTACTACTTAGATTACAAGGA
TGACAGGCGAGCATACGTGTCAAACTTCATGGACCATCTTGTCTCTTGGCATACTGT
CACTCTACGCATGATGCGTGCGGAGGCTTTTGTGAACCTTGGTGAACCAAATATCC
CAGTGGCATGAGATGATATGGATATGACCTGGAGTTGTCTCTGCATATTTCATCATC
ATGAGGGTTGCCAAGGGAAATCCTGAACCAAATCCAACTGGAAGAGGCGGAGAGT
TGTGGAGGTGGCGTGATGTACGACCTCATGCAACACACGGTGGACAAGCAATCTGC
TTGAAGATAAACGGCTGGGGTTTTGTCATTGTCCTTGATTGTTTGTACAAAGAAGAC
ATCTCCCAGTTTCAGGTCACGCTATAAAGCAGACATGGACGCTTGGGAGCATGTAG
GTAGACTTTGTAGTACGGGCTATCGGCCTAACTTCTGCTTGAAGCTACGGAATTTTC
TGTAAACCTTTACGCTTCAGAAGAGGTTCCCCTAGTGCTGCTAACAAGAGTCCCTA
GTTTCCACAACCTGCAGCCGTAGTTTCATCATTCTGTTGTAACAGAATCCAGCCCTT
GCGCGTTAAGGCACGCCAACATGAATATTTGTCTTGCTCCGAATCTTTTCGACYCTT
TGC

Figure 3.2.3. The generated 1072 bp FeSOD sequence obtained from *L. perenne* in this study. The partial 439 bp coding sequence isolated using the degenerate primers is shown in black caps with the degenerate FeSOD primers underlined. The further 133 bp of coding sequence generated using 3'-RACE is shown as the yellow highlight with the forward primer used for 3'RACE and for subsequent expression studies shown in red caps. The STOP codon (TGA) is identified in block red. The 3'-UTR is highlighted in aqua, with the reverse primer used for subsequent expression studies in blue caps. The Adapter reverse primer for 3'-RACE is not shown.

```
ORIGIN
        1 gatagatagc gcggcagagg aaagaggaga agaaaagatg gcggctttcg cctccgctct
       61 ccgcgttctc ccctcgccgc cggctgcggt gcctcgtcgg cttcgctcga gagaacaaag
      121 gcagggctgt agatctcgaa ggtattcaaa agtcgtggct tactacgctc tcactactcc
      181 gccgtataaa cttgatgccc tggaacctta tattagcaag aggacagttg aacttcactg
      241 gggtaagcat cagcaagact atgtggatag cttgaataag cagcttgcta ccagcatgtt
      301 ctatgggtac actctggagg aactaataaa agaagcatac aacaacggca acccattacc
      361 agaatataat aatgcagcac aggtatggaa ccatcacttc ttctgggaat caatgcagcc
      421 agaaggtggt gggtcaccag ggcgaggtgt cctgcagcag atagagaagg attttggctc
      481 ttttactaat tttagggaag agtttatacg ctcagcatta tcacttttgg ggtctggctg
      541 ggttttgctt gtcttgaaga gaaaagaacg aaaattatcg gtagtccata cacaaaatgc
      601 catcagtcca cttgcacttg gtgatattcc actcatcaat ctagacttgt gggagcatgc
      661 ttactacttg gattacaagg atgacaggcg aatgtatgtt acaaacttta tcgaccatct
      721 tgtctcttgg gatactgtca ctctacgcat gatgcgcgct gaggcttttg tgaaccttgg
      781 tgaaccaaat atcccagttg catgatatga gatgatatgg atatgaccta gagatatcta
      841 tgcatgtatt ctcatcatga gcgacgccga ggaatttcta gatcacatga tacctgatgc
      901 tgagattcgc atgcatgaga gacacttaca ccacctcatg tcctgcacgg tgaaatagtg
      961 gaaatctgct tgaggataaa cagctttggt tttatcgtca ccttggaatt ttgatatagc
     1021 atcaaagcaa ccttgacact agagcatgat tacagagtat gggccatcga tctaacttct
     1081 tcttgaagct gcaccacttc ttgcaaacgt ttatgcttca gaactaggac ccatggtccc
     1141 attatgcttt ttagattaga tcttcatcct aagtttcgac aactcatagc tgtagttttt
     1201 gtctttcttt tggcacagaa ttctgtcatt gttaagccta gctttgttcc ctctattatg
     1261 taacctgacc tttatgtccc cattgctcat tccttttgtc gacattgaat tatttgatgc
     1321 gatattttcg catccattac taagcttttg ctc
```

Figure 3.2.4. The reference sequence of *O.sativa* (AB014056) obtained from the NCBI database and used to predict the start (ATG) of the coding sequence for the FeSOD gene from *L. perenne* generated in this study. Highlighted in red are the start (ATG) and stop (TGA) codons of the coding sequence. Underlined nucleotides represent where the coding region (using degenerate primers and 3'RACE) for the FeSOD gene isolated in this study.

3.2.3 Analysis of 3' UTR sequences corresponding to the MnSOD gene isolated using degenerate primers

All 20 colonies that were sequenced returned high identity hits with MnSOD sequences in the NCBI database. Again, the largest sequence was selected for analysis and consequently used as the basis for the design of the MnSOD gene-specific primers used for expression analysis.

To determine the start of the 3'-UTR region in this MnSOD sequence, the STOP (TGA) codon, was identified by aligning with the STOP codon in the *Triticum aestivum* sequence that had highest identity (Fig 3.2.5).

A 197 bp MnSOD 3'-UTR region was observed and had a high max identity to a *Triticum aestivum* manganese superoxide dismutase (SOD) mRNA sequence (88 % identity) in BLASTn which was used to align the STOP codon (Table 3.2.2). The second most identical sequence is a *Triticum aestivum* manganese superoxide dismutase (SOD) mRNA sequence from another accession followed by a *Zea mays* clone 1671510 superoxide dismutase mRNA sequence with 89 % identity (Table 3.2.2). If the coding region amplified using the degenerate primers is included, with a further 71 bp of the coding sequence generated as part of the 3'RACE procedure and the 197 bp 3'UTR, a total sequence of 705 bp is obtained (Fig 3.2.6). Using a MnSOD sequence from *T.aestivum* (AF092524) as a reference sequence, a comparison with the full-length mRNA predicts that a further 152 bp of coding sequence is still required to obtain the full-length cDNA from *L. perenne* (Fig 3.2.7).

To confirm that the MnSOD 3'-UTR sequence is part of the same gene as that of the partial coding sequence generated using the MnSOD degenerate primers, a 56 bp sequence that overlapped from that generated using the degenerate primers (Fig. 3.1.2) with the same region generated using 3'-RACE (Fig. 3.2.6) was compared and found to be identical (data not shown).

Fig 3.2.5. **Results from the NCBI database BLAST-n analysis of the putative MnSOD sequence identification of STOP codon and subsequent 3'UTR sequence.** Query = MnSOD UTR sequence. Subject (AF092524.1) = *Triticum aestivum* sequence in the NCBI database. The figure illustrates the reading frame and identification of the stop codon. The entire 197 bp 3'-UTR sequence is shown as blue caps.

Accession	Description	Max score	Total score	Query coverage	E value	Max ident
AF092524.1	*Triticum aestivum* manganese superoxide dismutase (SOD) mRNA, nuclear gene encoding mitochondrial protein, complete cds	230	230	43%	5e-57	88%
EF392662.1	*Triticum aestivum* manganese superoxide dismutase (SOD) mRNA, partial cds	226	226	43%	6e-56	87%
EU958076.1	*Zea mays* clone 1671510 superoxide dismutase mRNA, complete cds	224	224	41%	2e-55	89%
EU952706.1	*Zea mays* clone 1286840 superoxide dismutase mRNA, complete cds	224	224	41%	2e-55	89%

Table 3.2.2. Sequences producing significant alignments to the 197 bp 3'-UTR MnSOD sequence of *L. perenne*

TTCACTGGGGGAAGCACCACGCCACCTACGTTGCCAACTACAACAAGGCGCTCGAG
CAGCTTGACGCCCGCTGTCTCTAAGGGCGACGCTTCCGCCGTCGTCCAACTCCAGG
GCGCCATCAAGTTCAACGGCGGCGGTCATGTGAACCATTCAATCTTCTGGAAGAAC
CTCAAGCCTACTAATGAGGGTGGGGGTGAGCCACCTCATGGTAAACTTGGCTGGGC
CATTGATGAGGACTTCGGTTCTTTTGACAAGCTTGTAAAGAAGATGAATGCGGAGG
GTGCTGCTTTACAAGGATCTGGATGGGTGTGGCTGGCGTTGGATAAAGAGGCAAAA
AAGCTTTCAGTTGAAACTACTGCTAATCAGGACCCTCTGGTGACTAAAGGAGCAAA
CCTGATTCCTTTGTTGGGGATTGATGTCTGGGAGCATGCTTACTATCTTGAACAACA
TCTGGAAGGTGGTGAACTGGAAATATGCTGGCGAAGAATACGAAAATGTGGCTGT
GTGATACTATGTCTGAATAGGCGTTGCTTTGCTCTTTGCTTGCCGACTGTGTTGGAT
CTTTATATGCAATAAATGCGTAATGCACAATGCAGATTTTGCGTTCTTGTTATGGCT
GTATTTGGTTGCCTTTGTTATACTCAGTGGCGCAATGCAGAGTCACATACGTTGTGC
AATTCTCTCTGCAAAATCATTGGTTGTGTC

Figure 3.2.6. The generated 705 bp MnSOD sequence obtained from *L. perenne* in this study. The partial 444 bp coding sequence isolated using the degenerate primers is shown in black caps with the degenerate MnSOD primers underlined. The further 71 bp of coding sequence generated using 3'-RACE is shown as the yellow highlight with the forward primer used for 3'RACE and for subsequent expression studies shown in red caps. The STOP codon (TGA) is identified in block red. The 3'-UTR is highlighted in aqua, with the reverse primer used for subsequent expression studies in blue caps. The Adapter reverse primer for 3'-RACE is not shown.

```
ORIGIN
        1 ccatggcgct ccgcacgttg gccgcgaaga aaaccctagg cctggcgctc ggcggcgcca
       61 ggggcgtggc gacgttcacg ctccccgacc tcccctacga ctacggtgcg ctggagccgg
      121 ccgtctccgg cgagatcatg cgcctgcacc accagaagca ccacgccacc tacgtcgccc
      181 actacaacaa ggcgctcgag cagctcgacg ccgccgtcag caagggggac gcgtccgccg
      241 tcgtccacct ccagagcgcc atcaagttca acggcggcgg tcatgttaac cattccatct
      301 tctggaagaa cctcaagcct atcagcgagg gtggtggtga ggcacctcat ggcaaacttg
      361 gctgggccat tgatgaagat tttggttcta ttgagaaact tataaagaag atgaatgcag
      421 agggtgcttt acaaggatct ggatgggtgt ggctagcttt ggataaagag gccaaagggc
      481 tttcagttga aactactcct aatcaggacc ctcttgtgac caaagggtca aacctgcatc
      541 ctttgttggg aattgatgtc tgggagcatg cgtactacct gcagtacaag aacgtgaggc
      601 cggactacct gaccaacatc tggaaggtgg tgaactggaa atatgctgga gaagagtatg
      661 aaaaagtgct tgcgtgattt gtctgatgag tagacagaca gtacttggct cgctcttgag
      721 tttcccgctg ttggatcttt gtatatgcag taataaaagt gggcactatt ccactgtcgg
      781 gaccttctgt acattgcata gaggtgacac tactgtctaa agcgcactag tgcatgtcca
      841 ttttggtact tgttactgtg cctgcgttgc taataaactc attcgctagt gctgtt
```

Figure 3.2.7. The reference sequence of *T.aestivum* (AF092524) obtained from the NCBI database and used to predict the start (ATG) of the coding sequence for the MnSOD gene from *L. perenne* generated in this study. Highlighted in red are the start (ATG) and stop (TGA) codons of the coding sequence. Underlined nucleotides represent where the coding region (using degenerate primers and 3'RACE) for the MnSOD gene isolated in this study.

3.2.4 Analysis of 3' UTR sequences corresponding to the CuSOD gene isolated using degenerate primers

All 20 sequences analysed against the NCBI database that were putative 3'-UTR sequences corresponding to the CuSOD gene did not provide identity to any SOD sequences already in the database. Thus further analysis of the 3'UTR region of the CuSOD gene was not carried out.

The sequences that were obtained did show some identity with a *Zea mays* full-length cDNA database sequences with 82 % identity followed by a *Zea mays* hypothetical protein with 82 % identity from the reading frame (Table 3.2.3). Also included in identity hits was a *Oryza sativa* Japonica Group cDNA sequence (78 %) and a *Solanum lycopersicum* cDNA sequence with 75 % identity.

3.2.5 Clustal analysis alignment of 3'UTR sequences and full length sequences obtained in this trial

To determine how closely related the MnSOD and FeSOD 3' UTR sequences were, a Clustal W alignment was carried out. A 43% identity was determined between the two SOD isoform 3' UTR sequences which is quite dissimilar (Fig 3.2.4).

Finally, an identity of 49 % between the full length sequences of FeSOD and MnSOD obtained as part of this study (including the 3'UTR sequences) was determined using Clustal W (Fig 3.2.9).

Accession	Description	Max score	Total score	Query coverage	E value	Max ident
BT086138.1	*Zea mays* full-length cDNA clone ZM_BFc0120E03 mRNA, complete cds	134	134	29%	3e-28	82%
NM_001143584.1	*Zea mays* hypothetical protein LOC100217228 (LOC100217228), mRNA >gb|BT038171.1| Zea mays full-length cDNA clone ZM_BFb0215M01 mRNA, complete cds	134	134	29%	3e-28	82%
AK068177.1	*Oryza sativa* Japonica Group cDNA clone:J013131A16, full insert sequence	134	134	37%	3e-28	78%
EZ063379.1	TSA*: Zea mays* contig64501, mRNA sequence	131	131	29%	4e-27	81%
BT066906.1	*Zea mays* full-length cDNA clone ZM_BFb0093H03 mRNA, complete cds	131	131	29%	4e-27	81%
EU944383.1	*Zea mays* clone 213734 mRNA sequence	131	131	29%	4e-27	81%
EF589280.1	*Oryza sativa* (indica cultivar-group) cultivar Pokkali unknown genomic sequence	114	114	33%	3e-22	77%
EF589282.1	*Oryza sativa* (indica cultivar-group) cultivar FL478 unknown genomic sequence	109	109	33%	1e-20	76%
EF589281.1	*Oryza sativa* (indica cultivar-group) cultivar IR29 unknown genomic sequence	109	109	33%	1e-20	76%
AP009053.1	*Oryza sativa* Japonica Group genomic DNA, chromosome 3, fosmid clone:OSJNOa070P15, complete sequence	109	109	33%	1e-20	76%
AK319996.1	*Solanum lycopersicum* cDNA, clone: LEFL1004AB11, HTC in leaf	100	100	32%	6e-18	75%

Table 3.2.3. Results from the NCBI database BLAST-n analysis of the putative CuSOD 3'UTR sequence. The queried sequence of the 3'RACE CuSOD sequences inputted into the NCBI database did not match any SOD sequences and was therefore not used for expression analysis. The identities that were obtained are shown.

```
FeSOD           GATGATATGGATATGACCTGGAGTTGTCTCTGCATATTTCATCATCATGAGGGTTGCCAA 60
MnSOD           ------------------------------------------------------------


FeSOD           GGGAAATCCTGAACCAAATCCAACTGGAAGAGGCGGAGAGTTGTGGAGGTGGCGTGATGT 120
MnSOD           ------------------------------------------------------------


FeSOD           ACGACCTCATGCAACACACGGTGGACAAGCAATCTGCTTGAAGATAAACGGCTGGGGTTT 180
MnSOD           ------------------------------------------------------------


FeSOD           TGTCATTGTCCTTGATTGTTTGTACAAAGAAGACATCTCCCAGTTTCAGGTCACGCTATA 240
MnSOD           ------------------------------------------------------------


FeSOD           AAGCAGACATGGACGCTTGGGAGCATGTAGGTAGACTTTGTAGTACGGGCTATCGGCCTA 300
MnSOD           ---------------------------------TACTATGTCTGAATAGGCGTTGCTTTG 27
                                                   *** ***   *   *   * *   *


FeSOD           ACTTCTGCTTGAAGCTACGGAATTTTCTGTAAACCTTTACGCTTCAGAAGAGGTTCCCCT 360
MnSOD           CTCTTTGCTTG------CCGACTGTGTTGGATCTTTATATGCAATAAATGCGTAATGCAC 81
                   * ******      * ** * *  ** *    * ** **   * * * *     *


FeSOD           AGTGCTGCTAACAAGAGTCCCTAGTTTCCACAACCTGCAGCCGTAGTTTCA-TCATTCTG 419
MnSOD           AATGCAGATTTTGCGTTCTTGTTATGGCTGTATTTGGTTGCCTTTGTTATACTCAGTGGC 141
                * *** * *     *      *  *  *   *    *  *** * ***  * *** *


FeSOD           TTGTAACAGAATC-CAGCCCTTGCGCGTTAAGGCACGCCAACATGAATATTTGTCTTGCT 478
MnSOD           GCAATGCAGAGTCACATACGTTGTGCAATTCT-CTCTGCAAAATCATTGGTTGTGTC--- 197
                      **** ** **  * *** **  *    * *  *** ** * *  **** *


FeSOD           CCGAATCTTTTCGACYCTTTGC 500
MnSOD           ----------------------
```

Figure 3.2.8. Clustal W alignment analysis of the FeSOD and MnSOD 3' UTR sequences along with identity. A consensus of 43 % was obtained when comparing the two sequences in terms of nucleotide identity.

Figure 3.2.9. Clustal W alignment analysis of the FeSOD and MnSOD full sequences obtained in this study. A 49 % consensus between the two sequences based on nucleotide identity was reached. The STOP codon has been highlighted in red to separate the 3'-UTR from the coding region.

3.3 Growth Analysis of *L. perenne* in Hydroponic Media

Seeds of perennial ryegrass (*L. perenne*) cultivar Grasslands Nui, accession number A11106 (AgResearch Grasslands, Palmerston North, New Zealand) were used in the hydroponic media to obtain healthy individual plants which would eventually be pooled together for SOD gene expression analysis.

Seedlings were first germinated under sterile conditions in petri dishes (Figure 2.1) and transferred to pottles for added space after germination had taken place. Once a sufficient root system had established (>2cm), seedlings were transferred to a full strength micro - half strength macro Hoagland's solution (Table 2.1) for eventual growth analysis.

Two hydroponic set-ups were constructed which were similar except for the age of seedlings used for the aluminium treatment (Figure 2.2). Both were treated with $AlCl_3$ to a final concentration of 0.2 mM. Seedlings were placed in pre-designated positions (observed in Figure 3.3.1) which were randomised. Each tray of seedlings was acclimatised for a week while the pH of the media was adjusted from pH 5.5 to pH 4.8 before the addition of $AlCl_3$.

3.3.1 Growth Analysis of the First Hydroponic Trial (Experiment I)

Root and shoot material was separated using a scalpel and a cut made at the root-shoot junction of each *L. perenne* plant. All material was pooled together and weighed in their respective groups before being placed in 50 mL falcon tubes and snap frozen in liquid nitrogen.

Over the time course, the pooled weight of root tissue for the control varied from 1.21 g (0.1 g mean weight of each root) to 2.15 g (0.18 g mean weight of each root) whereas the Al-treated root varied from 1.81 g (0.15 g) to 1.99 g (0.17 g) (Fig 3.3.1). In relation to aluminium treatment and the period of time the plants were exposed to $AlCl_3$ (0.2 mM), root growth appeared to be stimulated by the presence of aluminium under the conditions used. At the 0 hr time point both the control and Al-treated roots had a pooled weight of 0.81 g (0.15 g) but after 4hrs and 8 hrs of treatment, the mass of the

total root tissue had increased to 1.82 g and 1.99 g respectively. In comparison, pooled root tissue for the control had dropped to 1.21 g (4 hr) and 1.48 g (8 hr) but after 24 hr a mass of 2.15 g (0.18 g) was measured. After initial root stimulation seen at 4hr and 8hr of treatment, the Al-treated root tissue exhibited a slight decrease in mass with a final weight recording of 1.91 g at 24 hrs. However, as the data points represent the pooled weight of 12 seedlings, no statistical analysis was performed.

In comparison to the root, shoot tissue mirrored the 0 hr treatment by both giving initial weight recordings of 1.79 g (0.15 g mean weight per shoot) (Fig 3.3.1). Over 24 hr of treatment, the control shoot tissue weights ranged from 1.69 g to 2.45 g whereas the shoot tissue from the Al-treated samples ranged from 1.79 g to 2.38 g. Pooled shoot weights responded in a similar manner to that observed in the root tissue. At the 4 hr and 8 hr time points, the Al-treated shoot tissue was stimulated with measurements of (2.03 g) and (2.38 g) respectively. Again after 24 hrs of Al-treatment, growth was slightly inhibited with a decrease in shoot growth (2.36 g). Shoot tissue in the control responded in much the same way as root tissue after 4 hr and 8 hr treatment times. An initial decrease from 1.79 g (0 hr) to 1.69 g (4 hr) to a recording of 1.71 g (8 hr) was observed. A marked increase at 24 hr of 2.45 g mirrored the increase in root mass at the same time period in root tissue for the control. However, again, as the data points represent the pooled weight of 12 seedlings, no statistical analysis was performed.

A comparison between the shoot:root ratios between control and Al-treated samples yielded the following trends (Figure 3.3.2). With respect to the control, over time shoot biomass declined with a slight tendancy to produce more root biomass. At 4 hrs after treatment a shoot : root ratio recording of 1.4 was obtained with ratios of 1.16 and 1.14 for 8 hr and 24 hr respectively. In response to Al-treatment, different trends were obtained. Over time the shoot:root ratio increased from 1.12 after 4 hrs to 1.2 and 1.24 after 8hr and 24 hr. In terms of a direct comparison between the two treatments, the largest difference in shoot : root ratio occurred at 4 hr, with a high proportion of root mass observed in 24hr tissue compared to shoot.

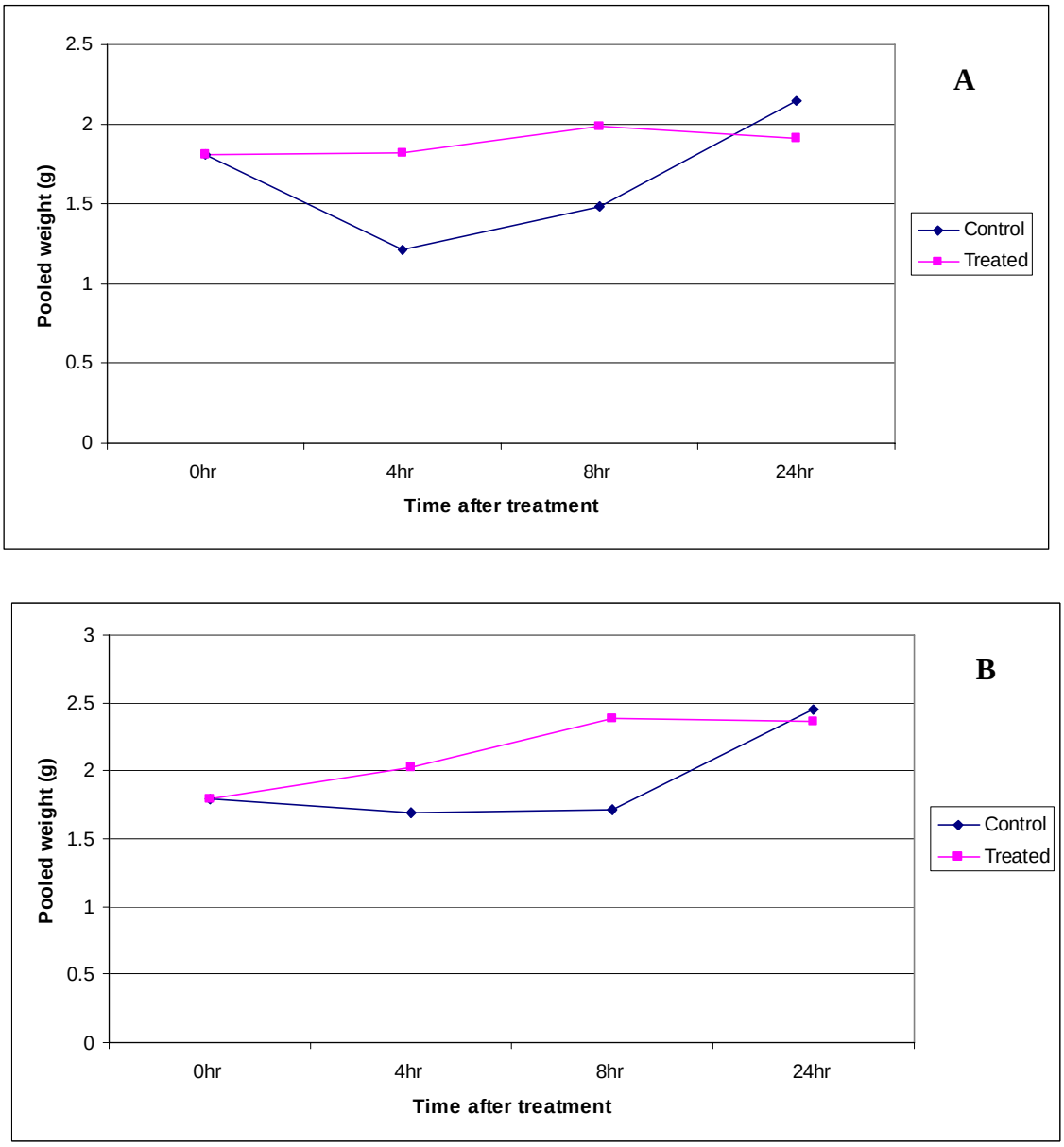

Figure 3.3.1. Growth analysis of the first hydroponic trial. Root (A) and shoot (B) pooled fresh weights (g) in response to aluminium treatment over time. Fresh weight was determined by pooling together 12 seedlings at each time point. Values are for the total pooled weight. Treated samples were subjected to 0.2 mM $AlCl_3$. Control samples were not treated with $AlCl_3$.

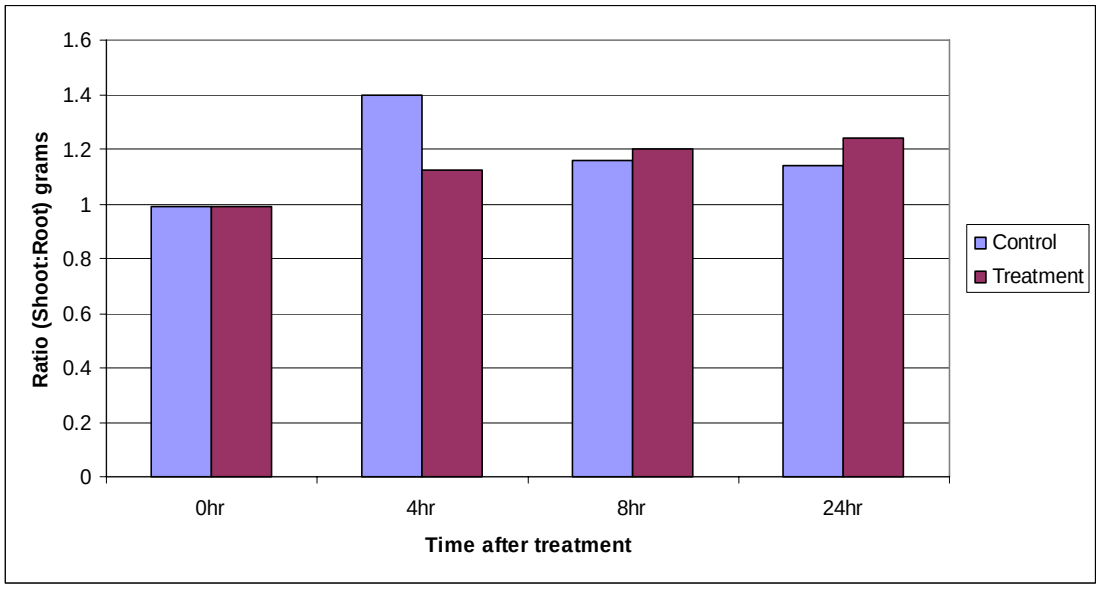

Figure 3.3.2. Growth analysis of the first hydroponic trial. Shoot : Root ratio comparison between control and Al-treated samples in response to 0.2 mM $AlCl_3$.

3.3.2 Growth Analysis for the Second Hydroponic Trial

A second hydroponics trial was designed to gauge the variability in root and shoot fresh weight between seedlings at each time point. This data provided the opportunity for some statistical analysis with the calculation of standard errors at each time point to gain a better understanding of the significance of the Al-treatment on the growth of *L. perenne*.

The mean weight for individual roots in the control treatment ranged from 8.5 mg (0 hr) to up to 9.1 mg (at 24 hr). Over the 24 hr of sampling, the average weight remained relatively consistent with recordings of 8.6 mg at 4 hr and 8.7 mg at 8 hr (Fig 3.3.3). In comparison Al-treated roots ranged from an average of 10.9 mg (4 hr), 13.6 mg (8 hr) and 12.4 mg at 24 hr. On average, the Al-treated roots weighed more than control roots but the differences are not significant at either the 4 hr or 24 hr time points after treatment (at the P=0.05 level). In contrast, root growth appeared to be stimulated after 8 hr of treatment with an average weight of 13.6 mg ± 1.2 for the Al-treated roots compared to the control 8.6 mg ± 1.1, and this difference was significant.

Similar results were observed for the shoot samples (Fig 3.3.3). Consistent average weights were recorded for control shoot samples within a range of 12.3 mg (0 hr) to 15.8 mg (4 hr). All four period points were not significantly different from each other but did seem to show a general trend of weight increase with time. Over time, the Al-treated shoot material slightly increased in weight from 19.2 mg (4 hr) to 19.7 mg (24 hr). In common with the Al-treated roots, Al-treated shoot material on average weighed more than the control shoot tissue, but these results were not significant at both the 4 hr and 24 hr time points (P=0.05). However, again at 8 hr after treatment, a significant difference was observed with the Al-treated shoots on average weighing 19.5 mg ± 2 and the control averaging 12.9 mg ± 2.3.

To determine whether root stimulation or a change in biomass had occurred, the shoot : root ratios were calculated (Fig 3.3.4). Over the time course, the Al-treated samples did not greatly differ from the control at each time point. Both treatments exhibited a high ratio at 4 hr with readings of 1.82 for the control and 1.75 for the Al-treated samples. A possible decrease in total shoot biomass or stimulation of root biomass consequently

followed with a decrease in the ratio at 8 hrs and 24 hrs. At 8 hr, the control ratio was 1.5 compared to the Al-treated of 1.42, and 1.59 for the control and 1.6 for Al-treated at 24 hr.

To better gauge the possible change in total biomass, Figure 3.3.4 was constructed. Over time, the average shoot weight remained constant with a range of 19.2 mg (4 hr) to 19.7 mg (24 hr). Average root weight also remained constant with readings of 10.9 mg (4 hr), 13.6 mg (8 hr) and 12.4 mg (24 hr). Further, no significant changes in biomass could be found at P=0.05.

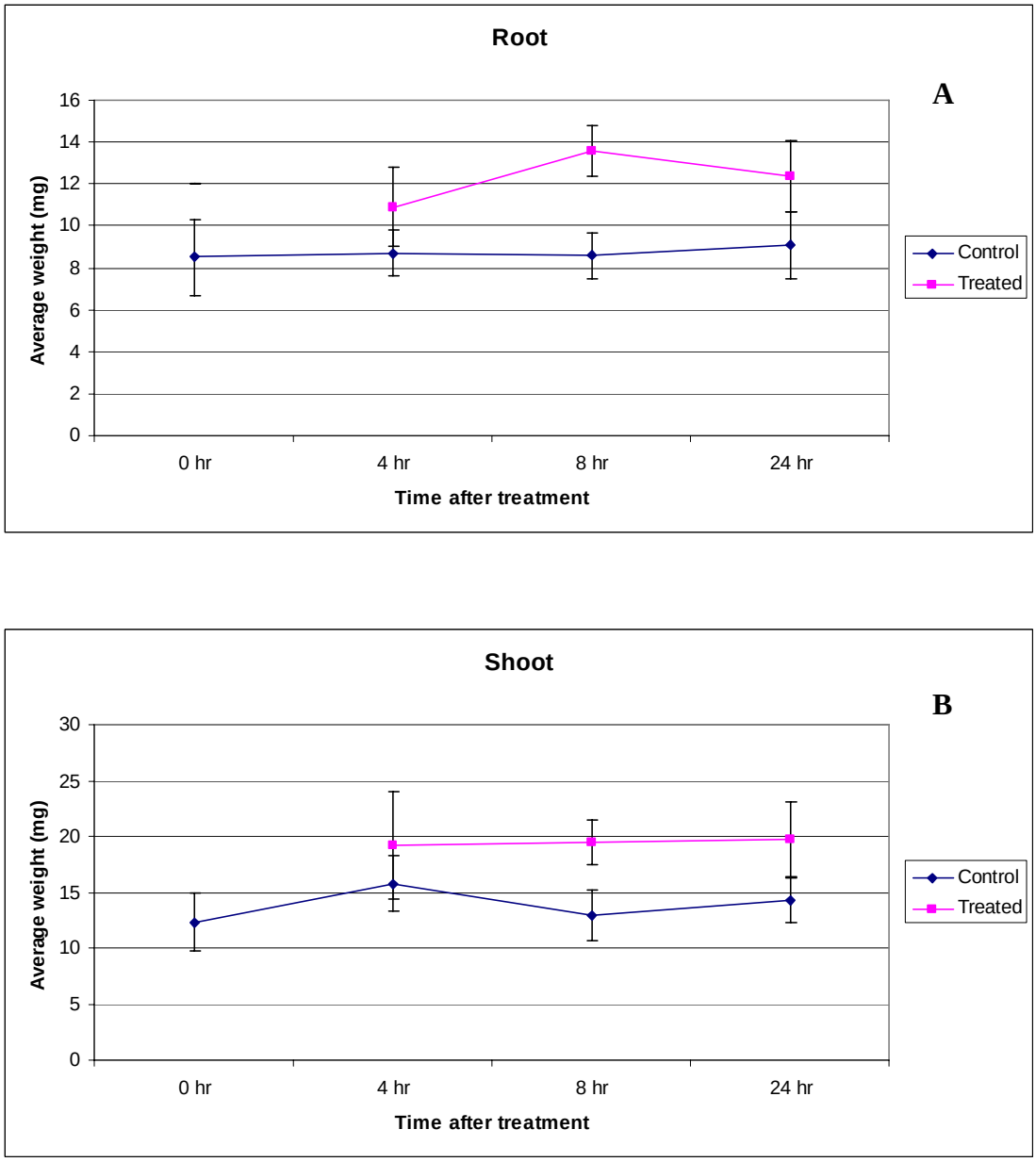

Figure 3.3.3. Growth analysis of the second hydroponic trial. Root growth (A) and shoot growth (B) in response in aluminium treatment (0.2 mM $AlCl_3$ or control) as indicated, over a short 24 hr period in *L.perenne*. Values are means ± SE, n = 9

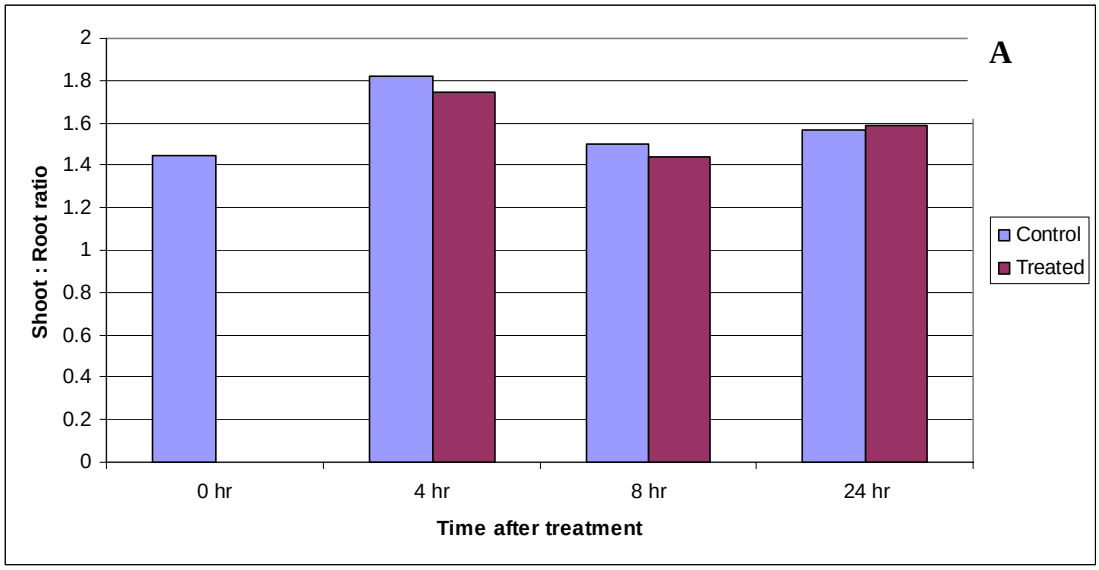

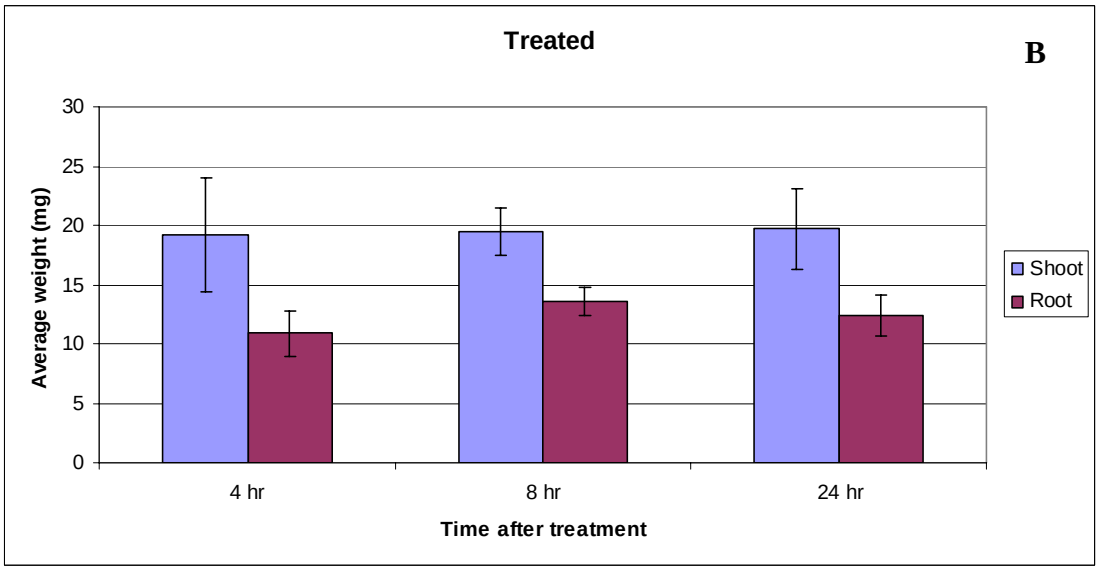

Figure 3.3.4. Growth analysis of the second hydroponic trial. Shoot : Root ratio comparison between control and Al-treated samples (A) and comparison between Al-treated shoot and root samples (B) of *L. perenne* in response to aluminium treatment (0.2 mM $AlCl_3$). Values for (B) are means ± SE, n=9.

3.4 Expression studies on isolated SOD isoforms in *L. perenne*

Expression of members of each gene family of the superoxide dismutase enzyme system in *L. perenne* in response to aluminium treatment was examined using samples collected over a 24 hr time period. Expression analysis was conducted using ethidium bromide stained products generated by the semi-quantitative Reverse Transcription – Polymerase Chain Reaction (sqRT-PCR). Individual plants were collected at each time point, separated into root and shoot material, which were then pooled and then used for RNA extraction.

Using sqRT-PCR, gene-specific primers designed to incorporate the 3'-UTR for the FeSOD and MnSOD genes were designed with the aim of specifically amplifying a single gene within the FeSOD or MnSOD gene families (if these families did comprise more than one gene). Prior to the actual experiment, a linearity assessment was conducted to determine the appropriate number of PCR cycles for each gene for which the template concentration was limiting. Actin was also used as a control to ascertain relative transcript abundance within each sample.

3.4.1 Analysis of FeSOD gene expression in L. perenne in response to 0.2 mM $AlCl_3$

Linearity studies carried out on the specific FeSOD gene isolated in this study in both root and shoot samples resulted in 34 cycles (Fig 3.4A) and 30 cycles respectively to be used in sqRT-PCR analysis. In response to Al-treatment, and in comparison to the control (non-treated), the FeSOD gene was not up- or down-regulated in shoot tissue. Under the conditions used, expression did not differ for this gene after 4, 8 or 24 hr after treatment with 0.2 mM $AlCl_3$ (Fig 3.4.0B). In relation to the control (non-treated) shoot samples expression of the FeSOD gene also remained unchanged.

Expression in the root samples mirrored the expression of the shoot samples (Fig 3.4.0E). In response to 0.2 mM $AlCl_3$, expression of the FeSOD gene did not differ over time in relation to the control (untreated) root samples.

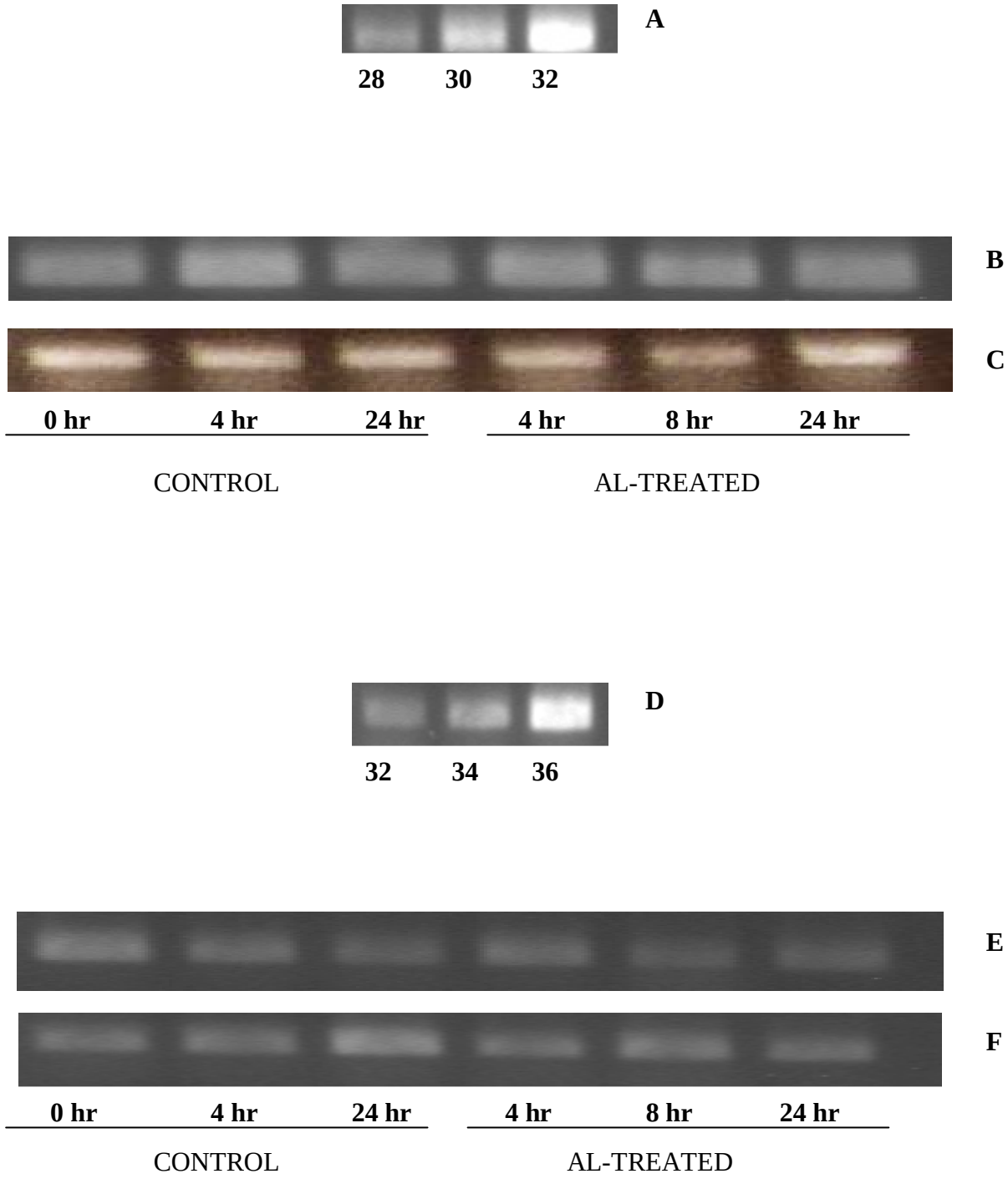

Figure 3.4.0. Semi-quantitative RT-PCR (sqRT-PCR) analysis of expression of a specific FeSOD gene. Responses to aluminium toxicity over time in *L.perenne* have been represented in both root and shoot. The linearity study is also included. Shoot (B) and root (E) expression analysis for FeSOD activity are compared against the internal control, actin (C, F). Linearity studies for the FeSOD primers in both shoot and root are also represented (A, D).

3.4.2 Analysis of MnSOD gene expression in L. perenne in response to 0.2 mM $AlCl_3$

Linearity studies carried out with the single MnSOD gene isolated in this study in both root and shoot samples resulted in the use of 28 cycles and 32 cycles respectively (Fig 3.4.1; A, D). In response to Al-treatment expression of the MnSOD gene did not differ significantly over 4, 8 or 24 hr of treatment in shoot samples when compared to expression in control tissues.

In root samples, a change in expression of the MnSOD gene occurred in response to 0.2 mM $AlCl_3$ (Fig 3.4.1; E). In comparison to the control root samples, a decrease in expression is observed at both 4 hr and 24 hrs after Al-treatment. Expression at 8 hrs is relatively constant in comparison to the expression levels observed in the control root sample at 0 hr and 4 hr. Therefore, over the 24 hrs of treatment expression of the MnSOD gene fluctuates when compared to the control sample.

3.4.3 Analysis of total CuSOD activity in L. perenne in response to 0.2 mM $AlCl_3$

As the isolation of a 3'-UTR sequence from the CuSOD gene was unsuccessful, degenerate CuSOD primers were used to monitor total CuSOD expression in response to 0.2 mM $AlCl_3$. With regard to linearity studies 30 cycles were used for both root and shoot expression (Fig 3.4.2; A, D). Total CuSOD gene expression was not affected by Al-treatment and this was seen in the shoot samples in comparison to the control samples (Fig 3.4.2B). Expression remained the same in Al-treated samples at 4, 8 and 24 hr. Expression in 0, 4 and 24 hr control (untreated) samples mirrored the expression response seen in the Al-treated samples.

In comparison to the shoot, expression in the roots was also not affected by Al-treatment. Total CuSOD activity in the treated root samples were similar after 4, 8 and 24 hrs of treatment. Expression levels in the treated samples were the same as the control root at 0 hr and 4 hr. Expression of CuSOD in control root samples at 24 hr was significantly increased compared to all other time points and samples (treated, control) (Fig 3.4.2E).

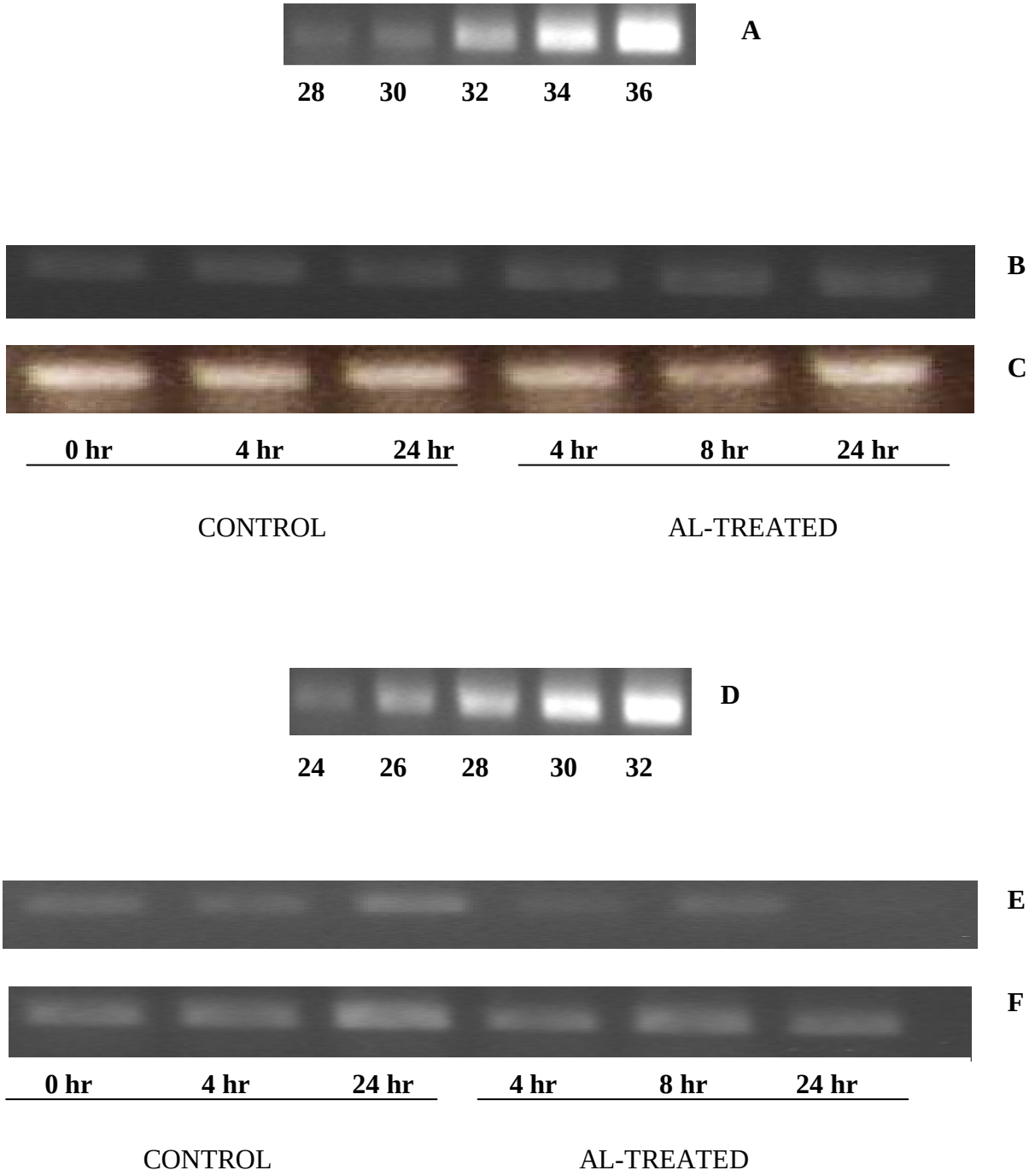

Figure 3.4.1. Semi-quantitative RT-PCR (sqRT-PCR) analysis of induction of the MnSOD UTR gene. Responses to aluminium toxicity over time in *L.perenne* have been represented in both root and shoot. Linearity study also included. Shoot (B) and root (E) expression analysis for MnSOD activity are compared against the control, actin (C, F). Linearity studies for the MnSOD primers in both shoot and root are also represented (A, D).

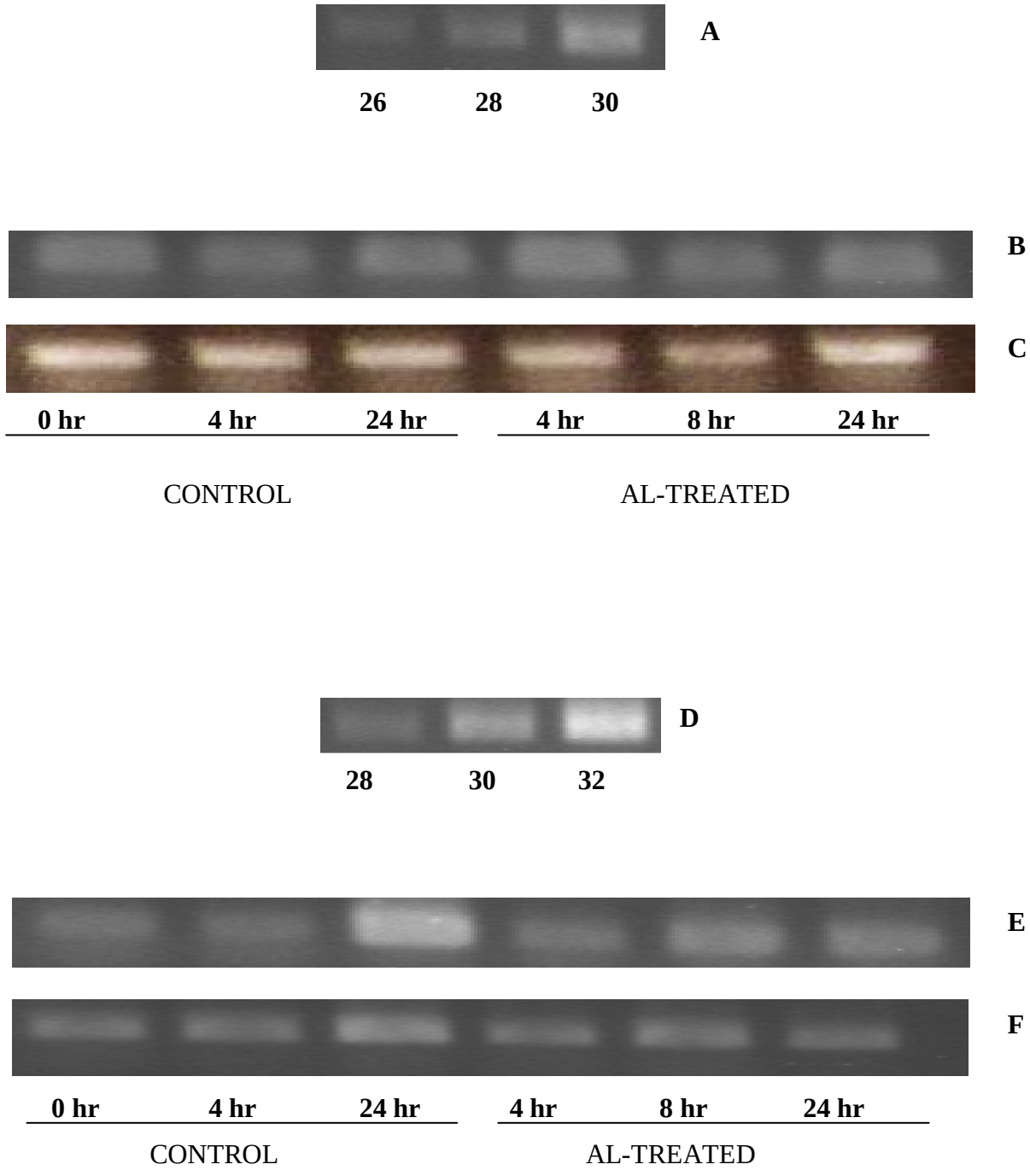

Figure 3.4.2. Semi-quantitative RT-PCR (sqRT-PCR) analysis of induction of total CuSOD gene expression (using degenerate CuSOD primers). Responses to aluminium toxicity over time in *L.perenne* have been represented in both root and shoot. Linearity study also included. Shoot (B) and root (E) expression analysis for CuSOD activity are compared against the control, actin (C, F). Linearity studies for the degenerate CuSOD primers in both shoot and root are also represented (A, D).

4. Discussion

The first part of this thesis aimed at the isolation and sequencing of genes from each of the isoforms found in a component of the antioxidant system, the superoxide dismutase (SOD) enzymatic system. The second part of this thesis sought to determine if an aluminium treatment (at a concentration of 0.2mM) had an effect on the growth of *L. perenne* seedlings growing in a hydroponic media. Finally, the expression of the isolated and identified SOD genes were analysed in aluminium-treated and non-treated root and shoot tissues over a short time course of 24 hours.

4.1 Aluminium treatment does not negatively affect root and shoot growth of *L. perenne* over a short treatment course

Under two constructed hydroponic experiments (that differed in the length of time seedlings were left in the hydroponic media prior to aluminium treatment and thus plant age) root and shoot growth were not significantly negatively affected by the addition of aluminium, in the form of the aluminium salt, $AlCl_3$, when added to a final concentration of 0.2mM.

4.1.1 Affect of aluminium on root growth in L. perenne

After 24 hours of treatment with aluminium to a final concentration of 0.2mM, *L. perenne* seedlings had a mean root weight of 12.4 mg ± 1.7 each compared to the control of 9.1 mg ± 1.6 (2^{nd} hydroponic trial) (Fig 3.3.3). This second trial was seen as an improvement on the first as it allowed for statistical analysis to be applied by individually weighing each seedling. Although this was the case, the different mean weights observed between the two treatments proved insignificant.

Although the first hydroponic trial dealt with pooled weights instead of individual weights (no statistical analysis could be gathered because of this) the results were very similar when compared with the second trial. The pooled weight of roots after 24 hours from the aluminium treatment weighed 1.91 g while the control pooled root weighed 2.15 g (Fig 3.3.1). This is a difference in individual weight of 0.02 g per seedling which is very close to the standard error seen in the second hydroponic trial.

These results are interesting as they seem to contradict the literature (Achary et al., 2008; Giannakoula et al., 2008). However it must be noted that this trial was completed over a very short time frame (24 hours). It is often identified in field and hydroponic trials that aluminium concentrations detrimentally inhibit the growth of root tissue but it should also be noted that root growth was not measured in this thesis, only changes in the fresh weight over time. As early as 1965, Clarkson, 1965, observed root growth on aluminium laced soils was observed to be inhibited in *Allium cepa*. Since then root growth, which is the product of cell division and elongation, has been shown to be affected by the presence of aluminium in a number of species (Ciamporova, 2000).

The use of a final concentration of 0.2mM $AlCl_3$ may have caused a reduction of root growth over a longer period of time in *L. perenne* as similar concentrations of aluminium have reduced the growth of individual roots in other species. For example, in a study on the effect of aluminium on *Phaseolus aureus* (mungbean), concentrations of 2mM and 5mM caused a reduction in root length of 8.05 cm ± 0.57 and 5.29 cm ± 0.77 from a non-treated mean root length of 11.68 cm ± 0.14 (Abdullahi et al., 2003). However, this effect was observed after two weeks in aluminium treatment.

Similar results were seen in shorter term studies involving *Glycine max* (soybean) where control root length (untreated) roots measured 20.5 cm ± 0.2 but after treatment with 500 µM of aluminium caused a reduction in mean length of roots to 12.4 cm ± 0.1 after 48 hours of treatment. This reduction in root length is explained by the binding of aluminium to nucleic acids and a reduction in cell division. Interestingly, the same study observed an increase in mean root length with 200 µM treatment, the same concentration used in this thesis (0.2 mM). The result yielded an increased root length of 22.1 ± 0.2, but this was not significant after 48 hours of aluminium treatment. (Balestrasse et al., 2006). Such a result is comparable with the hydroponic trials and the conditions of aluminium treatment used in this thesis. A result similar to this one could show that under the conditions used a concentration of 0.2mM of aluminium in solution may not affect root growth when measured as fresh weight in such a short time frame.

As well, tolerance to aluminium could be quite high in *L. perenne* cv. Nui, although a number of authors have documented that grasses have a low tolerance to aluminium

toxicity (i.e. reduction in cell elongation, reduced root growth, plants exhibiting toxic symptoms) (Wenzl et al., 2001; Poozesh et al., 2007) The variability between grass species in response to aluminium toxicity resistance ranges from 1 to 50 µM (Al^{3+}), with a number of grass species such as *Festuca rubra* and *Holcus lanatus* being able to tolerate aluminium at 10-20 µM (Poozesh et al., 2007). Certain cultivars of *L. perenne* have been identified that can not tolerate levels above 2 µM, but variance in resistance have been observed in a number of other cultivars of *L. perenne* (Wenzl et al., 2001; Poozesh et al., 2007). From the literature c.v Nui has not been evaluated but when exposed to 200 µM albeit for 24 hours, no apparent changes were observed.

Results such as these depend on resistance mechanisms that cultivars of species have genetically programmed or evolved in response to metal toxicity. Not all results are going to be clear cut as many cultivars of wheat and barley are known to be tolerant of aluminium levels that would commonly be toxic to other plant species. Cultivars of *Zea mays*, *Triticum aestivum* and *Hordeum vulgare* have all been documented to show extreme tolerance to toxic levels of aluminium (Taylor & Foy, 1985.; Pintro et al., 1998.; Gunse et al., 2000.; Pan et al., 2001). It must also be noted that there are differences between field and hydroponic trials as the speciation of aluminium differs. Polynuclear complexes of aluminium (usually found occurring in soils) are more toxic to plants than monomeric, less charged species of aluminium (usually used in hydroponic trials) (Rengel, 1996). These mechanisms will be discussed later.

4.1.1.1 Affect of aluminium on root morphology in L. perenne

Although this thesis aimed to isolate genes of the SOD enzymatic system and studying their expression in response to aluminium treatment, it must also be noted that aluminium causes morphological changes to plant roots. Over the 24 hours of treatment with 0.2mM of aluminium, root morphology was not observed to deviate from control root morphology (note : these are morphological changes observed visually). One major change in relation to root morphology was the amount of time the *L. perenne* seedlings remained in hydroponic media. Seedling roots of *L. perenne* in the first hydroponic trial remained in solution before treatment for an extra two weeks compared to the second hydroponic trial. These roots (1st trial) were a lot darker in colour and larger in circumference when compared with those in the second trial. Roots of the second trial were up to 50 % smaller in circumference and creamy-white in colour. This is a significant change in morphology, that occurred in just over two weeks of being treated to a media suited for efficient tissue growth to occur but not attributed at all to aluminium treatment. Seedlings of *L. perenne* that remained in media were transferred into solution after germination and initial growth (14 days) but the first trial seedlings remained in hydroponic media for four weeks (final age being 42 days) while the second trial seedlings remained in solution for only two weeks (final age being 31 days).

Long term affects of aluminium toxicity on root morphology have also been well documented. Roots of a number of species (*Allium cepa, Triticum aestivum, Zea mays*) have appeared stunted and thickened in response to aluminium treatment after long term treatment (1-2 weeks) (Jones et al., 2006; Achary et al., 2008; Giannakoula et al., 2008). It has also been documented that roots may become irregularly curved and change colour in response to aluminium toxicity after four weeks of treatment (seedlings were 42 days old once harvested) (Eleftheriou et al., 1993; Budikova et al., 1997). Such morphological changes induced by aluminium treatment resulted in reduced root biomass, resulting in poor pasture growth. Though the roots used in this trial differed in colour and size between the two hydroponic trials, this was not in response to aluminium treatment but due to the favourable growth conditions of the media and age of the root system.

4.1.2 Affect of aluminium on shoot growth in L. perenne

Shoot biomass (mean weight) in response to 0.2mM $AlCl_3$ for 24 hours did not change significantly compared to the untreated control shoot tissue. With concern to the second hydroponic trial, Al-treated shoot tissue weighed more on average than the control (also seen in aluminium treated root tissue in second trial) but this was not significant (Fig 3.3.3). A mean weight of 19.7 mg for Al-treated shoot tissue (24 hr) and a mean weight of 14.8 mg for control tissue (24 hr) proved insignificant due to high variability in the data set. In comparison to the first hydroponic trial, which used pooled weights, the Al-treated tissue again would have been insignificant in weight difference compared to the control when looking at individual seedling shoot weight gain.

Significant changes in shoot growth would have been surprising as root growth was not affected, as determined by a significant weight change per seedling (a large change in root weight may also cause signalling to aerial parts and in doing so, reduce shoot biomass). Any change in fresh weight would have also been surprising as inhibition of root cell elongation is believed to occur in a matter of minutes (30 min - 2 hours) at even micromolar concentrations to aluminium toxicity (Mimmo et al., 2009). This inhibition enables the induction of signal transduction events which eventually leads to a cascade in signalling and perception by the aerial parts of the plant (shoot tissue). Though the root tissue may perceive these changes quite rapidly, it would be surprising to notice the changes (in weight) in the shoot over such a small time frame of 24 hours after aluminium treatment. Such a cascade of events may have occurred in this study using *L.perenne* as the plant species but anatomical analysis was not carried out. However, Meriga et al (2004) did observe a reduction in shoot growth in as little as 40 hours after treatment with 80 µM of aluminium in two cultivars of rice. Both cultivars exhibited a reduction in root growth after 40 hours but signalling on the perceived aluminium toxicity in the shoots only resulted in a lower growth reduction in the shoots compared to the roots.

4.1.3 Affect of aluminium treatment on total biomass in L. perenne

As aluminium toxicity at different concentrations (depending on the plant species) causes a decrease in root length and subsequent reduction in shoot growth, it would be helpful in determining if a change in total plant biomass would occur after such a limited time as used in this thesis.

A shoot to root ratio compares a treated sample with a control sample, with the higher ratio suggesting either an increase in total shoot biomass or a subsequent decrease in root growth. Documented cases of a change in biomass using shoot to root ratios (shoot : root) have not been noted in literature, but one has been constructed for the two hydroponic trials used in this investigation. In comparison to the control, aluminium treated plants exhibited a higher shoot biomass ratio at 8 hr and 24 hr after being treated (1^{st} hydroponic trial) (Fig 3.3.2). This could possibly indicate a shift between decreased root growth or a reduction in the total weight of both plant tissues with the roots responding a lot faster to the detrimental nature of 0.2 mM of aluminium. These results were comparable to that found in the second trial where an increased biomass was observed at 24 hr for the aluminium treated tissues. Two trends may exist when looking at biomass (weight changes), a change in total biomass of the plant in response to aluminium or a change in partitioning of growth, i.e a change in the root to shoot ratio.

Most documented cases do not deal with change in biomass ratios but delve into reductions in overall plant weight in response to toxic levels of aluminium. Analysis into aluminium treatment of mungbean (Abdullahi et al., 2003) at a concentration of 2mM is sufficient to cause significant reductions in seedling epicotyl and root length and also seedling height. These seedlings were treated for 2 weeks with $AlCl_3$, with an eventual total biomass reduction (fresh weight) of up to 50 % when treated with 2mM. At 5mM the total biomass was reduced 90 % compared to the untreated control. Long term studies in *L. perenne* at a 0.2 M concentration of $AlCl_3$, as used in this thesis, may in fact, lead to a similar response. However, after 24 hours of exposure to aluminium treatment, as carried out in this study, did not cause a reduction.

4.2 Sequencing and Isolation of Genes Encoding the SOD Enzymatic System in *L. perenne*

To enable expression analysis to be undertaken on the SOD enzymatic system in *L. perenne*, molecular methods were used to isolate at least one unique gene for each member of the SOD isoform system initially based on degenerate Cu/ZnSOD, FeSOD and MnSOD primers and then using 3'RACE to generate a unique 3'-UTR.

4.2.1 Evolutionary Nature of the SOD enzymatic system and L. perenne

The SOD enzymatic system is a key member of the antioxidant pathway in both eukaryotic and prokaryotic bodies, protecting cells from the harmful by-products of aerobic metabolism. They are grouped as metalloenzymes that occur in three different molecular forms based on their prosthetic metals, a Cu/ZnSOD, FeSOD and a MnSOD, and whose function is to catalyse the disproportionation of superoxide radicals which are generated during oxidative reactions. To understand the importance of the system, SOD deficient organisms such as *E.coli* are extremely hypersensitive to oxygenic environments and result in eventual death (Bowler et al., 1992; Fink & Scandalios, 2002).

Until comparatively recently, it was believed that not all three isoenzymes existed in higher plants. In most higher plants, MnSODs and Cu/ZnSODs were uniformally distributed throughout the plant but in the case of FeSODs, these enzymes were only thought to exist in prokaryotic organisms and tree species from the *Ginkoaceae*, *Nymphacea* and *Cruciferae* (Bridges & Salin, 1981; del Rio et al., 1985). But more recently, genes belonging to FeSOD have been isolated from a number of angiosperm species that lack close phylogenetic relationships to these families such as tobacco, *Arabidopsis thaliana*, rice and soybean (Murao et al., 2004). Although this is the case, there are still a few species that either lack all three isoenzymes or only contain one isoform (e.g. the CuSOD isoenzyme in sunflower) rather than three (Corpas et al., 2006).

The degenerate primers in this study which were designed and based around the conserved sequences in *O. europaea* (Corpas et al., 2006), were used to determine if all

three isoforms of the SOD system existed in *L. perenne*. Using pGEM for transformation of a DNA insert into *E.coli* DH5α, colonies were then sequenced for SOD sequences expressed in root tissue of *L. perenne*. One-hundred colonies were sequenced for each of the three SOD isoforms commonly found in higher plants and analysed against the genebank database using BLASTn to search for identity with other graminaceous species.

All three returned high identities with graminaceous species showing that among these groups, sequence identity is very similar. Of interest in this study, was the ability of the degenerate FeSOD primers to amplify a sequence that showed high identity to MnSOD sequences in the database and which consequently was used to design gene-specific MnSOD primers using 3'RACE.

The consensus sequence used for CuSOD analysis had high identity to *Oryza sativa* (84%) but also to a number of other species such as *Zea mays* and *Olea europaea* (79%) (Table 3.1.0). In comparison, the consensus FeSOD sequence used for analysis had high identity to *Zea mays* (82%), and *Oryza sativa* (69%) (Table 3.1.1). Also using BLASTn, a number of other eukaryotes such as the liverwort, *Marchantia paleacea* with an identity of 72% (over a query coverage of 42%) and also the algae, *Dunaliella salina* with an identity of 74% (24% query coverage) were identified. Similarly, the MnSOD sequence used for analysis had high identity to *Triticum aestivum* (86%) and *Saccharum officinarum* (85%) but also identity to a number of other organisms such as *Dimocarpus longan* (fruit similar to lychee) (76%) and *Zantedeschia aethiopica*, a lilly native to South Africa (76%). Moreover, the ability of the FeSOD degenerate primers to pick up MnSOD sequences has been observed before. Kaminaka et al. (1999) isolated a FeSOD gene from rice that lacked FeSOD activity and was able to demonstrate that recombinant proteins of the gene expressed in *E. coli* showed MnSOD enzyme activity. This could possibly mean plants lacking FeSOD activity may obtain an MnSOD activity derived from the related FeSOD gene. However, activity analysis of the genes as recombinant proteins was not undertaken as part of this thesis.

This information signifies the importance of the conservation of isoform SOD sequences among higher plants and other organisms. The amino acid sequence alignment observed by Fink & Scandalios (2002) shows a high homology among the

proteins that they studied. Their work on the phylogenetic relationships between non-plants and plants was able to show that plant SOD sequences group together, while viruses and other non-plant organisms form their own groups. This could explain why low homology (identity) was observed for the sequences isolated in this study as higher plants group together due to their close phylogenetic relationship while other organisms such as prokaryotes have evolved differently compared to other multicellular organisms.

All three sequences generated in this study were nucleotide (and amino acid) aligned in Clustal W to identify a relationship between isoforms due to the fact that high homology has been noted in a number of studies (Bowler et al., 1992; Gupta et al., 1993; Fink and Scandalios, 2002). At the amino acid level, the MnSOD and FeSOD sequences exhibited an identity of 38% compared to CuSOD which had an identity of 23% with MnSOD and 19% with FeSOD. In terms of structure, MnSOD and FeSOD are similar, while Cu/Zn is structurally unrelated (Bowler et al., 1992). Moreover, the phylogenetic distribution of the three isoenzymes tends to indicate that MnSOD and FeSOD are both ancient and may have evolved before the diversion of the prokaryotic and eukaryotic lineages (Bowler et al., 1992). Amino acid deduction for sequences of the three isoforms also suggests that the Cu/ZnSOD isoenzyme is unrelated and may have evolved separately in some eukaryotes at a later date (Alscher et al., 2002; Fink & Scandalios, 2002). A suggestion for such an evolution has been made by Alscher et al (2002) and Exley (2004) which is that as evolution progressed, the metal requirements of each SOD isoenzyme differed in response to soluble metals available and the changing oxygenic status that occurred through each geological era.

4.2.2 Gene relationships amongst SOD isoforms in L. perenne

Each of the three isoenzymes of the SOD enzymatic system is not coded by one gene but in some species an isoenzyme is in fact, comprised of a multi gene family (Corpas et al., 2006). Multiple forms of SOD have been found in plant species to date, including *Zea mays* which comprises at least nine isoenzymes of the SOD enzymatic system so contains a number of genes that code for each isoenzyme. Five of these isoenzymes are dimeric Cu/Zn containing proteins, while one Mn-containing tetrameric enzyme exists. (Fink & Scandalios, 2002). The most documented case of a multi gene family existing for the SOD isoenzyme system is *Arabidopsis thaliana* which contains three genes encoding Cu/ZnSOD, three genes encoding FeSOD and one coding for MnSOD (Kliebenstein et al., 1998).

Due to the fact that it is currently unknown how many genes code for each isoenzyme identified in *L. perenne*, the protocol of 3'RACE was used to isolate a unique gene for each SOD isoform. A 500 bp FeSOD sequence was analysed showing high identity (85%) to an FeSOD sequence obtained from *Oryza sativa* in BLASTn. The sequence obtained originated from the untranslated region which is able to provide gene-specific sequences for the isoform gene, but this cannot be guaranteed in some cases due to similar sequence homology between gene sequences. The 3'UTR sequence for the FeSOD gene that was used for expression analysis was also analysed to identify if it matched with the reading frame generated using the degenerate primers. A match identified the sequence as a gene from the reading frame. This analysis was also carried out on the MnSOD sequence which contained a 3'UTR sequence length of 197 bp which showed a high identity of 88% with a MnSOD sequence originating from *Triticum aestivum*. This step was undertaken to reduce the chances of obtaining expression patterns related to a number of genes of each isoform in *L. perenne*.

Unfortunately, the identity hits that showed high similarity with the FeSOD-3'UTR sequence obtained in this thesis were from molecular characterisation studies of cDNA and not sequences isolated in response to metal or environmental stresses. But the MnSOD-3'UTR sequence which had high identity to *Triticum aestivum* (AF092524) is a sequence obtained from genebank which is a full-length mRNA that has been subjected to aluminium treatment. AF092524 is a 896 bp mRNA sequence which has been

isolated from aluminium treated wheat roots. Unfortunately this sequence is unpublished and only remains on the NCBI database, and so no details of the concentration or duration of the aluminium treatment are given.

4.3 Expression analysis of the three genes coding for isoforms of the SOD enzymatic system

In terms of FeSOD gene expression, the results of sqRT-PCR analysis showed that under the conditions used expression of the gene was neither up-regulated or down-regulated over time in response to treatment with aluminium at 0.2mM in either root or shoot tissue. Both Al-treated root and shoot samples over the time course of treatment (4-24hr) had comparable levels of expression when compared to the control (non-treated samples) (Fig 3.4.0). Similar results were observed for the expression analysis of the MnSOD gene isolated in this study. Expression of the MnSOD gene in response to aluminium treatment did not change over time in comparison to the non-treated samples used in sqRT-PCR analysis in shoot tissue. A slight reduction in expression was observed in Al-treated root samples at both 4 hr and 24 hr after treatment in comparison to the control (non-treated) root samples (Fig 3.4.1).

Although a specific gene could not be isolated (in terms of a 3'-UTR sequence) for the CuSOD isoform, the use of the same degenerate primers that were utilised at the beginning of this study (Corpas et al., 2006) were used to identify if total CuSOD activity was induced (or decreased). Degenerate primers used in this study would function by expressing all related CuSOD genes that exist in *L. perenne* when observing expression analysis. Expression did not appear to change in response to Al-treatment but it must be noted that expression of the control (non-treated) 24 hr point is much higher. This can be explained by a much higher actin expression at this point, resulting in greater expression of the total CuSOD activity (Fig 3.4.2).

4.3.1 Possible explanation of observed expression results

The comparison of expression analysis used in this study have been documented in other plant species, but where the enzyme activity of the three isoenzymes has differed in response to different environmental stresses. CuSOD enzyme activity can remain static while MnSOD enzyme activity can be up-regulated while FeSOD enzyme activity is down-regulated (Achary et al., 2008). However, it cannot be discounted that the genes coding the specific isoenzymes isolated in this study are housekeeping genes, i.e. genes whose expression does not change in response to a stress such as aluminium. It is even possible that under the conditions used, aluminium at 0.2mM is not a sufficient concentration to cause oxidative stress in *L. perenne* cv. *Nui*. Further work is needed to elucidate the responses observed. In saying this, plants function in two ways in response to aluminium stress, detoxifying harmful aluminium species externally (excretion of organic acids) or internal detoxification of aluminium (the antioxidant pathway, and other tolerance mechanisms).

4.3.1.1 Organic acids

Excretion of organic acids at the rhizophere-media interface has been shown to cause a reduction in expression of key components of the antioxidant pathway. This is one method that tolerant plant species use to combat aluminium toxicity by chelating aluminium or detoxifying it either within the plant (tolerance) or at the rhizosphere interface (exclusion). Stimulation of organic acid excretion in response to aluminium was first reported in *P. vulgaris* in 1991 cited in Rangel et al., 2007.

Compelling experimental evidence suggests a number of plant species including several dicots and monocots exclude aluminium ions from entering root tip cells by secreting organic acids (dicarboxylic and triboxylic acids) such as malate, citrate and oxalate acids that eventually immobilise the ions by forming stable non-toxic complexes (Furukawa et al., 2007; Liu et al., 2007; Pineros et al., 2008). The most common organic acids released are malate and citrate but plant species differ in the type of organic acid secreted and the sensitivity to aluminium in respect to secretion patterns (amount of organic acid produced to detoxify aluminium) of organic acids (Liu et al., 2009). Furukawa et al. (2007) even goes as far as separating plants based on two mechanisms

of organic acid excretion, the first being that a number of plant species secrete organic acids immediately in response to aluminium while the second mechanism is a delay in the excretion of organic acids after exposure to aluminium which suggests that gene induction is required (Furukawa et al., 2007).

Within plant species, Al-resistant cultivars are identified by the exclusion of aluminium from root cells in response to organic acids that have been secreted, and in doing so, result in the exclusion of aluminium from the roots. Liu et al. (2007) observed that Al-resistance in *Triticale* cultivars was positively correlated with the levels of malate and citrate secretion which resulted in reduced levels of aluminium accumulation in root apices of ten cultivars after nine hours of exposure to 50 µM of $AlCl_3$. Thus, exclusion of organic acids can be immediate or delayed and allow the detoxification of aluminium in media.

With respect to this study the excretion of organic acids is a possibility and may explain why expression levels of the SOD genes remained static over the time of treatment. However, this aspect was not addressed directly.

4.3.1.2 SOD activity in response to oxidative stress

Conflicting documented cases surround total SOD enzyme activity with regards to aluminium toxicity and other environmental stresses. In contrast, to the expression of two genes (MnSOD, FeSOD) and possible total expression analysis of one isoform of the SOD system (CuSOD) in this study, most literature analyses total SOD enzyme activity in plants. However, aluminium toxicity has been documented in some cases to down-regulate or fail to induce a response in SOD enzyme activity in rice (Kuo & Kao, 2003). Detached leaves of rice treated with 5mM $AlCl_3$ resulted in lower overall SOD enzyme activity than those that were not treated over a time course of three days. Leaves were excised and kept in petri dishes in media with added aluminium. However, other components of the antioxidant pathway such as catalase and glutathione reductase (enzyme activity) increased in response to Al-treatment (Kuo & Kao, 2003). Such a response could possibly result in increased levels of superoxide anions reacting with hydrogen peroxide that had not been converted by catalase to form hydroxyl radicals in the leaves of rice.

At the isoform level, expression seems to differ. Oxidative stress resulting from aluminium toxicity in *Allium cepa* (bulbs set for rooting for two days) resulted in varied gene expression of MnSOD, FeSOD and CuSOD isoforms in response to concentrations of $AlCl_3$ ranging from 0-100 µM after 4 hours. Results identified the up-regulation in expression of the CuSOD isoform in a dose-responsive manner but FeSOD only slightly increased in response to increased aluminium treatment. Moreover, the MnSOD isoform did not exhibit any increase in expression but remained static in response to increased levels of aluminium. Overall (*A. cepa* study) total SOD enzyme activity increased in response to increased levels of aluminium (Achary et al., 2008). Similar results were observed in cultivars of *Oryza sativa* where total SOD enzyme activity increased in response to 160 µM $AlCl_3$ after 15 days of exposure but at the isoform level, expression activity varied. Roots treated with 160 µM of the aluminium solution exhibited an increase of 39% in enzyme activity of the CuSOD isoform, 52% for FeSOD and 53% for the MnSOD isoform (Sharma & Dubey, 2007). Further to this study, levels of hydrogen peroxide increased significantly in response to the increased conversion of superoxide ions to hydrogen peroxide, which increased catalase enzyme levels were unable to convert efficiently which resulted in cell death in *Oryza sativa* root tip cells. This downside to increased SOD enzyme activity has been noted before with plants overexpressing isoforms of the SOD enzymatic system resulting in toxic levels of hydrogen peroxide being formed (del Rio et al., 1985; Gupta et al., 1993; Basu et al., 2001).

It has been identified that changes in isoform expression in response to aluminium toxicity can result in isoforms being repressed or promoted in response to metal deficiency. In the fern *Matteuccia struthiopteris,* FeSOD gene expression could be regulated by controlling the levels of Fe and Cu in the media solution. Results indicated that expression of the FeSOD gene was induced by Cu depletion but was also induced by the addition of Fe (Murao et al., 2004). Thus element concentrations in hydroponic media may play a part in expression of SOD genes in response to Al-toxicity.

The slight decrease in expression of the MnSOD gene at 4 hr and 24 hr after treatment with 0.2 mM of AlCl3 (Fig. 3.4.1) and static expression levels of the FeSOD gene and total expression in the CuSOD isoform provide further proof that isoform expression

can differ between the three SOD isoenzymes in response to Al-treatment. In response to ozone mediated stress in *Arabidopsis thaliana*, three CuSOD genes, two FeSOD genes and one MnSOD gene all responded differently over time but enzyme activity of total SOD expression increased in relation to the stress (Kliebenstein et al., 1998). Differential expression of genes may elucidate to the fact that only some genes expressed are responsible for the detoxification to aluminium in different cellular compartments while static expressed genes may be required for another cellular process or require a higher level of toxicity to be induced. Further insight of the role of SOD in the response to Al-treatment in *L. perenne* could be gained through the measurement of total enzyme activity for each isoenzyme.

4.4 Future Work

This study has provided insights into defence mechanisms surrounding *Lolium perenne* and its response to aluminium treatment, looking particularly at a key component of the antioxidant pathway, the superoxide dismutase (SOD) enzymatic system. Cloning and sequencing of genes expressed during aluminium toxicity were analysed and although expression analysis did not detect anything of great interest, potential avenues of research interest could be followed. Consideration of the growth of *L. perenne* in response to aluminium also could see potential research in long term growth studies.

- Morphological studies of root growth and internal cell structure and function could be studied in longer term growth trials at a range of aluminium concentrations.

Aluminium toxicity has been observed to cause deformities in normal root morphology and cause detrimental effects to cell cytoskeleton structure resulting in deformed root shape, brittleness and off-colour.

- Analysis of organic acid secretion at the rhizosphere interface in response to aluminium toxicity in *L. perenne* should be undertaken. This analysis could involve a number of cultivars of *L. perenne* to determine tolerance levels

- If possible, a number of SOD related genes for each of the isoforms should be isolated to determine if any of these are differentially expressed over time in response to aluminium concentrations. Also other components of the antioxidant pathway such as catalase could be analysed, both at the gene and enzyme activity level.

- Design an improved method for hydroponic studies so as to allow replication studies at differing concentrations of aluminium with reduced standard errors – that is, provide more sound statistical analysis

5. References

Abdullahi, B.A., Gu, X., Gan, Q., Yang, Y. (2003). Brassinolide amelioration of aluminum toxicity in mungbean seedling growth. Journal of Plant Nutrition, **26** (9), 1725-1734.

Achary, V.M.M., Jena, S., Panda, K.K., Panda, B.B. (2008). Aluminium induced oxidative stress and DNA damage in root cells of *Allium cepa* L. *Ecotoxicology and Environmental Safety*, **70**, 300-310

Ali, B., Hasan, S.A., Hayat, S., Hayat, Q., Yadav, S., Fariduddin, Q., Ahmad, A. (2008). A role for brassinosteroids in the amelioration of aluminium stress through antioxidant system in mung bean (*Vigna radiate* L. Wilczek). *Environmental and Experimental Botany*, **62**, 153-159

Asada, K. (1994). Production and action of active oxygen species in photosynthetic tissues. In C.H.Foyer and P.M.Mullineaux (Eds.). *Causes of photooxidative stress and amelioration of defense systems in plants* (pp. 77-104). CRC Press : USA

Balestrasse, K.B., Gallego, S.M., Tomaro, M.L. (2006). Aluminium stress affects nitrogen fixation and assimilation in soybean (*Glycine max*.). *Plant Growth Regulation*, **48**, 271-281.

Basu, U., Good, A.G., Taylor, G.J. (2001). Trangenic *Brassica napus* plants overexpressing aluminium-induced mitochondrial manganese superoxide dismutase cDNA are resistant to aluminium. *Plant, Cell and Environment*, **24**, 1269-1278

Boscolo, P.R.S., Menossi, M., Jorge, R.A. (2003). Aluminium-induced oxidative stress in maize. *Phtyochemistry*, **62**, 181-189

Bowler, C., Montagu, M.V., Inze, D. (1992). Superoxide dismutase and stress tolerance. Annu. *Rev. Plant. Physiol.*, **43**, 83-116

Budikova, S., Ciamporova, M., Ovecka, M., Polonyi, J. (1997). Structural characterization of maize root tip under aluminium stress. *Acta Fac. Rer. Nat. Univ. Comen. Physiol. Plant*, **29**, 47-52.

Ciamporova, M. (2000). Diverse responses of plant root cells to aluminium stress. *Plant* Soil, **225**, 1-4.

Clarkson, D.T. (1965). The effect of aluminium and some other trivalent metal cations on cell division in the root apices of *Allium cepa*. *Annals of Botany*, **29**, 309-315

Corpas, F.J., Fernandez, A., Carreras, A., Valderrama, R., Luque, F., Esteban, F., Rodriguez, M., Chaki, M., Pedrajas, J.R., Sandalio, L.M., del Rio, L.A., Barroso, J.B. (2006). The expression of different superoxide dismutase forms is

cell-type dependent in olive (*Olea europaea* L.) leaves. *Plant Cell Physiology*, **47** (7), 984-994.

Cruz, C., Bio, A.F.M., Dominguez-Valdivia, M.D., Aparicio-Tejo, P.M., Lamsfus, C., Martins-Loucao, M.A. (2006). How does glutamine synthetase activity determine plant tolerance to ammonium? *Planta*, **223**, 1068-1080

Dalton, D.A. (1995). Antioxidant defenses of plants and fungi. In S.Ahmad (Ed.). *Oxidative stress and antioxidant defenses in biology* (pp. 298-342). Chapman & Hall : USA

Del Rio, L.A., Sandalio, L.M., Yanez, J., Gomez, M. (1985). Induction of a manganese-containing superoxide dismutase in leaves of *Pisum sativum* L. by high nutrient levels of zinc and managanese. *Journal of Inorganic Biochemistry*, **24**, 25-34

Dominguez-Valdivia, M.D., Aparicio-Tejo, P.M., Lamsfus, C., Cruz, C., Martins-Loucao, M.A., Moran, J.F. (2008). Nitrogen nutrition and antioxidant metabolism in ammonium-tolerant and sensitive plants. *Physiologia Plantarum*, **132**, 359-369

Eleftheriou, E.P., Moustakas, M., Fragiskos, N. (1993). Aluminate induced changes in morphology and ultrastructure of *Thinopyrum* roots. *Journal of Experimental Botany*, **44**, 427-436.

Epstein, E., Bloom, A.J. (2005). *Mineral nutrition of plants : principles and perspectives* (2nd Ed.). Sinauer Associates Inc : USA

Exley, C. (2003). The pro-oxidant activity of aluminium. *Free Radical Biology & Medicine*, **36** (3), 380-387

Ezaki, B., Gardner, R.C., Ezaki, Y., Matsumoto, H. (2000). Expression of aluminium-induced genes in transgenic *Arabidopsis* plants can ameliorate aluminium stress and/or oxidative stress. *Plant Physiology*, **122**, 657-665

Ezaki, B., Suzuki, M., Motoda, H., Kawamura, M., Nakashima, S., Matsumoto, H. (2004). Mechanism of gene expression of Arabidopsis glutathione s-transferase, AtGST1, and AtGST11 in response to aluminium stress. *Plant Physiology*, **134**, 1672-1682

Fink, R.C., Scandalios, J.G. (2002). Molecular evolution and structure-function relationships of the superoxide dismutase gene families in angiosperms and their relationship to other eukaryotic and prokaryotic superoxide dismutases. *Archives of Biochemistry and Biophysics*, **399** (1), 19-36

Fukuda, T., Saito, A., Wasaki, J., Shinano, T., Osaki, M. (2007). Metabolic alterations proposed by proteome in rice roots grown under low P and high Al concentration under low pH. *Plant Science*, **172**, 1157-1165

Furukawa, J., Yamaji, N., Wang, H., Mitani, N., Murata, Y., Sato, K., Katsuhara, M., Takeda, K., Ma, J.F. (2007). An aluminium-activated citrate transporter in barley. *Plant Cell Physiol.*, **48** (8), 1081-1091

Giannakoula, A., Moustakas, M., Mylona, P., Papadakis, I., Yupsanis, T. (2008). Aluminium tolerance in maize is correlated with increased levels of mineral nutrients, carbohydrates and proline, and decreased levels of lipid peroxidation and Al accumulation. *Journal of Plant Physiology*, **165**, 385-396

Gibeaut D.M., Hulett J., Cramer G.R., Seemann J.R. (1997). Maximal biomass of Arabidopsis thaliana using a simple, low-maintenance hydroponic method and favourable environmental conditions. *Plant Physiology*, **115**, 317-319

Gratao, P.L., Gomes-Junior, R.A., Delite, F.S., Lea, P.J., Azevedo, R.A. (2006). Antioxidants stress responses of plants to cadmium. In N.A.Khan and Samiullah (Eds.), *Cadmium toxicity and tolerance in plants* (pp. 1-34). Alpha Science International Ltd : Oxford

Gunse, B., Poschenrieder, C., Barcelo, J. (2000). The role of ethylene metabolism in the short term responses to aluminium by roots of two maize cultivars different in Al-resistance. *Environmental and Experimental Botany*, **43**, 73-81.

Guo, Z., Ou, W., Lu, S., Zhong, Q. (2006). Differential responses of antioxidative system to chilling and drought in four rice cultivars differing in sensitivity. *Plant Physiology and Biochemistry*, **44**, 828-836

Gupta, A.S., Heinen, J.L., Holaday, A.S., Burke, J.J., Allen, R.D. (1993). Increased resistance to oxidative stress in transgenic plants that overexpress chloroplastic cu/zn superoxide dismutase. *Proc. Natl. Acad. Sci.*, **90**, 1629-1633

Jones, D.L., Blancaflor, E.B., Kochian, L.V., Gilroy, S. (2006). Spatial coordination of aluminium uptake, production of reactive oxygen species, callose production and wall rigidification in maize roots. *Plant, Cell and Environment*, **29**, 1309-1318

Kaminaka, H., Morita, S., Tokumoto, M., Yokoyama, H., Masumura, T., Tanaka, K. (1999). Molecular cloning and characterization of a cDNA for an iron-superoxide dismutase in rice (*Oryza sativa*). *Biosci. Biotechnol. Biochem*, **63,** 302-308

Khan, M.S.H., Tawaraya, K., Sekimoto, H, Koyama, H., Kobayashi, Y., Murayama, T., Chuba, M., Kambayashi, M., Shiono, Y., Uemura, M., Ishikawa, S., Wagatsuma, T. (2009). Relative abundance of D5-sterols in plasma membrane lipids of root-tip cells correlates with aluminum tolerance of rice. *Physiologia Plantarum*, **135,** 73-83

Kobayashi, T., Ogo, Y., Itai, R.N., Nakanishi, H., Takahashi, M., Mori, S., Nishizawa, N. (2007). The transcription factor IDEF1 regulates the response to and tolerance of iron deficiency in plants. *PNAS*, **104** (48), 19150-19155

Kochian, L.V. (1995). Cellular mechanisms of aluminium toxicity and resistance in plants. *Annu. Rev. Plant Physiol*., **46**, 237-260

Kochian, L.V., Hoekenga, O.A., Pineros, M.A. (2004). How do crop plants tolerate acid soils? Mechanisms of aluminium tolerance and phosphorus efficiency. *Annu. Rev. Plant Biol*., **55**, 459-493

Kovermann, P., Meyer, S., Hortensteiner, S., Picco, C., Scholz-Starke, J., Ravera, S., Lee, Y., Martinoia, E. (2007). The *Arabidopsis* vacuolar malate channel is a member of the ALMT family. *The Plant Journal*, **52**, 1169-1180

Kuo, M.C., Kao, C.H. (2003). Aluminium effects on lipid peroxidation and antioxidative enzyme activities in rice leaves. *Biologica Plantarum*, **46** (1), 149-152

Liu, Q., He, L.S., Wang, Z.Y., Zheng, S.J. (2006). Differential aluminium resistance and organic acid anions secretion in triticale. *Communications in Soil Science and Plant Analysis*, **38**, 1991-2004

Liu, D., Zou, J., Wang, M., Jiang, W. (2008). Hexavalent chromium uptake and its effects on mineral uptake, antioxidant defence system and photosynthesis in *Amaranthus viridis* L. *Bioresource Technology*, **99**, 2628-2636

Liu, J., Magalhaes, J.V., Shaff, J., Kochian, L.V. (2009). Aluminium-activated citrate and malate transporters from the MATE and ALMT families function independently to confer Arabidopsis aluminium tolerance. *The Plant Journal*, **57**, 389-399

Mates, J.M. (2000). Effects of antioxidant enzymes in the molecular control of reactive oxygen species toxicology. *Toxicology*, **153**, 83-104

Matsumoto, H. (2002). Metabolism of organic acids and metal tolerance in plants exposed to aluminium. In M.N.V Prasad and K.Strzalka (Eds.). *Physiology and biochemisty of metal toxicity and tolerance in plants* (pp. 95-110). Kluwer Academic Publishers : The Netherlands

Meriga, B., Reddy, B.K., Rao, K.R., Reddy, L.A., Kishor, P.B.K. (2004). Aluminium-induced production of oxygen radicals, lipid peroxidation and DNA damage in seedlings of rice (*Oryza sativa*). *J. Plant. Physiol*., **161**, 63-68

Mimmo, T., Sciortino, M., Ghizzi, M., Gianquinto, G., Gessa, C.E. (2009). The influence of aluminium availability on phosphate uptake in *Phaseolus vulgaris* L. and *Phaseolus luntaus* L. *Plant Physiology and Biochemistry*, **47**, 68-72

Morgan, M.J., Lehmann, M., Schwarzlander, M., Baxter, C.J. (2008). Decrease in manganese superoxide dismutase leads to reduced root growth and affects tricarboxylic acid cycle flux and mitochondrial redox homeostasis. *Plant Physiology*, **147**, 101-114

Mullen, C.L., Scott, B.J., Evans, C.M., Conyers, M.K. (2006). Effect of soil acidity and liming on Lucerne and following crops in central-western New South Wales. *Australian Journal of Experimental Agriculture*, **46**, 1291-1300

Murao, K., Takamiya, M., Ono, K., Takano, H., Takio, S. (2004). Copper deficiency induced expression of Fe-superoxide dismutase gene in *Matteuccia struthiopteris*. *Plant Physiology and Biochemistry*, **42**, 143-148

Navrot, N., Rouhier, N., Gelhaye, E., Jacquot, J. (2007). Reactive oxygen species generation and antioxidant systems in plant mitochondria. *Physiologia Plantarum*, **129**, 185-195

O'Brien, K.M., Dirmeier, R., Engle, M., Poyton, R.O. (2004). Mitochondrial protein oxidation in yeast mutants lacking manganese-(MnSOD) or copper- and zinc-containing superoxide dismutase (CuZnSOD). *The Journal of Biological Chemistry*, **279** (50), 51817-51827

Pan, J., Zhu, M., Chen, H. (2001). Aluminium-induced cell death in root tip cells of barley. *Environmental and Experimental Botany*, **46**, 71-79

Pintro, J., Barloy, J., Fallavier, P. (1998). Uptake of aluminium by the root tips of an al-sensitive and al-tolerant cultivar of *Zea mays*. *Plant Physiol. Biochem*., **36** (6), 463-467

Polesskaya, O.G., Kashirina, E.I., Alekhina, N.D. (2004). Changes in the activity of antioxidant enzymes in wheat leaves and roots as a function of nitrogen source and supply. *Russian Journal of Plant Physiology*, **51** (5), 615-620

Poozesh, M., Cruz, P., Choler, P., Bertoni, G. (2007). Relationship between the Al resistance of grasses and their adaptation to an infertile habitat. *Annals of Botany*, **99**, 947-954

Prasad, M.N.V. (2004). *Heavy metal stress in plants – from biomolecules to ecosystems* (2nd Ed.). Springer : India

Rangel, A.F., Rao, I.M., Horst, W.J. (2007). Spatial aluminium sensitivity of root apices of two common bean (*Phaseolus vulgaris* L.) genotypes with contrasting aluminium resistance. *Journal of Experimental Botany*, **58** (14), 3895-3904

Rangel, A.F., Rao, I.M., Horst, W.J. (2009). Intracellular distribution and binding state of aluminum in root apices of two common bean (*Phaseolus vulgaris*) genotypes in relation to Al toxicity. *Physiologia Plantarum*, **135**, 162-173

Rengel, Z. (1996). Uptake of aluminium by plant cells. *New Phytologist*, **134**, 389-406

Richards, K.D., Schott, E.J., Sharma, Y.K., Davis, K.R., Gardner, R.C. (1998). Aluminium induces oxidative stress genes in *Arabidopsis thaliana*. *Plant Physiol*., **116**, 409-418

Rodriquez-Serrano, M., Romero-Puertas, C., Pazmino, D.M., Testillano, P.S., Risueno, M.C., del Rio, L.A., Sandalio, L.M. (2009). Cellular response of pea plants to cadmium toxicity: cross talk between reactive oxygen species, nitric oxide, and calcium. *Plant Physiology*, **150**, 229-243

Ryan, P.R., Raman, H., Gupta, S., Horst, W.J., Delhaize, E. (2009). A second mechanism for aluminium resistance in wheat relies on the constitutive efflux of citrate from roots. *Plant Physiology*, **149**, 340-351

Ruley, A.T., Sharma, N.C., Sahi, S.V. (2004). Antioxidant defense in a lead accumulating plant, *Sesbania drummondii*. *Plant Physiology and Biochemistry*, **42**, 899-906

Sartie, A.M. (2006). *Phenotypic assessment and quantitative trait locus (QTL) analysis of herbage and seed production traits in perennial ryegrass (Lolium perenne L.).* PhD Thesis. Massey University, New Zealand

Sawaki, Y., Iuchi, S., Kobayashi, Y., Kobayashi, Y., Ikka, T., Sakurai, N., Fujita, M., Shinozaki, K., Shibata, D., Kobayashi, M., Koyama, H. (2009). STOP1 regulates multiple genes that protect Arabidopsis from proton and aluminum toxicities. *Plant Physiology*, **150**, 281-294

Scott, B.J., Ewing, M.A., Williams, R., Humphries, A.W., Coombes, N.E. (2008). Tolerance of aluminium toxicity in annual *Medicago* species and Lucerne. *Australian Journal of Experimental Agriculture*, **48**, 499-511

Seawright, M.P. (2005). *Physiological and biochemical response of endophyte infected Lolium perenne to water stress and to plant hormone treatment when water sufficient*. MSc Thesis. Massey University, New Zealand

Sharma, P., Dubey, R.S. (2007). Involvement of oxidative stress and role of antioxidative defense system in growing rice seedlings exposed to toxic concentrations of aluminium. *Plant Cell Rep*, **26**, 2027-2038

Siegel, F.R. (2002). *Environmental geochemistry of potentially toxic metals*. Springer : USA

Simonovicova, M., Huttova, J., Mistrik, I., Siroka, B., Tamas, L. (2004). Root growth inhibition by aluminium is probably caused by cell death due to peroxidase-mediated hydrogen peroxide production. *Protoplasma*, **224**, 91-98

Simonovicova, M., Tamas, L., Huttova, J., Mistrik, I. (2004). Effect of aluminium on oxidative stress related enzymes activities in barley roots. *Biologia Plantarum*, **48** (2), 261-266

Sun, P., Tian, Q., Zhao, M., Dai, X., Huang, J., Li, L., Zhang, W. (2007). Aluminium-induced ethylene production is associated with inhibition of root elongation in *Lotus japonicus* L. *Plant Cell Physiol.*, **48** (8), 1229-1235

Tamas, L., Huttova, J., Mistrik, I. (2003). Inhibition of al-induced root elongation and enhancement of al-induced peroxidase activity in al-sensitive and al-resistant barley cultivars are positively correlated. *Plant and Soil*, **250**, 193-200

Tamas, L., Budikova, S., Huttova, J., Mistrik, I., Simonovicova, M., Siroka, B. (2005). Aluminium-induced cell death of barley-root border cells is correlated with peroxidase- and oxalate oxidase-mediated hydrogen peroxide production. *Plant Cell Rep.*, **24**, 189-194

Taylor, G.J., Foy, C.D. (1985). Mechanisms of aluminium tolerance in *Triticum aestivum* L. (wheat). I. differential pH induced by winter cultivars in nutrient solutions. *Amer. J. Bot*., **72** (5), 695-701

Van Camp, W., Montagu, M.V., Inze, D. (1994). Superoxide dismutases. In C.H.Foyer and P.M.Mullineaux (Eds.). *Causes of photooxidative stress and amelioration of defense systems in plants* (pp. 317-342). CRC Press : USA

Vitoria, A.P., Lea, P.J., Azevedo, R.A. (2001). Antioxidant enzymes responses to cadmium in radish tissues. *Phytochemistry*, **57**, 701-710

Wang, W., Pan, J., Zheng, K., Chen, H., Shao, H., Guo, Y., Bian, H., Han, N., Wang, J., Zhu, M. (2009). Ced-9 inhibits Al-induced programmed cell death and promotes Al tolerance in tobacco. *Biochemical and Biophysical Research Communications*, **383**, 141-145

Wenzl, P., Mancilla, L.I., Mayer, J.F., Rao, I. (2001). The high level of aluminium resistance in signalgrass is not associated with known mechanisms of external detoxification in root apices. *Plant Physiology*, **125**, 1473-1484

Whitehead, D.C. (2000). *Nutrient elements in grassland : soil-plant-animal relationships*. CABI Publishing : United Kingdom

Witcombe, J.R., Hollington, P.A., Howarth, C.J., Reader, S., Steele, K.A. (2008). Breeding for abiotic stresses for sustainable agriculture. *Philosophical Transactions of the Royal Society B*, **363**, 703-716

Yang, J., Li, Y., Zhang, Y., Zhang, S., Wu, Y., Wu, P., Zheng, S. (2008). Cell wall polysaccharides are specifically involved in the exclusion of aluminium from the rice root apex. *Plant Physiology*, **146**, 602-611

Zhang, J., He, Z., Tian, H., Zhu, G., Peng, X. (2007). Identification of aluminium-responsive genes in rice cultivars with different aluminium sensitivities. *Journal of Experimental Botany*, **58** (8), 2269-2278

Zhen, Y., Qi, J., Wang, S., Su, J., Xu, G., Zhang., M., Miao, L., Peng, X., Tian, D., Yang, Y. (2007). Comparative proteome analysis of differentially expressed proteins induced by Al toxicity in soybean. *Physiologia Plantarum*, **131**, 542-554

Zheng, S.J., Yang, J.L. (2005). Target sites of aluminium phytotoxicity. *Biologia Plantarum*, **49** (3), 321-331

Zhou, S., Sauve, R., Thannhauser, T.W. (2009). Proteome changes induced by aluminium stress in tomato roots. *Journal of Experimental Botany*, **60** (6), 1849-1857